Flexible Energy Resources for Enhancing Power Distribution System Resilience

by Zijiang Yang

B.S. in Electrical Engineering, May 2017, Illinois Institute of Technology

A Thesis submitted to

The Faculty of
The School of Engineering and Applied Science
of The George Washington University
in partial satisfaction of the requirements
for the degree of Master of Science

May 19, 2019

Thesis directed by

Payman Dehghanian
Assistant Professor of Electrical and Computer Engineering

Dedication

This MS Thesis is lovingly dedicated to my parents (Xiong and Zhaoying), my sisters (Pushan), and Xiaolu, without whom my achievements so far could never be accomplished. They are the ones always nursing me with affections and love. Their support and encouragement have sustained me throughout my university life.

Acknowledgments

I would like to express my sincere gratitude to my advisor, Prof. Payman Dehghanian, for his guide, understanding, wisdom, patience, encouragements, and for supporting me reach this point. Thanks also to my committee members, Prof. Robert Harrington, and Prof. Shahrokh Ahmadi, for their time and patience.

Appreciation goes to my friends and the member of the Smart Grid Laboratory, specifically Shiyuan Wang, Bo Wang, Li Li, Mohannad Alhazmi, Mostafa Nazemi, Jinshun Su, Bhavesh Shinde for making my time at the George Washington University a wonderful experience.

Most of all, I am fully indebted to my parents for their terrific support, without which, the pursuit of this advanced degree would never have been started and accomplished.

Abstract

Flexible Energy Resources for Enhancing Power Distribution System Resilience

In the past decades, high-impact low-probability (HILP) events are observed more and more frequent. While such severe HILP events cause prolonged and extensive electric outages, the conventional reliability view is insufficient to coping with the challenges on the modern power system. Improving the resilience of the power system, hence, becomes increasingly important and urgent. The use of advanced technologies including the remote-controlled switches and distributed energy sources bring additional flexibility to the power system operation when the emergency conditions or the outages caused by HILP events unfold. Mobile power sources (MPSs) including truck-mounted mobile emergency generators, truck-mounted mobile energy storage systems, and electric vehicles have a great potential in harnessing their mobility for enhancing the power system resilience.

This thesis mainly focuses on investigating the potential roles of the MPS in improving the power system resilience, specifically, facilitating the distribution system restoration following natural hazards. The distribution system reconfiguration (real-time topology change) is also taken into account to best utilize the network built-in flexibility and help power delivery during emergencies. A mixed-integer nonlinear programming model is proposed for deriving a strategy for MPS dispatch and distribution system reconfiguration under a given repair strategy. The model is further linearized into a mix-integer linear programming formulation. The coordination of the proposed MPS and photovoltaic (PV) generation is also investigated. Eventually, the impact of the repair strategy on the contribution of MPS dispatch and PV generation on promoting distribution system restoration is studied.

Table of Contents

List of Figures

List of Tables

Nomenclature

A. Sets and Indices

$i, j \in \mathbf{B}$	Indices/set of nodes.
$m \in \mathbf{M}$	Indices/set of mobile power sources (MPSs).
$t, \tau \in \mathbf{T}$	Indices/set of time periods.
$(i, j) \in \mathbf{L}$	Indices/set of branches.
$N_{\mathbf{B}}, N_{\mathbf{T}}, N_{\mathbf{L}}$	Number of all nodes, time periods, branches.
$\mathbf{B}^{\text{sub}}$	Set of substation nodes.
$\mathbf{B}_m$	Set of candidate nodes that can be connected to MPS m.
$\mathbf{B}_t^{\text{source}}$	Set of nodes that are selected to be the sources of the fictitious flows at time t.
$\mathbf{L}^{\text{switch}}$	Set of branches equipped with remotely-controlled switches (RCSs).
$\mathbf{L}_t^{\text{damaged}}$	Set of branches that are damaged and have not been repaired at time t.
$\mathbf{G} \in \mathbf{M}$	Set of all mobile emergency generators (MEGs).
$\mathbf{S} \in \mathbf{M}$	Set of all mobile energy storage systems (MESSs).
$\mathbf{V} \in \mathbf{M}$	Set of all mobile electric vehicle (EV) fleets.
$\mathbf{M_i}$	Set of MPSs that can be connected to node i.

B. Parameters and Constants

χ_i	Priority of the load demanded at node i.
$\beta_{ij,t}$	Binary damage status of the branch (i, j) at time t. (1 if the branch is undamaged or has been repaired, 0 otherwise).
$P_{i,t}^{\text{demand}}$	Real power demand of node i at time t (kW).
$Q_{i,t}^{\text{demand}}$	Reactive power demand of node i at time t (kVar).
α_{ij}^0	Binary parameter representing the initial status of branch (i,j) (1 if the branch is connected, 0 otherwise).
N_t^{island}	Number of islands due to the damaged and unrepaired branches at time t.
N_i^{mps}	Number of MPSs that are allowed to be connected to node i.

$T^{\text{travel}}_{m,ij}$	Travel time of MPS m from node i to node j.
Δt	Duration of one time period.
M	A large enough positive number.
$\underline{\text{SOC}}_m$	Minimum state of charge (SOC) of MESS or EV fleet m (kWh).
$\overline{\text{SOC}}_m$	Maximum SOC of the MESS or EV fleet m (kWh).
$\overline{P}^{\text{ch}}_m, \overline{P}^{\text{dch}}_m$	Maximum charging and discharging power of MESS or EV fleet m (kW, kVar).
$\overline{P}_m, \overline{Q}_m$	Maximum real and reactive power output of MPS m (kW, kVar).
$\overline{P}_{ij}, \overline{Q}_{ij}$	Real and reactive power capacity of branch (i, j) (kW, kVar).
r_{ij}, x_{ij}	Resistance and reactance of branch (i, j) (Ω).
$\underline{\text{Vsqr}}_i$	Minimum squared voltage magnitude at node i (kV^2).
$\overline{\text{Vsqr}}_i$	Maximum squared voltage magnitude at node i (kV^2).
C^{tr}_m	Transportation cost coefficient of MPS m.
C^{P}_m	Power rating price of MESS or EV fleet m (\$/kWh).
k_m	Degradation slope of MESS or EV feelt m.
δ_m	Generation cost of MEG m (\$/kWh).
$\eta^{\text{ch}}_m, \eta^{\text{dch}}_m$	Charging and discharging efficiency of MESS or EV fleet m.
P^{travel}_m	Energy consumption rate of EV fleet m when traveling (kW).
$d^{\text{fic}}_{i,t}$	Fictitious load of node i at time t.
PVC	Value of loss of solar energy (\$/kWh)
$\overline{P}^{s}_{i,t}$	Maximum available real power from solar farm connected to node i at time t (kW)

C. Functions and Variables

$pd_{i,t}, qd_{i,t}$	Real and reactive power demand supplied at node i at time t (kW, kVar).
$pg_{i,t}, qg_{i,t}$	Real and reactive power at substation node i at time t (kW, kVar).
$pf_{ij,t}, qf_{ij,t}$	Real and reactive power flow on branch (i, j) at time t (kW, kVar).
$\text{SOC}_{m,t}$	SOC of MESS or EV fleet m at time t (kWh).

$p^{\text{ch}}_{m,t}, p^{\text{dch}}_{m,t}$ Charging and discharging power of MESS or EV fleet m at time t (kW).

$p_{m,t}, q_{m,t}$ Real and reactive power output of MPS m at time t (kW, kVar).

$p^{\text{mps}}_{i,t}, q^{\text{mps}}_{i,t}$ Real and reactive power output of MPSs at node i at time t (kW, kVar).

$Vsqr_{i,t}$ Squared voltage magnitude at node i at time t (kV^2).

$fl_{ij,t}$ Fictitious flow on branch (i, j) at time t.

$fg_{i,t}$ Fictitious supply at source node i at time t.

$p^{\text{SC}}_{i,t}$ Curtailed power of solar farm connected to node i at time t (kW).

$p^{s}_{i,t}$ Real power generated by solar farm connected to node i at time t (kW).

D. Binary Variables

$\alpha_{ij,t}$ Connection status of branch (i, j) at time t
(1 if the branch is connected, 0 otherwise).

$c_{m,t}, d_{m,t}$ Charging and discharging status of MESS or EV fleet m at time t
(1 if charging or discharging, 0 otherwise).

$\varphi_{m,t}$ Traveling status of MPS m at time t
(1 if the MPS is traveling, 0 otherwise).

$\mu_{m,i,t}$ Connection status of MPS m to node i at time t
(1 if connected, 0 otherwise).

Chapter 1: Introduction

1.1 Problem Statement

In the recent years, more frequent realization of the high-impact low-probability (HILP) hazards and catastrophe have resulted in prolonged electricity outages, excessive equipment damages, and even more severe economic loss and disruptions in our modern society [1, 2]. The HILP events include two categories: (i) natural hazards, such as hurricanes, earthquakes tornadoes, windstorms, wildfires, ice storms, etc; (ii) man-made disasters, such as cyber attacks or physical attack on power system infrastructure.

Table 1.1: Statistics of Outage Events in the U.S. Between 1984-2006 [3]

Statistics for Outage Cause Categories

	% of events	Mean size in MW	Mean size in customers
Earthquake	0.8	1,408	375,900
Tornado	2.8	367	115,439
Hurricane/Tropical Storm	4.2	1,309	782,695
Ice Storm	5	1,152	343,448
Lightning	11.3	270	70,944
Wind/Rain	14.8	793	185,199
Other cold weather	5.5	542	150,255
Fire	5.2	431	111,244
Intentional attack	1.6	340	24,572
Supply shortage	5.3	341	138,957
Other external cause	4.8	710	246,071
Equipment Failure	29.7	379	57,140
Operator Error	10.1	489	105,322
Voltage reduction	7.7	153	212,900
Volunteer reduction	5.9	190	134,543

Table 1.1 shows the statistics of 933 outage events, reported by the North American Electric Reliability Corporation (NERC), between 1984 to 2006 [3]. Extreme weathers and natural disasters have relatively low frequencies, but a greater impact on electric power supply and a larger size of affected electricity customers, among these outage cause categories.

Earthquake

Earthquakes are one of the most unpredictable hazards which can cause striking damages in the radial power distribution system (DS). Among the past records on disastrous earthquakes, one can highlight the 6.9 magnitude earthquake in Armenia on December 7, 1988 engendering thousands of people died and injured and two substations seriously damaged or almost entirely wrecked and transformers, circuit breakers, and capacitor banks critically damaged [4], the Loma Prieta earthquake in the greater San Francisco Bay Area in California in 1989 which affecting 12,000 of the one million customers out of electric service after 48 hours, destroyed the Moss Landing power plant and caused $6 billion in property damage [4, 5], the Northridge earthquake that struck Los Angeles on January 17, 1994, affecting 2.5 million local customers [6], the Hyogo-ken Nanbu earthquake that attacked Hanshin-Awaji region on January 17, 1995, resulting approximately in 2.6 million households out of power services [7], the severe Bam earthquake in 2003 causing $90 million costs in the reconstruction of electricity in Iran [8], the Wenchuan earthquake in 2008 which caused extreme damages in 966 substations, 274 transmission lines at multiple voltage levels and 1700 circuits [9], the Tohoku earthquake in 2011 impacting about 8.9 million households in 18 prefectures among 4 electric power companies [10], a magnitude 5.8 earthquake in Virginia in 2011 that knocked down the North Anna Nuclear Power Station and led to thorough damage evaluations that last more than 10 weeks before the power station restarted, and recently in 2017 in Iran, the Sarpol-e Zahab earthquake with 7.3 moment magnitude resulting in a prolonged city-wide blackout for weeks [11]. Most significantly, earthquakes can ruin all kinds of power system facilities and infrastructure, both above and under ground, and the swift reconstruction of the underground facilities is impractical [4].

Tornado, Windstorm and Hurricane

Hurricanes principally affect the transmission and distribution lines. Hurricane Hugo hits the Carolinas rendering $6.5 billion property damaged alone. 70% of the 430,000

customers of the largest supplier of electricity in South Carolina suffered a blackout during the storm and 140,000 customers were out of electricity even after five days [4]. Southeastern US was swept by hurricane Gloria, hurricane Isabel and hurricane Wilma respectively in September 1985, September 2003 and October 2005; each of these hurricanes led to approximately 10,000 MW power loss. To be specific, hurricane Isabel about 2.5 million outages, hurricane Gloria almost three million outages and hurricane Wilma 3.2 million outages [12]. Additionally, hurricane Katrina smashed Southeastern US in August 2005 affecting 2.7 million customers in eight states, resulting in approximately $84.8 billion to $157.5 billion damage cost [13]; the electricity service remained unavailable for around 250,000 customers even almost one month after the storm. The damaged electric assets included 72,47 utility poles, 8,281 transformer, and 1,515 transmission structures. Beside, 300 substations were shut down and multiple power plants, of which three nuclear plants could not work well [14]. Specifically, hurricane Katrina destroyed almost two-thirds of the transmission and distribution system, leading to all 195,000 customers of Southern Company's Mississippi Power subsidiary were without electricity. In transmission level, only three of 122 transmission lines survived while more than 300 transmission towers were damaged, including 47 metal towers in the 230 kV bulk power system. In the distribution level, 9,000 poles and 2,300 transformers were missing and around 65% of equipment were destroyed, incorporating 23,500 spans of conductor [15]. Tropical storm Irene hit the State of Connecticut on August 28, 2011, affecting more than 800,000 power customers suffering prolonged electricity outage up to 9 days and resulting in approximately $200 million in damage [16]. Hurricane Sandy struck the Northeast U.S. on October 22, 2012, followed by around 10% customers in New York and New Jersey stayed out of electricity for 10 days, causing over 100,000 primary electrical lines damaged, affecting approximately 8 million customers for electricity interruption and total damage of nearly $ 50 billion in the area [13, 17–19]. Two 500-kV transmission lines, four 220-kV transmission lines, eight 110-kV transmission lines were damaged due to a tornado that slapped Jiangsu Province,

China in 2016 and affected the electricity service of 135,000 households [20].

Snowstorm and Ice Storm

Southern China was struck by a snow storm in 2008 resulting in 129 lines faults and the failure of 2,000 substations as well as 14.66 million households out of electricity supply [18, 20]. In 1998, the New England/Eastern Canada Ice Storm knocked down 770 electric transmission towers, more than 26,000 distribution poles, 4,000 transformers and up to 1,800 miles of transmission and distribution lines needed to be rebuild or replaced. Following the ice storm, more than 5.2 million customers were out of electricity and numerous customers remained without electricity up to three weeks while the full restoration of the power took more than one month [21]. The estimated damaged was estimated up to $4 billion [22].

Physical Attack

Between 1980 to 1989, a total of 386 strikes on the U.S. energy assets were recorded by the U.S. Department of Energy [4]. An uncertain number of gunmen struck the Metcalf Transmission Substation owned by the Pacific Gas and Electric (PG&E) outside San Jose, California in April 2013. The well-planned attack severely destroyed 17 transformers and engender damage of more than $15 million, though no large electricity outages happened, since the power flows were rerouted by the operators from neighboring generators [13].

Cyber Attack

On December 23, 2015, about 225,000 customers were out of power for around 6 hours in Ukraine due to a cyber attack. The well-known Microsoft Office macro vulnerabilities, along with spear-phishing schemes and malware was utilized by the attackers to break into the internal networks of three utilities. Further, the Supervisory Control and Data Acquisition (SCADA) system was modified by the attackers and became uncontrollable by the operators while the control centers were out of power and disable cyber monitoring and the control systems, until the SCADA system was shut down. After the attack, even though the service was restored via employing manual operation in a short time relatively,

the control centers were not entirely ready for use in several months [23].

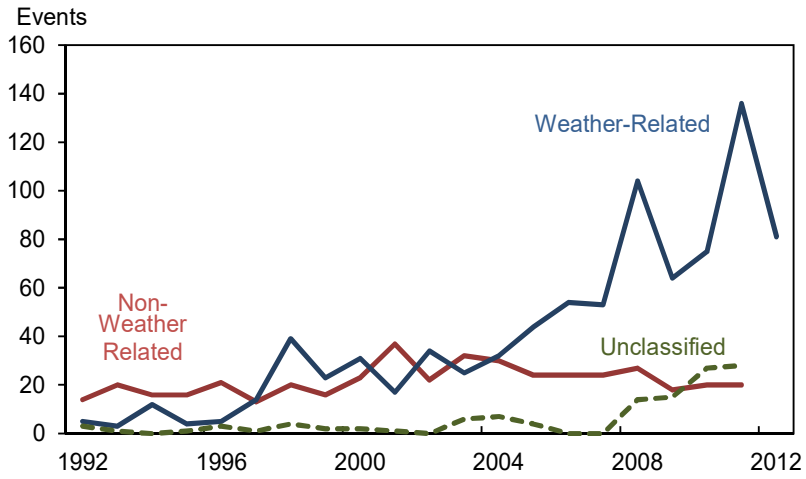

Figure 1.1: Observed outages to the bulk electric system between 1992-2012 [24]

Figure 1.1 reveals that the frequency of bulk electric system outages due to extreme weather has grown significantly in recent years [24]. Meanwhile, human-made physical attack or cyber attack still need to be concerned. The occurrence of such catastrophic HILP-caused electricity outages has been observed to be on the rise over the past decade and the U.S. infrastructure is more and more dependent on electricity. This calls for further effective strategies beyond the traditional reliability view for improving the grid resilience to ensure a continuous and resilient supply of electricity to the end customers and maintain the basic services such as the economic system and emergency services when dealing with the aftermath of seismic hazards [20, 25, 26].

1.2 The Concept of Resilience

Unlike the widely adopted terminology "reliability" in many traditional principles, Power system resilience is an emerging concept and its definition is unclear and unfocused thus far; nonetheless, the definition has a common comprehension. "Resilience" and "Reliability" seem to have a similar but essentially distinct meaning. The key characteristic difference between resilience and reliability is presented in Table 1.2 [18].

Table 1.2: The Concept Contrast Between Reliability and Resilience [18]

Reliability	Resilience
High-probability, low-impact	Low-probability, high-impact
Static	Adaptive, ongoing, short- and long-term
Evaluates the power system states	Evaluates the power system states *and t*ransition times between states
Concerned with customer interruption time	Concerned with customer interruption time *and* the infrastructure recovery time

The existing reliability metrics do not concentrate on the consequence of individual HILP events. Beyond minimizing the probability of extensive and prolonged outages, resilience also takes the following into account: acknowledgment of the occurrence of such outages, preparation to cope with them, minimization of the outage effect, rapid restoration of the service and learning from the experience to enhance the future performance [13].

National Academies of Sciences, Engineering, and Medicine [13] provides a definition in 2017 for resilience as follows: "*Resilience is not just about lessening the likelihood that these outages will occur. It is also about limiting the scope and impact of outages when they do occur, restoring power rapidly afterwards, and learning from these experiences to better deal with events in the future.*"

PJM Interconnection provides a definition in March 2017 as follows [27]: "*Resilience, in the context of the bulk electric system, relates to preparing for, operating through and recovering from a high-impact, low-frequency event. Resilience is remaining reliable even during these events*". This definition is more specific to the HILP events.

In President Barack Obama's Presidential Policy Directive [28], the term "resilience" refer to "*the ability to prepare for and adapt to changing conditions and withstand and recover rapidly from disruptions. Resilience includes the ability to withstand and recover from deliberate attacks, accidents, or naturally occurring threats or incidents*".

A definition of resilience for energy system is provided by UK Energy Research Center [29] as follows:"*Resilience is the capacity of an energy system to tolerate disturbance and to continue to deliver affordable energy services to consumers. A resilient energy system*

can speedily recover from shocks and can provide alternative means of satisfying energy service needs in the event of changed external circumstances."

Among the existing definitions of resilience, four aspects of the system resilience are summarized in [30] as follows:

- The state of electricity services of a power system can be described by resilience when confronting an interruption or outage. The description of resilience contains the extent of the service degradation, the rapidity of service recovery, and the recovery extent of the service. As can be seen, resilience does not only reveal a discrete state of whether a disturbance has happened or not, but also demonstrates the level of disturbance.

- The system resilience is determined by its design and its operation. These affect the degradation degree during a disturbance, the swiftness of the recovery and the completion of the recovery. For instance, a more redundant system that considers recovery strategies and additional contingency operation modes might undergo fewer and shorter interruptions. On the other hand, such a redundant system is more strenuous to reconstruct.

- Different resilience levels of the system can be resulted from different response at different costs. For instance, the system rebuilt with additional resources and a more efficient set of equipment can provide higher quality of service than the original level after the disaster recovery.

- The system resilience changes over time. The service of a system could be enhanced with regular maintenance and upgrade but at a cost. On the other hand, the service of a system without regular maintenance and upgrade has a lower operating cost but it can be anticipated that the quality of service and will lessen in the future.

The National Infrastructure Advisory Council (NIAC), USA provided comes up with four main features of resilience in [31]:

- **Robustness**: The capability to maintain operation or withstand when disaster occurs, especially HILP events. Besides the system structure or design, it also relates to the system redundancy in case of some important components damages, along with the investment and maintenance of the critical infrastructure.

- **Resourcefulness**: The capability to expertly handle the occurred disaster. It incorporates determining the strategies and priority of the action that should be taken to both control and diminish the hazard, convey the decision to the people to execute. This feature mainly relates to the human, and not the adopted technology.

- **Rapid Recovery**: The capability to restore the system to its normal operating condition as soon as possible following the hazards. It relates to elaborately prepared contingency plans, capable emergency operations and strategic resources distribution and crews dispatch.

- **Adaptability**: The manner to learn from a hazard. It relates to the enhancement of the robustness, resourcefulness and recovery abilities of the system for the future hazards via new tools and technologies.

The Cabinet Office, U.K. also provides four main characteristics of infrastructure resilience in [32] as follows:

- **Resistance:** provides the strength or protection to withstand the disaster and its main effect to further mitigate the damage or disturbance.

- **Reliability:** the infrastructure components make sure to be inherently designed to maintain operation under certain conditions.

- **Redundancy:** the availability of backup equipment or spare capacity to allow the operation to be switched or redirected to alternative routes.

- **Response and Recovery:** rapid and effective response to and recovery from the hazards.

Additionally, Electric Power Research Institute (EPRI) in the U.S. also determines the three elements of resilience which are prevention, survivability, recovery for distribution system in [33] as demonstrated in Figure 1.2:

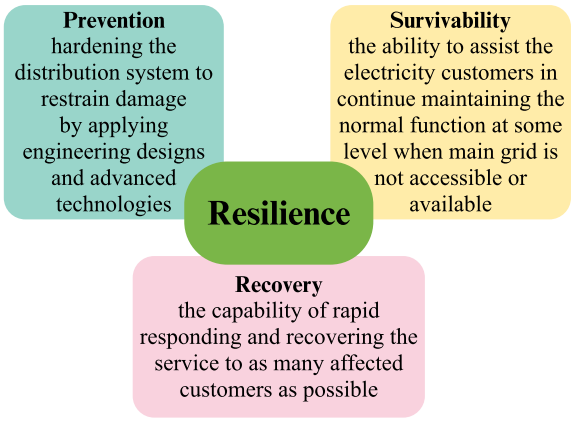

Figure 1.2: Elements of resilience by Electric Power Research Institute (EPRI) [33]

Notice that these elements and aspects of the system resilience can also lead to its measurement (or metrics). Most of the existing definitions of resilience refer to the capability of the system to withstand and rapidly recover from HILP events.

A conceptual resilience curve is proposed in [18] to describe the variations in the system resilience level over time in regard to a HILP event, as illustrated in Figure 1.3, where R represents the resilience level of the system. With respect to a HILP event, the power system experiences the following states [18, 34]:

- **Resilient State $t_0 \sim t_e$:** before the HILP event happens at t_e, the power system should be robust and resistant to withstand the first strike of the HILP event by sufficiently predict the time and location of the external disturbance and preventive actions (e.g. preventive generation rescheduling) taken by the system operator, aiming to enhance the disturbance resilience of the infrastructure.

- **Event Progress $t_e \sim t_{pe}$:** during the HILP event progress, the system is degraded to post-event degradation state, where the system resilience decrease to R_{pe}. Emergency or corrective actions (e.g. generation re-dispatch alone or generation re-dispatch

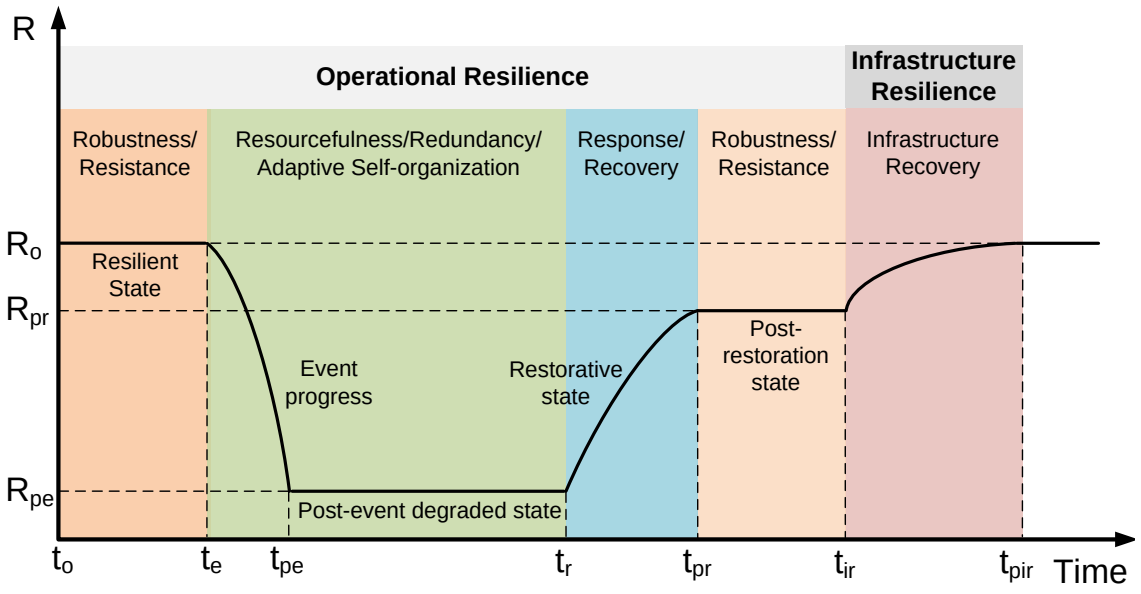

Figure 1.3: The conceptual resilience curve related to a HILP event [18]

coordinating with dynamic-boundary microgrid operation) can be taken to reduce the effect of the external disturbance.

- **Post-Event Degraded State $t_{pe} \sim t_r$:** after the event strike, the system enters the post-event degraded state. At this stage, the key resilience features are the *resourcefulness*, *redundancy*, *adaptive self-organization*, they offer the necessary *corrective operational flexibility* to accommodate and cope with the changing situation. This assists in minimizing the consequence of the event and the degradation in the system resilience level (e.g. $R_0 - R_{pe}$) while appropriate and effective coordination and preparation enable rapid beginning of the restoration state.

- **Restorative State $t_r \sim t_{pr}$:** the system should manifest fast *response* and *recovery* ability to recover the system resilience level from R_{pe} to R_{pr}. R_{pr} may be the pre-event resilience level R_0 or a desired resilience level that is not as high as R_0.

- **Post-Restoration State $t_{pr} \sim t_{ir}$ and Infrastructure Recovery $t_{ir} \sim t_{pir}$:** Following the restorative state, the consequence of the event on the system resilience and its performance during the event need to be evaluated and analyzed to enhance the

infrastructure resilience for future similar or unpredictable events. Depending on the severity of the event, the system may need longer time to recover the infrastructure in $t_{ir} \sim t_{pir}$.

1.3 Quantitative Metrics for Resilience

Even though the traditional reliability metrics have been widely used and are comparatively mature, a survey of publicly owned utilities in 2013 reveals that the outages caused by major events may be overlooked when measuring the performance of the utilities only using the existing reliability metrics. The contribution of planning, operational strategies and used technologies on facilitating the recovery and reducing the impact of extensive and prolonged outages may not be reflected by the traditional reliability criteria. Similar to the definition of resilience, there is no widely recognized resilience metrics up to the present while some efforts have been in progress in the literature [13, 35–38]. Establishing widely-accepted metrics of the system resilience is progressively significant and urgent, as it is impossible to address the priority of system enhancements and reinforcements needed to (i) monitor or reveal the changes as they unfold; (ii) define the enhancement strategies for system resilience; or (iii) to balance the resilience improvements with the related costs [39]. This is particularly needed as the enhanced system resilience to significant shocks will affect different interdependent ecosystems alike which indirectly affect the social welfare and every aspect of our economy [40–44].

According to [45], several requirements are crucial for establishing a resilience metric as follows:

- **Be Useful:** the developed metrics used by humans or computational analysis (or both) should contribute to decision making, incorporating system planning decisions, real-time operational decisions, and policy decisions.

- **Provide a Mechanism for Comparison:** the same metric can distinguish the re-

silience of different systems where one has improvement in infrastructure or operation while the other has not.

- **Be Usable in Operations and Planning Contexts:** the same metric should be beneficial to both operating decision (e.g. system pre-configuration followed by a hurricane) and planning decisions (e.g. burial of electrical conductor).

- **Exhibit Extendability:** the metrics should be applicable in different timescales and different geographical extents and situations while it can adapt to the progressing technology and growingly complicated analytics of the future.

- **Be Quantitative:** the metrics should be both qualitative and quantitative.

- **Reflect Uncertainty:** the metrics should be able to evaluate the uncertainties quantitatively while the certainty of this value can be considered in the made decision based on the resilience metrics [46].

- **Support a risk based approach:** Besides the instant system impacts, one particular hazard or a series of the hazards, the vulnerability of the system and the potential impact on people should be indicated by the metrics.

- **Capture Recovery Time:** the outage duration should be revealed by the metrics in either direct or indirect way.

Resilience metrics can be divided into two categories: qualitative metrics and quantitative metrics. Comparing with the qualitative metrics, quantitative metrics are helpful for the efficacy assessment of some resilience measures or comparison between the resilience level of different systems. Only quantitative metrics are discussed in this section.

The quantitative resilience metrics basically are divided into three categories: the analytic method, the simulation-based method and the statistical analysis, where the analytical method utilizes the system failure probability in a particular situation while the simulation-

based method is most popular and can effortlessly be bond with specific hazard scenarios and compute the impact of the hazards [20].

One example of the analytical method is presented in [47], where resilience is defined as a "probability that the network performs its intended function" at a given duration when the component fails due to external causes, as a means to "describe the distribution of network reliability".

One example of the simulation-based method is demonstrated in [45]. The resilience metrics are used for cost analysis of resilience improvement. Based on the resilience metrics, the widely used IEEE 118 bus test case is utilized to analyze the resilience of an existing system as a resilience baseline and compare with possible investment portfolios to optimize the investments for resilience enhancement at a given fixed budget. Another example is in [48], where the power flow analysis and resilience metrics are exploited to compare the ratio and area between the desired performance and real performance of the power system. In addition, [49] uses the failure probability (vulnerability) of transmission lines as the metric of the real-time operational resilience under both extreme weather and loading conditions.

The statistical analysis is applied to the system that has collected historical natural hazard data. In [50], the duration of the unexpected interruption caused by the distribution system failure is employed as a metric of the resilience and the analysis is based on the historical data of the outage duration in the City of Phoenix, Arizona between 2002 and 2005. Another example is exemplified in [51], where the rapidity of restoration is a metric of the system resilience and the historical data of power delivery and telecommunications is utilized which was gathered after the landfall of Hurricane Katrina.

A basic representation of the resilience metric is proposed in [52], as presented in the following equation:

$$R_i(S_p, F_r, F_d, F_o) = S_p \frac{F_r}{F_o} \frac{F_d}{F_o}$$

where S_p is the speed recovery factor, F_o is the original stable level of system performance,

F_d is the performance level forthwith the disturbance, F_r is the performance at a new stable level after the recovery efforts have been depleted. This metric contains the resilience capabilities and the recovery time.

While the definitions and metrics of resilience are not in consensus and widely used, the traditional reliability indices, the loss of load frequency (LOLF) and loss of load expectation (LOLE) is used as resilience metric to assess and compare different strategies for system resilience improvement in [53].

Four metrics of resilience, similar to but somewhat different from the main features addressed by NIAC in [31], are proposed by Kwasinski in 2016 in [54] as demonstrated in Figure 1.4:

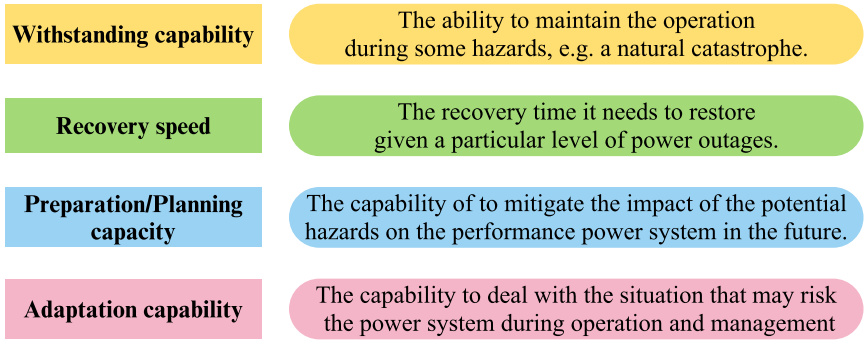

Figure 1.4: Resilience metrics by Kwasinski [54]

The Grid Modernization Laboratory Consortium (GMLC) supported by the Department of Energy (DOE) proposed example resilience metrics in [55], as presented in Table 1.3.

The GMLC metrics analysis highlighted the incorporation of statistical measures of uncertainty (e.g. the affected customers' types and the path of a hurricane) and the reporting of resilience metrics while all impacts are estimated as probability distributions [13].

Another quantitative metric system called the ΦΛΕΠ resilience metric system is proposed in [34] to evaluate the resilience level of a system, as presented in Table 1.4.

To be specific, the metrics refer to how fast and how low resilience drops in the event progress state, how extensive the post-event degraded state is, and how promptly does the network recover in the restorative state.

Table 1.3: Resilience Metrics Proposed by the Grid Modernization Laboratory Consortium of the U.S. Department of Energy (DOE) [55]

Consequence Category	Resilience Metric
Direct	
Electrical Service	Cumulative customer-hours of outages
	Cumulative customer energy demand not served
	Average number (or percentage) of customers experiencing an outage during a specified time period
Critical Electrical Service	Cumulative critical customer-hours of outages
	Critical customer energy demand not served
	Average number (or percentage) of critical loads that experience an outage
Restoration	Time to recovery
	Cost of recovery
Monetary	Loss of utility revenue
	Cost of grid damages (e.g., repair or replace lines, transformers)
	Cost of recovery
	Avoided outage cost
Indirect	
Community Function	Critical services without power (e.g., hospitals, fire stations, police stations)
	Critical services without power for more than N hours (where backup power exists by outage exceeds fuel supply, i.e., $N >$ hours of backup fuel requirement)
Monetary	Loss of assets and perishables
	Business interruption costs
	Impact on Gross Municipal Product (GMP) or Gross Regional Product (GRP)
Other critical assets	Key production facilities without power
	Key military facilities without power

Table 1.4: the ΦΛΕΠ Resilience Metric System [34]

Phase	**State**	**Resilience metric**	**Symbol**
I	Disturbance progress	How *fast* resilience drops? How *low* resilience drops?	Φ Λ
II	Post-disturbance degraded	How *extensive* is the post-disturbance degraded state?	E
III	Restorative	How *promptly* does the network recover?	Π

1.4 Thesis Outline

The remainder of the thesis is organized as follows. **Chapter 2** reviews several applications in the past work and literature to enhance the power system resilience in two aspects: long-term structural resilience and short-term operational resilience. The related applications for long-term structural resilience include the deployment of battery storage and photovoltaic (PV) generation. The related application for short-term operational resilience contains mobile power sources, microgrid operation and control, and the use of remote-controlled

switches.

Chapter 3 explores the potential of mobile power sources in promoting the post-disaster restoration of the distribution system (DS) and consequently improving the system resilience. The DS reconfiguration is also taken into account to help deliver the power via changing the connection status of the distribution branches equipped with remote-controlled switches (RCSs). A mixed-integer nonlinear programming (MINLP) optimization model is proposed for deriving the MPS routing and scheduling strategy under a certain repair plan. The formulation is further linearized, hence the complexity of computation decreases. Three case studies are applied to verify the efficacy of the proposed MPS dispatch method.

Chapter 4 investigates the impact of the PV generation existing in the DS on the proposed MPS dispatch method and the potential of coordinating the proposed method with the existing PV generation to boost the DS post-disaster restoration. The same damage scenarios and repair strategies as in Chapter 3 are employed to compare the effectiveness of the proposed method in the cases with and without the PV generation.

In **Chapter 5**, the same test system and damage scenarios are applied in the case studies with different repair plans to explore the effect of the repair strategies on the contribution of the proposed MPS dispatch method and the PV generation to facilitating the DS restoration following natural hazards and emergency events.

Chapter 6 presents the research conclusions and summarizes the main findings of this thesis. Future work is also provided in this chapter.

Chapter 2: Literature Review

2.1 Introduction

Resilience is characterized as a function of time, thus power system resilience can be divided into two categories: long-term resilience and short-term resilience. This chapter investigates the previous research that focused on the system resilience, both long-term and short-term.

Long-term resilience is generally focusing on the grid structural resilience, which refers to the adaptability of the system infrastructure in the face of new hazards and changing situations [53]. It, hence, relates to planning and design of the power system and a long-term decision paradigm. Although the power system has a long history of planning, the planning and design efforts in the past decades have mainly focused on the improvements in the power system reliability, to be specific, aiming at optimizing the operations (e.g. saving the operating cost) during normal operating conditions and at the same time withstanding the credible events that have been repeatedly confronted by the operators. However, the planning and design for resilience are distinct, which virtually involve all aspects of the power system. The design of the system needs a holistic view, both considering the resilience of the individual components in the grid and the resilience of the entire power system grid-scale. Typically, the enhancement of the component reliability can lead to improvements in the system resilience [13], while the improvements in the component and infrastructure may be a medium-term and long-term effort (e.g., preventive maintenance plans) which may not be accomplished in a short time frame [56–77].

On the contrary, short-term resilience, essentially the operational resilience, typically refers to the ability of the system to control the damage, mitigate the impacts, maintain the electricity service and restore the service to the affect customers via taking the full advantage of the existing and available electric assets when the hazards or catastrophe occur. It involves some characteristics that a resilient power system has before (e.g. robustness/resistance),

during (e.g. resourcefulness/redundancy), and after (e.g. recovery) a hazard or interruption event, as illustrated in Figure 1.3 in Section 1.2. The efficacy of the preventive and corrective measures for system restoration, such as the correct discernment and understanding of the collected information and data, the problem addressing, recognition of the available flexible resources, the priority of measures, determination of the most suitable measures, essentially rely on the capability of the system operators who develop the restoration strategies [35–38, 53, 78–83].

2.2 Research and Applications in Enhancing Long-Term Power System Resilience

Power system resilience can be enhanced by exploiting several advanced technologies and flexible energy resources. One example of advanced technology in the modern power grid is battery storage. Compared with the conventional generator, battery storage devices can store the energy when the system load is low and supply power when the system load is high or emergencies occur, rendering several advantage of rapid response, high efficiency, and low maintenance costs. Deploying battery storage devices enables the power grid to have more operational flexibility. In [84], a resilience-oriented framework for deploying battery energy storage systems (BESSs) in the power distribution system (DS) to enhance the system resilience against high-impact low-probability (HILP) events is proposed. In this work, the earthquake disasters are characterized; afterward, a mechanism for DS vulnerability evaluation and a methodology for finding the optimal location and capacity of BESS units are presented to assist the system planners and decision makers to allocate BESSs in DS, aiming at hardening the system robustness. Besides the battery energy storage system, photovoltaic (PV) generation is another promising solution as a distributed energy resource (DER) in the grid and can be utilized during hazards, though attributed with the disadvantage of variable power output due to its uncertainty [1]. A scheme for system resilience improvement via a multi-objective optimization model is proposed in [85] for finding the optimal capacity and allocated location of PV generation and battery storage so that PV generation and battery

storage can be more accessible for both the load and non-black-start (NB-S) generating units during extreme HILP events.

Deploying dedicated fiber-optic communication networks and sectionalizing switches used for isolation of damaged components is beneficial to DS resilience while the DS network can be reconfigured automatically to mitigate the impact of the faults. One example of such advanced DS mechanisms is established by Chattanooga Electric Power Board (EPB), which is one of the largest publicly owned electric power providers in the U.S, with $111 million funding from the Department of Energy (DOE) via the Smart Grid Investment Grant program. Smart grid technology was applied to the DS to improve its robustness via deploying a dedicated fiber-optics communication system, advanced metering infrastructure, smart distribution switches, and other facilities to realize an effective restoration automatically. The worth and the effectiveness of deploying the distribution automation technology were verified when thousands of hours of outage time were avoided thanks to smart switches while 250 times inefficient repair crew dispatches were avoid due to the outage information provided by smart switches and advanced analytics for post-disaster analysis [86–92]. Meanwhile, the fiber-optic system provides a basis for the technologies that required significant high data exchange rates, e.g. phasor measurement units (PMUs), a device used to estimate the magnitude and phase angle of the voltage or current in the grid [93–101].

2.3 Research and Applications in Enhancing Short-Term Power System Resilience

Mobile power sources (MPSs), including truck-mounted mobile emergency generators (MEGs), truck-mounted mobile energy storage systems (MESSs) and electric vehicles (EVs) have great potentials to be employed as grid-support resources during power grid emergency operating conditions to supply the critical loads and enhance the resilience of distribution system (DS) via a swift disaster restoration. Additionally, power distribution system resilience to HILP events can be elevated by holistic planning, operation, and control

of microgrids in which critical loads can be supplied during emergencies [102, 103]. Due to the evolving battery technology and the increasing demand for a more resilient power system, the application of MPS and microgrid recently has been more and more focused.

2.3.1 Application of Microgrid in Enhancing Power System Resilience

A microgrid is defined as "an energy system consisting of distributed generation, demand management, and other DERs that can connect and disconnect from the bulk power system based on operating conditions" [13]. Microgrids, as the physical islands (PI) in a local area, can be formed by exploiting DERs to provide continuous power supply to electric utilities and customers after a fault. In [104], a real-time operational approach is proposed to form multiple microgrids energized by distributed generation (DG) in the radial DS, aiming at restoring critical loads from the power outages via a mixed-integer linear programming (MILP) optimization model. In [105], microgrids are formed by DG and mobile generator to serve the local demand in a given portion of the grid during the restoration after a fault occurs and the improvement of reliability is verified by a reduced energy not supplied (ENS). A methodology for minimizing the operation costs in normal operating condition and provide power supply to the affected customers in outage areas are studied in [106] by scheduling the output of the controllable DGs and energy storage systems and optimally-sectionalized DS into self-supplied microgrid via stochastic formulations. A hierarchical control strategy is proposed in [107] to apply to an existing direct current (DC) microgrid in the Illinois Institute of Technology (IIT) to improve the economics and resilience of the DC microgrid. A resilience-oriented microgrid optimal scheduling model is presented in [108] aiming at minimizing the microgrid load curtailment by scheduling available resources when the main grid is inaccessible in a prolonged outage duration, considering the uncertainties of load demand, generation and the time and duration of the main grid supply interruption. In this work, the problem is decomposed to normal operation (when the main grid could supply the microgrid) and resilience operation (when the main grid power is not available) and efforts

were proposed to improve the operational resilience by regulating the unit commitments, energy storage schedules, and loads schedules. Microgrid as an efficient mechanism to supply the critical loads during emergencies is studied in [109]. In this work, the restoration problem is transformed to a maximum coverage problem in a form of linear integer program by introducing the concepts of restoration tree and load group, considering DERs' dynamic performance. The DERs, however, are typically deployed at fixed locations across the grid and thus are only able to support the local load points within a PI and maybe some in neighboring PIs, but certainly not the demanded loads in further-away PIs [46, 110].

2.3.2 Application of Mobile Power Sources in Enhancing Power System Resilience

Comparing with stationary microgrids with fixed-location DERs and stationary battery storage systems, mobile power sources (MPSs) which include mobile emergency generators (MEGs), electric vehicles (EVs), and truck-mounted mobile energy storage systems (MESSs) offer greater advantages to boost the DS resilience primarily driven by their mobility [111–115]. The application of MPSs for enhanced resilience of DS has been studied in several research efforts [116–118].

The investment in MESSs in radial DS to reduce the cost in normal operations and relocation of MESSs under HILP events (e.g., natural disasters) to improve the power grid resilience are studied in [119], where the proposed optimization is a two-stage stochastic mixed-integer second order conic program (MISOCP) with binary decision variables representing the relocation of MESSs. This work also compares the results of the cases with and without stationary energy storage units. In [120], aiming at minimizing the post-disaster restoration cost, the coordination of MESS and DS network reconfiguration for forming microgrids is formulated as a MILP model to facilitate critical loads service restoration. MESSs can transfer the energy among multiple microgrids in the DS by traveling to and locating at different locations in proper time. The utilization of plug-in EVs in a microgrid is investigated in [111–115, 121] to improve the voltage profile and reduce the power loss

of the microgrid that incorporates plug-in EVs, renewable energy sources, energy storage system and DG. In the model presented in [121], the uncertainty of the renewable energy sources is formulated by a stochastic optimization approach while the power loss can be significantly reduced with plug-in EVs that can charge (or discharge) active power and/or absorb (or inject) reactive power. Proactive preparedness prior to an imminent hurricane is investigated in [122], including the allocation of generation resources (i.e. diesel oil, electric batteries, and electric buses) in the system that incorporates distributed generators, microgrids, charging stations and critical loads, considering resource transportation cost, initial distribution of electric buses and severity of the expected hurricane. Due to the uncertainty of the damage caused by the hurricane, the allocation problem is formulated as a mixed-integer stochastic nonlinear program, which is further simplified into a MILP problem by a proposed heuristic method. EVs can be charged to store energy not only to meet its own transportation requirements, but also as an emergency power source to supply electricity to critical loads during emergencies. The impact of the vehicle to grid (V2G) service both on the individual EV and the power system operation is studied in [123] where EVs can act as generation sources and/or as responsive loads according to the power system operating states. Additionally, the result shows the cost of the vehicle owners can be reduced and the impact of EVs on the grid is insignificant regarding power loss and voltage regulation. An algorithm for Vehicle-to-Home (V2H) technology, as a simplified variation of the vehicle-to-Grid (V2G) mechanism, is proposed in [124], using electric vehicles as backup power sources to support the end customers during grid interruptions, with the objective of maximizing the backup energy duration. Multiple homes, electric vehicles and photovoltaic generation are considered in this work, though the electric network constraints are not considered. The pre-positioning and real-time allocation of MEG are studied in [125] by two-stage dispatch framework, aiming at minimizing the outage duration of loads considering loads' priorities, demand sizes, and MEG routing problem. The problem is formulated as a scenario-based two-stage stochastic optimization problem, where the first

stage is to find the optimal pre-positioning location of the MEGs ahead of a natural disaster while the second stage real-time dispatches MEGs from the pre-positioning location to some portion of the network to restore critical loads by forming microgrids.

Furthermore, following a HILP hazard, the configuration of the DS may change due to the unavailability of some distribution branches and other elements. DS network reconfiguration plays a significant role in rerouting and delivering the power from MPSs to critical loads by switching some branches on and off and maintain the radial network topology. The distribution branches can be equipped with remote-controlled switches (RCS) that facilitate a network reconfiguration for the dynamic formation of the microgrid as emergency operating conditions unfold. Several models of DS network reconfiguration have been studied. The distribution system reconfiguration is formulated in [126] by three new convex models, which are mixed-integer quadratic programming, mixed-integer quadratically constrained programming model and mixed-integer second-order cone programming. In [127], a heuristic nonlinear constructive algorithm for DS reconfiguration is presented with more computation time but higher accuracy. In [128], a DS reconfiguration methodology based on the Ant Colony Algorithm (ACA) is proposed with an objective of reaching the minimum power loss and better load balancing in a radial DS considering the existence of DGs. The meta heuristic Harmony Search Algorithm (HSA) is used in [129] for DS network reconfiguration and finding the optimal location of DG units to minimizing the real power loss and boost voltage profile in DS. In [2, 78–83], the network reconfiguration at transmission level is employed as temporarily corrective tool for load restoration in coping with the predicted hazards as well as in normal operating conditions for economic gains and financial benefits.

Chapter 3: Mobile Power Sources Dispatch Coordinating With Distribution System Reconfiguration for Post-Disaster Restoration

3.1 Introduction

In this chapter, in order to improve the power system operational resilience, the potential of mobile power sources (MPSs) for the distribution system (DS) restoration after natural disaster strikes is investigated. Meanwhile, due to the unavailability of some distribution branches and in order to reroute and deliver the power from MPSs to critical loads, the DS network reconfiguration is also taken into account to enable the formation of dynamic microgrids by switching some branches on and off during the restoration process.

The rest of this chapter is organized as follows. First, a simple illustrative diagram is presented which demonstrates the process of post-disaster restoration assisted by the MPS dispatch. Afterward, a mixed-integer nonlinear programming (MINLP) model is proposed for routing and scheduling of MPSs coordinated with the DS network reconfiguration to improve the DS resilience against the natural hazards. The MINLP model is further linearized into a mixed-integer linear programming (MILP) model to decrease the computation complexity. Multiple types of MPSs, e.g., truck-mounted mobile emergency generators (MEGs), truck-mounted mobile energy storage systems (MESSs) and electric vehicle (EV) fleets, are dispatched considering the repair schedules of the damaged branches to facilitate the DS restoration process. Eventually, case studies of three different damage scenario and their numerical results are presented to describe how the DS restoration is facilitated with the routing and scheduling of MPSs coordinated with DS reconfiguration.

3.2 Proposed Framework for Power Grid Restoration via Routing and Scheduling of MPSs Coordinated With DS Reconfiguration

Based on Figure 3.1, the unavailability of some distribution branches following a HILP event results in a number of physical islands (PIs) in which some or all load points are disconnected from the main grid. The optimal scheduling and routing of MPS can be achieved via the proposed optimization formulation with the aim of enhancing the DS resilience. Having identified the damaged branches in Stage I, the MPS can be moved to other PIs in which some portions of critical loads can be recovered by the excessive power provided by MPS, while the branches equipped with remote-controlled switches (RCS) can open or close for optimal power delivery. Meanwhile, the other damaged branches are repaired by repair crews and this loop is repeated until all damaged branches are repaired and all load points are supplied by the main grid. The system is then fully restored and the DS resilience function reaches its maximum.

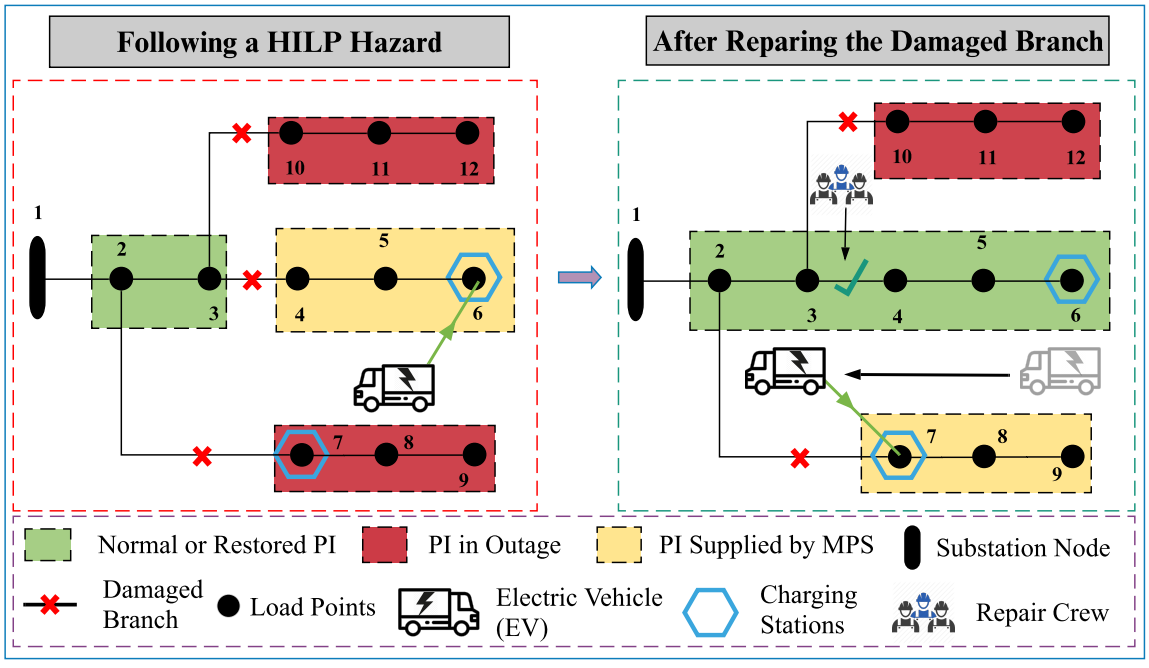

Figure 3.1: Simple illustrative diagram of MPSs' assistance on enhancing resilience

3.3 Formulation

This section presents a model for routing and scheduling of mobile power sources (MPSs) coordinated with the distribution system (DS) reconfiguration. In this model, three types of MPS are considered, including truck-mounted mobile emergency generators (MEGs), truck-mounted mobile energy storage systems (MESSs) and electric vehicle (EV) fleets. Meantime, the DS reconfiguration is also considered (i.e. switching the distribution lines on and off) to help deliver the power from MPSs and substation (if available). Thus, the objective function is aimed at maximizing the total loads supplied considering their priorities and minimizing the total cost produced by the MPSs including the transportation cost of the MPSs, battery degradation cost, and the cost of power generation of MEGs. Motivated by [118], the extended objective function (3.1) includes four terms, as follows:

$$\begin{aligned}\max\Big(&\sum_{t\in\mathbf{T}}\sum_{i\in\mathbf{B}}\chi_i\cdot pd_{i,t}-\sum_{t\in\mathbf{T}}\sum_{m\in\mathbf{M}}C_m^{\mathrm{tr}}\cdot\varphi_{m,t}-\\&\sum_{t\in\mathbf{T}}\sum_{m\in\{\mathbf{S},\mathbf{V}\}}C_m^{\mathrm{P}}\cdot(p_{m,t}^{\mathrm{ch}}+p_{m,t}^{\mathrm{dch}})-\sum_{t\in\mathbf{T}}\sum_{m\in\mathbf{G}}\delta_m\cdot p_{m,t}\Big)\end{aligned}\tag{3.1}$$

The first term is the total loads supplied weighted by the priority of the load points χ_i, i.e. the weighted sum of supplied loads, over the entire restoration time period $\mathbf{T}$; the second term is the transportation cost of MPSs, due to the trips they make during the restoration phase; the third term reflects the cost of battery degradation of EV fleets and MESSs when charging and discharging during the restoration process; and the last term is the relative cost of the MEG outputs. The second term is added to minimize the traveling time of MPSs to avoid unnecessary transportation since the MPSs should not travel around once all loads are restored. Meanwhile, if there may exist various MPS dispatch strategies that can achieve the same restoration result, the strategy achieving the optimal result with the MPSs with the minimum transportation costs will be selected. The transportation cost coefficient

C_m^{tr} of MPS m is a constant representing the relative transportation cost of each MPS. The third term is aimed to reduce the battery degradation cost so that the redundant charging and discharging are avoided during the restoration phase. The MEGs consume the fuel to generate power and provide the energy for transporting themselves. The last term is added to minimize the cost associated with the power output of MEGs so that the unnecessary real power output from MEGs is reduced. Additionally, if there are multiple MEGs with different generation cost (represented by δ_m) available for dispatch, the strategy using the MEGs with lower generation cost to generate power is selected. Note that in general the objective of maximizing the loads supplied is dominant.

Along with the objective function, a number of constraints need to be taken into account for the DS restoration problem as follows.

- ***MPS Connection Constraints:*** Following a HILP disaster, the MPSs rapidly travel and get connected in the PIs to supply electricity where needed. Since the MPSs need associated facilities to connect to the grid, the load points equipped with corresponding connecting facilities can be set as the candidate nodes of MPSs. At each time period, each MPS can be connected to at most one pre-determined candidate node, as enforced in (3.2). MPSs cannot connect to the load points that are not equipped with associated facilities, as stated in constraint (3.3). Constraint (3.4) indicates that the allowed number of MPSs connected to a node is limited to stations' capacity at each candidate node. Constraint (3.5) states that the MPSs cannot travel to other nodes when connected to a candidate node.

$$\sum_{i \in \mathbf{B}_m} \mu_{m,i,t} \leq 1, \ \forall m \in \mathbf{M}, \forall t \in \mathbf{T} \tag{3.2}$$

$$\sum_{i \in \mathbf{B} \setminus \mathbf{B}_m} \mu_{m,i,t} = 0, \ \forall m \in \mathbf{M}, \forall t \in \mathbf{T} \tag{3.3}$$

$$\sum_{m \in \mathbf{M}_i} \mu_{m,i,t} \leq N_i^{\text{mps}}, \ \forall i \in \bigcup_{m \in \mathbf{M}} \mathbf{B}_m, \forall t \in \mathbf{T} \tag{3.4}$$

$$\varphi_{m,t} = 1 - \sum_{i \in \mathbf{B}_m} \mu_{m,i,t},\ \forall m \in \mathbf{M}, \forall t \in \mathbf{T} \tag{3.5}$$

- ***MPS Routing Constraints:*** Constraint (3.6) ensures that the MPSs transportation among different DS nodes satisfies the required travel time, where $T^{\text{travel}}_{m,ij}$ denotes the required traveling time of MPS m between node i and node j

$$\mu_{m,i,t+\tau} + \mu_{m,j,t} \leq 1, \forall m \in \mathbf{M},\ \forall i, j \in \mathbf{B}_m,\ \forall \tau \leq T^{\text{travel}}_{m,ij},\ \forall t + \tau \leq N_{\mathbf{T}} \tag{3.6}$$

  For better understanding, constraint (3.6) is explained with a simple example presented as follows. Assume that the MPS m needs 2 time periods to travel between node i and node j, i.e. $T^{\text{travel}}_{m,ij} = 2$; then the following constraints are restricted:

$$\mu_{m,i,t+1} + \mu_{m,j,t} \leq 1,\ \forall t + 1 \leq N_{\mathbf{T}} \tag{3.7}$$

$$\mu_{m,i,t+2} + \mu_{m,j,t} \leq 1,\ \forall t + 2 \leq N_{\mathbf{T}} \tag{3.8}$$

  Then, as Equations (3.7) and (3.8) show, if $\mu_{m,j,t} = 1$ (MPS m is connecting to node j at time t), then $\mu_{m,i,t+1} = 0 = \mu_{m,i,t+2} = 0$ (MPS m cannot be connected to node i at time $t+1$ and $t+2$ since it takes 2 time periods to travel from node j to node i).

- ***MPS Power Scheduling Constraints:*** It is assumed that the truck-mounted MESSs and MEGs consume the fuel for their transportation and the MEGs can be refueled with tanker truck during the restoration process [130] while EV fleets consume electric energy when they are in transport. The change in the state of charge (SOC) of MESSs over time is determined by their charging and discharging behaviors, as represented in (3.9) while the SOC of EV fleets is determined by their charging and discharging as well as travel behaviors as stated in (3.10). Constraint (3.11) restricts the ranges of SOC of MESSs and EV fleets over all time periods. Constraint (3.12) and (3.13) respectively restrict the ranges of charging and discharging power for MESSs and EV

fleets according to the corresponding rated power. Charging and discharging of MESS and EV are mutually exclusive over all time periods, as represented in (3.14) which also indicates that the MPS disconnected from DS can neither charge nor discharge. Constraint (3.15) and (3.16) set the range of real and reactive power output of MEG according to its rated power, respectively, and enforce MEG to have zero real and reactive output when it is disconnected from the DS.

$$\mathrm{SOC}_{m,t} = \mathrm{SOC}_{m,t-1} + (\eta_m^{\mathrm{ch}} \cdot p_{m,t}^{\mathrm{ch}} - p_{m,t}^{\mathrm{dch}} / \eta_m^{\mathrm{dch}}) \cdot \Delta t, \forall m \in \mathbf{S},\ \forall t \geq 1 \tag{3.9}$$

$$\mathrm{SOC}_{m,t} = \mathrm{SOC}_{m,t-1} + (\eta_m^{\mathrm{ch}} \cdot p_{m,t}^{\mathrm{ch}} - p_{m,t}^{\mathrm{dch}} / \eta_m^{\mathrm{dch}} - \varphi_{m,t} \cdot P_m^{\mathrm{travel}}) \cdot \Delta t,\ \forall m \in \mathbf{V},\ \forall t \geq 1 \tag{3.10}$$

$$\underline{\mathrm{SOC}}_m \leq \mathrm{SOC}_{m,t} \leq \overline{\mathrm{SOC}}_m, \forall m \in \{\mathbf{S}, \mathbf{V}\}, \forall t \in \mathbf{T} \tag{3.11}$$

$$0 \leq p_{m,t}^{\mathrm{ch}} \leq c_{m,t} \cdot \overline{P}_m^{\mathrm{ch}}, \forall m \in \{\mathbf{S}, \mathbf{V}\}, \forall t \in \mathbf{T} \tag{3.12}$$

$$0 \leq p_{m,t}^{\mathrm{dch}} \leq d_{m,t} \cdot \overline{P}_m^{\mathrm{dch}}, \forall m \in \{\mathbf{S}, \mathbf{V}\}, \forall t \in \mathbf{T} \tag{3.13}$$

$$c_{m,t} + d_{m,t} \leq \sum_{i \in \mathbf{B}_m} \mu_{m,i,t}, \forall m \in \{\mathbf{S}, \mathbf{V}\}, \forall t \in \mathbf{T} \tag{3.14}$$

$$0 \leq p_{m,t} \leq \sum_{i \in \mathbf{B}_m} \mu_{m,i,t} \cdot \overline{P}_m, \forall m \in \mathbf{G}, \forall t \in \mathbf{T} \tag{3.15}$$

$$0 \leq q_{m,t} \leq \sum_{i \in \mathbf{B}_m} \mu_{m,i,t} \cdot \overline{Q}_m, \forall m \in \mathbf{G}, \forall t \in \mathbf{T} \tag{3.16}$$

- ***DS Radiality Constraints:*** For the radiality of a system consists of n nodes (buses), there are two conditions which need to be satisfied [131]: (i) in the system, the number of connected branches (lines) is equal to $n-1$; (ii) all load nodes are connected to the source node (equivalent to all are connected).When some branches in the system are damaged, several physical islands (PIs) are formed. The radiality requirements

remain to be satisfied for each PI resulted from the damaged branches, since each PI can be regarded as a subsystem consisted of some numbers of nodes. Therefore, in such scenarios, the two conditions which need to be satisfied for the radiality of the entire system become: (1) at each PI, the number of connected branches is equal to the total number of nodes in the PI - 1; (2) all load points are connected to a determined source node in each PI.

Assume that the total number of nodes in the system is $N_{\mathbf{B}}$, and the number of PI resulted from the damaged branches is N, the number of nodes in the k-th PI is n_k. Then the condition (1) is represented as follows:

$$\text{the number of closed branches in the k-th PI} = n_k - 1 \tag{3.17}$$

If the sum over equation (3.17) up for all PI, equation (3.18) is derived.

$$\text{the number of closed branches in the whole system} = \sum_{k=1}^{N} n_k - N \tag{3.18}$$

Since $\sum_{k=1}^{N} n_k = N_{\mathbf{B}}$, constraint (3.19) is derived and satisfies the first condition.

$$\sum_{(i,j)\in\mathbf{L}} \alpha_{ij,t} = N_{\mathbf{B}} - N_t^{\text{island}}, \quad \forall t \in \mathbf{T} \tag{3.19}$$

As for the second condition, for better illustration, the IEEE 33-node test system is used as presented in Figure 3.2. The original 33-node DS is radial and all load points are connected to the substation node as the source node. When a HILP natural disaster strikes and some branches in the DS are damaged, six PIs are formed. Some PIs that are isolated from the main grid only contain load nodes and no energy source. In each PI, one node is considered as a fictitious source node (notice that this node does not need to actually supply power to other nodes) and the remaining nodes are fictitious

load points. The fictitious source node and fictitious load nodes are the source and the destination of fictitious power flow, respectively. The amount of the fictitious flow into a load node $d^{\text{fic}}_{i,t}$ is set as 1 at all nodes. Since the fictitious flows can only be provided by the fictitious source node, the second condition is satisfied in constraint (3.20)-(3.22) that enforce each load node to receive one unit of the fictitious flow from the fictitious source node at each PI.

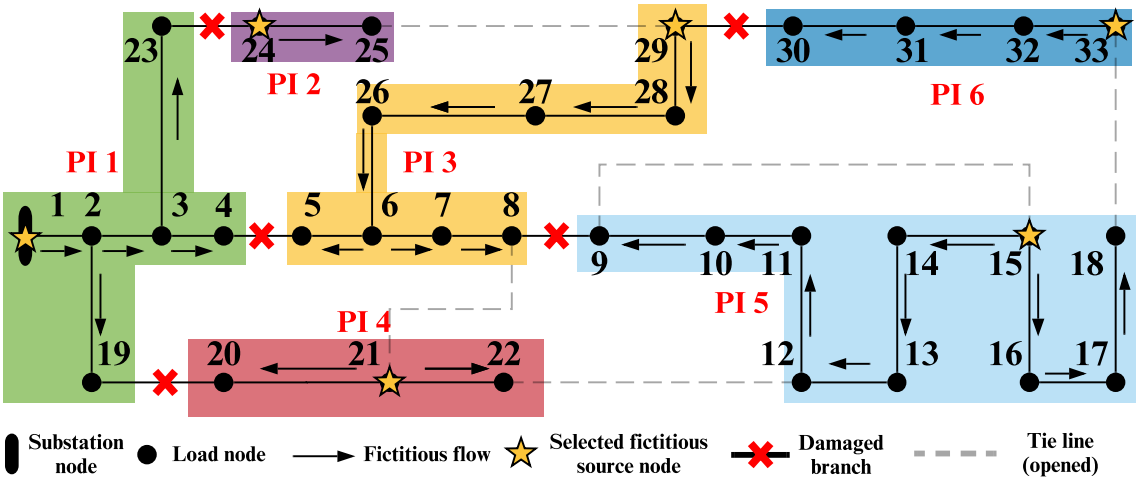

Figure 3.2: Illustrative example for distribution system (DS) radility requirements

Constraints (3.20)-(3.21) ensure the fictitious flow balance for the fictitious load and source nodes, respectively. Constraint (3.22) enforces the fictitious flow to be zero in open branches. The large enough positive number M relaxes this constraint when some branches are open (See [131] for additional details on the fictitious network and radiality conditions). Finally, constraints (3.19)-(3.22) ensure that the DS remains radial over all time periods.

$$\sum_{(j,i)\in\mathbf{L}} fl_{ji,t} - \sum_{(i,j)\in\mathbf{L}} fl_{ij,t} = d^{\text{fic}}_{i,t}, \quad \forall i \in \mathbf{B}\backslash\mathbf{B}^{\text{source}}_{t}, \forall t \in \mathbf{T} \tag{3.20}$$

$$\sum_{(i,j)\in\mathbf{L}} fl_{ij,t} - \sum_{(j,i)\in\mathbf{L}} fl_{ji,t} = fg_{i,t}, \quad \forall i \in \mathbf{B}^{\text{source}}_{t}, \forall t \in \mathbf{T} \tag{3.21}$$

$$-\alpha_{ij,t} \cdot M \leq fl_{ij,t} \leq \alpha_{ij,t} \cdot M, \quad \forall (i,j) \in \mathbf{L}, \forall t \in \mathbf{T} \tag{3.22}$$

- ***Branch Status Constraints:*** According to (3.23), the damaged branch must be open if it has not yet been repaired at time t. Constraint (3.24) states that the undamaged branches that are not equipped with remote-controlled switches (RCS) remain in their initial status over all time periods.

$$\alpha_{ij,t} \leq \beta_{ij,t}, \quad \forall (i,j) \in \mathbf{L},\ \forall t \in \mathbf{T} \tag{3.23}$$

$$\alpha_{ij,t} = \alpha^{0}_{ij}, \quad \forall (i,j) \in \mathbf{L} \backslash \{\mathbf{L}^{\text{damaged}}_{t}, \mathbf{L}^{\text{switch}}\},\ \forall t \in \mathbf{T} \tag{3.24}$$

- ***MPS Power Output Constraints:*** Constraints (3.25)-(3.26) indicate that the real or reactive power injection or extraction at a candidate node for MPS siting is equal to the sum of the real or reactive power output of the MPSs. The non-MPS nodes are attributed zero real and reactive power from MPSs as expressed in (3.27).

$$\begin{aligned} p^{\text{mps}}_{i,t} = & \sum_{m \in \mathbf{M}_i \cap \{\mathbf{S},\mathbf{V}\}} \mu_{m,i,t} \cdot p^{\text{dch}}_{m,t} - \sum_{m \in \mathbf{M}_i \cap \{\mathbf{S},\mathbf{V}\}} \mu_{m,i,t} \cdot p^{\text{ch}}_{m,t} \\ & + \sum_{m \in \mathbf{M}_i \cap \mathbf{G}} \mu_{m,i,t} \cdot p_{m,t}, \quad \forall i \in \bigcup_{m \in \mathbf{M}} \mathbf{B}_m, \forall t \in \mathbf{T} \end{aligned} \tag{3.25}$$

$$q^{\text{mps}}_{i,t} = \sum_{m \in \mathbf{M}_i} \mu_{m,i,t} \cdot q_{m,t}, \quad \forall i \in \bigcup_{m \in \mathbf{M}} \mathbf{B}_m, \forall t \in \mathbf{T} \tag{3.26}$$

$$p^{\text{mps}}_{i,t} = q^{\text{mps}}_{i,t} = 0, \quad \forall i \in \mathbf{B} \backslash \bigcup_{m \in \mathbf{M}} \mathbf{B}_m, \forall t \in \mathbf{T} \tag{3.27}$$

- ***Power Balance Constraints:*** Constraints (3.28)-(3.29) describe the real and reactive power balance conditions at all nodes, respectively. The range of the demanded load to be supplied is bounded in constraint (3.30). Constraint (3.31) enforces the recovery rate of the supplied loads not to decrease. The power factor of the demand is assumed to be fixed in (3.32). The real and reactive power flows in the online branches are respectively limited by their real and reactive power capacities in (3.33)-

(3.34). Constraints (3.33)-(3.34) also enforce the real and reactive power flow in open branches to be zero.

$$\sum_{(j,i)\in\mathbf{L}} pf_{ji,t} - \sum_{(i,j)\in\mathbf{L}} pf_{ij,t} = pd_{i,t} - pg_{i,t} - p_{i,t}^{\text{mps}}, \quad \forall i \in \mathbf{B}, \forall t \in \mathbf{T} \tag{3.28}$$

$$\sum_{(j,i)\in\mathbf{L}} qf_{ji,t} - \sum_{(i,j)\in\mathbf{L}} qf_{ij,t} = qd_{i,t} - qg_{i,t} - q_{i,t}^{\text{mps}}, \quad \forall i \in \mathbf{B}, \forall t \in \mathbf{T} \tag{3.29}$$

$$0 \leq pd_{i,t} \leq P_{i,t}^{\text{demand}}, \forall i \in \mathbf{B}, \ \forall t \in \mathbf{T} \tag{3.30}$$

$$pd_{i,t-1}/P_{i,t-1}^{\text{demand}} \leq pd_{i,t}/P_{i,t}^{\text{demand}}, \forall i \in \mathbf{B}, \ \forall t \geq 1 \tag{3.31}$$

$$qd_{i,t} = (Q_{i,t}^{\text{demand}}/P_{i,t}^{\text{demand}}) \cdot pd_{i,t}, \forall i \in \mathbf{B}, \ \forall t \in \mathbf{T} \tag{3.32}$$

$$-\alpha_{ij,t} \cdot \overline{P}_{ij} \leq pf_{ij,t} \leq \alpha_{ij,t} \cdot \overline{P}_{ij}, \forall (i,j) \in \mathbf{L}, \forall t \in \mathbf{T} \tag{3.33}$$

$$-\alpha_{ij,t} \cdot \overline{Q}_{ij} \leq qf_{ij,t} \leq \alpha_{ij,t} \cdot \overline{Q}_{ij}, \forall (i,j) \in \mathbf{L}, \forall t \in \mathbf{T} \tag{3.34}$$

- ***Power Flow Constraints:*** Based on the DistFlow branch equations in [132], constraint (3.35) and (3.36) represent the power flow equation. The large enough positive number M value is a relaxation parameter to relax these two constraints for open branches. Constraint (3.37) states the boundary for the voltage magnitudes across the network.

$$Vsqr_{i,t} - Vsqr_{j,t} \leq (1-\alpha_{ij,t}) \cdot M + 2 \cdot (r_{ij} \cdot pf_{ij,t} + x_{ij} \cdot qf_{ij,t}), \quad \forall (i,j) \in \mathbf{L}, \forall t \in \mathbf{T} \tag{3.35}$$

$$Vsqr_{i,t} - Vsqr_{j,t} \geq (\alpha_{ij,t}-1) \cdot M + 2 \cdot (r_{ij} \cdot pf_{ij,t} + x_{ij} \cdot qf_{ij,t}), \quad \forall (i,j) \in \mathbf{L}, \forall t \in \mathbf{T} \tag{3.36}$$

$$\underline{\text{Vsqr}}_i \leq Vsqr_{i,t} \leq \overline{\text{Vsqr}}_i, \forall i \in \mathbf{B}, \forall t \in \mathbf{T} \tag{3.37}$$

In summary, the formulation for routing and scheduling of MPSs coordinated with the DS reconfiguration is as follows:

1. Objective Function: Equation (3.1)
2. Constraints: Equation (3.2) - (3.6), equation (3.9) - (3.16), equation (3.19) - (3.37)

Note that constraints (3.25) and (3.26) include non-linear terms in the form that a binary variable (e.g. $\mu_{m,i,t}$) is multiplied by a continuous variable (e.g. $p^{\text{dch}}_{m,t}$). This makes the optimization problem a mixed-integer non-linear programming (MINLP) model with very high computation complexity.

A linearization technique is exploited as illustrated below [133]. For instance, the nonlinear term $\mu_{m,i,t} \cdot p^{\text{dch}}_{m,t}$ can be substituted by $P^{\text{dch}}_{m,i,t}$ and the following constraints are employed:

$$0 \leq P^{\text{dch}}_{m,i,t} \leq \mu_{m,i,t} \cdot \overline{P}^{\text{dch}}_{m} \tag{3.38}$$

$$p^{\text{dch}}_{m,t} + (\mu_{m,i,t} - 1) \cdot \overline{P}^{\text{dch}}_{m} \leq P^{\text{dch}}_{m,i,t} \leq p^{\text{dch}}_{m,t} \tag{3.39}$$

where, if $\mu_{m,i,t} = 1$, then we have $P^{\text{dch}}_{m,i,t} = p^{\text{dch}}_{m,t}$; if $\mu_{m,i,t} = 0$, then $P^{\text{dch}}_{m,i,t} = 0$. The same approach can also applied to the term $\mu_{m,i,t} \cdot p^{\text{ch}}_{m,t}$, $\mu_{m,i,t} \cdot p_{m,t}$ and $\mu_{m,i,t} \cdot q_{m,t}$.

Afterward, the MINLP formulation is linearized into a mixed-integer linear programming (MILP) problem and, therefore, the computation complexity is significantly reduced.

3.4 Case Study: Modified IEEE 33-Node Test System

3.4.1 System Characteristics, Assumptions, and Data

In this section, the proposed method is applied on the modified IEEE 33-node test system which contains one substation node, 37 distribution lines (including 5 tie lines) to verify the method effectiveness. In this thesis, the stations that have grid connection facilities for electric vehicle (EV) fleets are charging stations [134, 135], and the stations that have the grid connection facilities for mobile energy storage systems (MESSs) and mobile emergency generators (MEGs) are designated as the MESS stations [136]. Assume that there are 3 charging stations and 3 MESS stations available in the distribution system (DS), as shown in Figure 3.3. Additionally, 8 remote-controlled switches (RCSs) are allocated [137] as depicted in Figure 3.3. It is assumed that 3 MPSs are available: MESS 1 with 500 kW/776 kWh capacity [138], MEG 1 with 800 kW/600 kVar capacity [139], EV fleet 1 incorporating 2 electric buses with 150 kW/150 kWh capacity [135] and 0.25 kW energy consumption rate for transportation [140]. The tie lines in the DS are normally open. Only the branches equipped with RCS can be switched during the restoration process. The priority of load nodes are randomly generated between 1 and 10, which are lower than the typical interruption cost of various types of customers [141]. The connection status of tie lines are open while the rest branches are closed during normal operation.

All MPSs are located at the substation node and fully charged to prepare for potential emergency events. When the natural hazards or emergency events occur, once the damaged branches are identified as well as the repair plan is proposed, the MPSs will depart from the substation node to supply the critical loads. Three different damage scenarios are considered in this section.

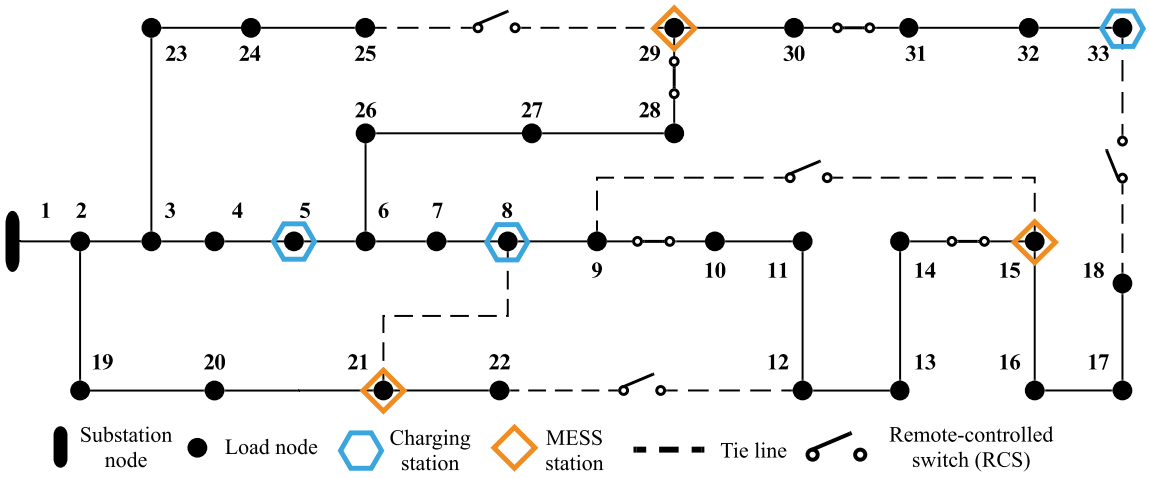

Figure 3.3: The modified IEEE 33-node test system

3.4.2 Case Study 1: Damage Scenario 1

Assume that 9 branches are damaged after the hazard strikes as depicted in Figure 3.4, and the repair plan is adopted as shown in Table 3.1. According to the repair plan, the whole restoration process is set as **T** = 24 time periods while each time period is $\Delta t = 0.5hr$.

Table 3.1: Repair Order of Damaged Branches in Case Study 1

Time period (*t*)	3	6	7	9	13	16	20	22	24
Repaired branch	19-20	8-9	9-10	12-13	16-17	30-31	27-28	24-25	23-24

The strategy of MPSs dynamic dispatch is obtained as presented in Table 3.2. The symbol "→" denotes that the MPS is during transportation. The activity of the branches equipped with RCS is demonstrated in Table 3.3.

Table 3.2: Location of MPSs in Each Time Period in Case Study 1

---		**Time Period**								
		1	**2~3**	**4~7**	**8**	**9~12**	**13~14**	**15**	**16~17**	**18~24**
MPS	**EV 1**	**node 1**	→	**node 33**			→	**node 5**	→	**node 33**
	MESS 1	**node 1**	→	**node 15**	→	**node 29**				
	MEG 1	**node 1**	→	**node 29**						

The recovery rate in each time period is depicted in Figure 3.5. Curves for the case

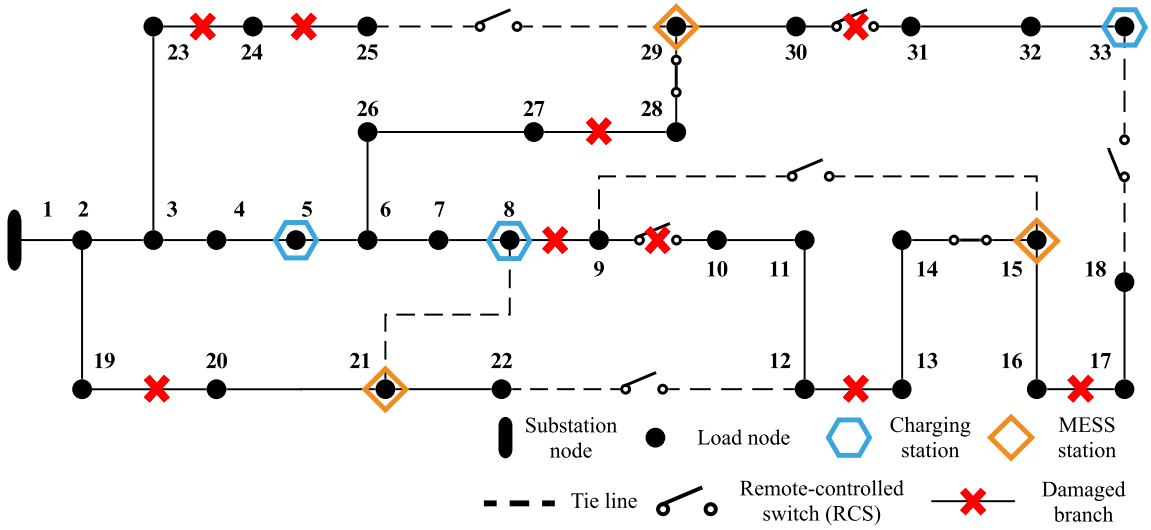

Figure 3.4: Damage scenario in case study 1

Table 3.3: Distribution System (DS) Reconfiguration Actions in Case Study 1

Time period	Remote-controlled switch (RCS) actions
$t = 1$	close branch 9-15, 12-22, 18-33, 25-29
$t = 7$	open branch 12-22, close branch 9-10 (reparied)
$t = 9$	open branch 9-15
$t = 16$	close branch 30-31 (repaired)
$t = 17$	close branch 9-15, open branch 14-15
$t = 20$	open branch 9-15,18-33, close branch 14-15
$t = 24$	open branch 25-29

only using DS reconfiguration method and the benchmark case without any MPS supply and DS reconfiguration are included for comparison. As can be seen in Figure 3.5, without MPS and DS reconfiguration, the benchmark case has the lowest recovery rate over the restoration process. With MPS and DS reconfiguration employed, the proposed method restore the system to 89% at $t = 16$ and to 100% at $t = 22$. To be specific, with MPS and DS reconfiguration, the proposed method achieves a load outage recovery of around 30% higher than the benchmark case at time period $t = 4 \sim 8$ and at least 20% higher than the case with DS reconfiguration alone at $t = 4 \sim 19$.

The curves for the system load demand, SOC of EV fleet 1, SOC of MESS 1, real power output of MEG 1 are demonstrated in Figure 3.6.

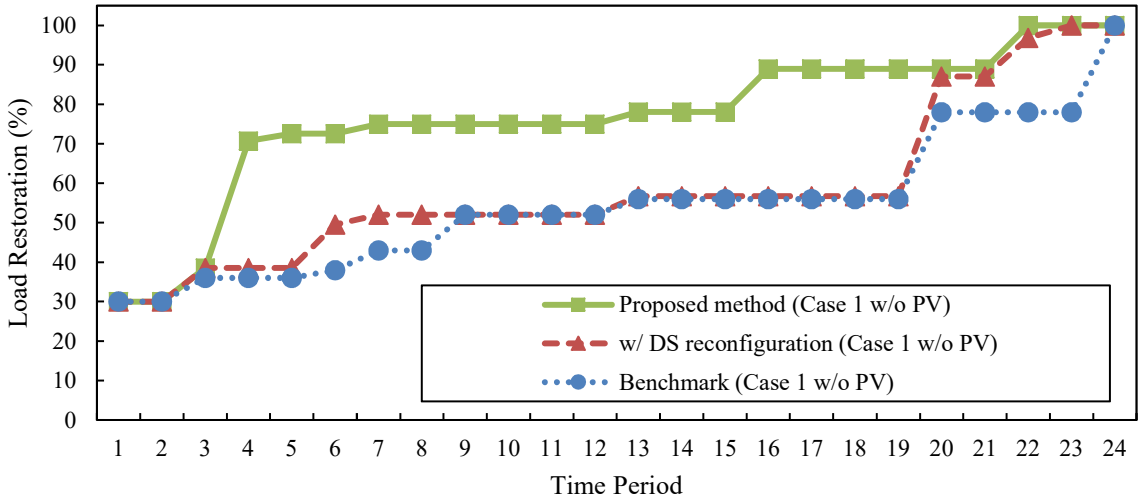

Figure 3.5: Load restoration in each time period using different strategies: Case Study 1

Based on Tables 3.1 to 3.3 and Figures 3.4 and 3.6, the strategy of MPSs dispatch coordinated with the DS reconfiguration attains a better system restoration. Specifically, following a HILP event, all three MPSs should be departed from the substation node at $t = 1$ to supply the critical loads while tie lines 9-15, 12-22, 18-33, and 25-29 which are normally open (i.e., offline) should be closed (i.e., online) in order to change the DS topology such that several PIs can be linked to facilitate the MPSs contribution in recovery of load outages in the subsequent time periods. Note that branch 14-15 and 28-29 are already online during the normal operating conditions, while branches 9-10 and 30-31 are offline due to the post-event damages. Some time periods in the restoration process are illustrated in Figures 3.7 to 3.11. At time $t = 3$, branch 19-20 is repaired by repair crews. At time $t = 4$, EV fleet 1, MESS 1, and MEG 1 are respectively connected to node 33, node 15, and node 29 to supply critical loads. EV fleet 1 supplies node 18 rather than node 33 since node 18 has higher priority. At $t = 9$, branch 8-9, branch 9-10 and branch 12-13 have been repaired at earlier time periods; MESS 1 moves to node 29 and ready to supply the critical loads in the subsequent time periods. MESS 1 recharge itself at $t = 5 \sim 6$ since branch 8-9 is repaired and node 15 is reconnected to the main grid. At $t = 15$, EV fleet 1 travel to node 5 to get charged to supply loads in the following time periods. At $t = 18$, EV fleet 1 transport to node 33 and continue

to supply the critical loads. At $t = 22$, branch 24-25 is repaired, and the DS is fully restored.

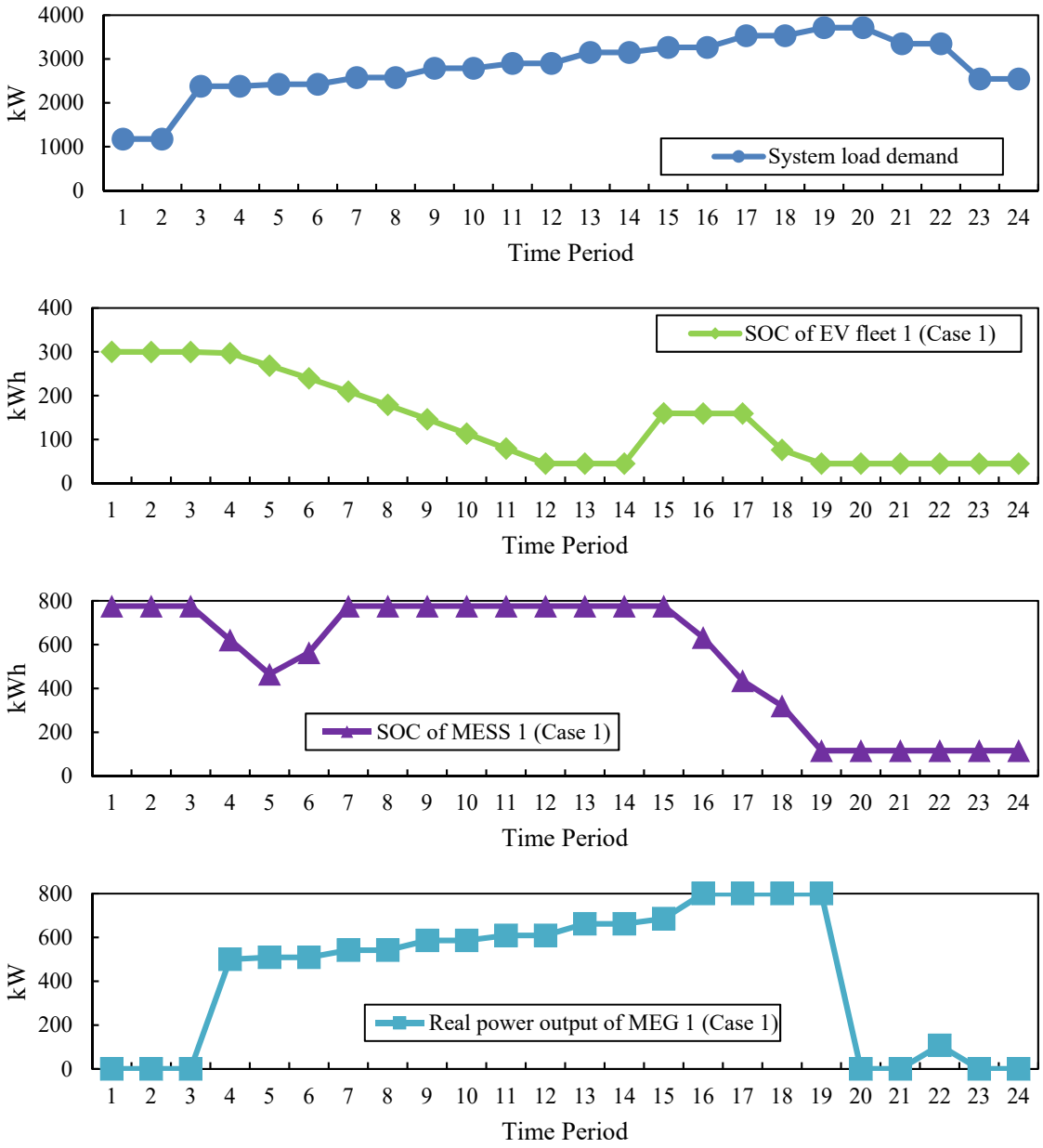

Figure 3.6: SOC of EV fleet 1, SOC of MESS 1, real power output of MEG 1 and system load demand in each time period: Case Study 1

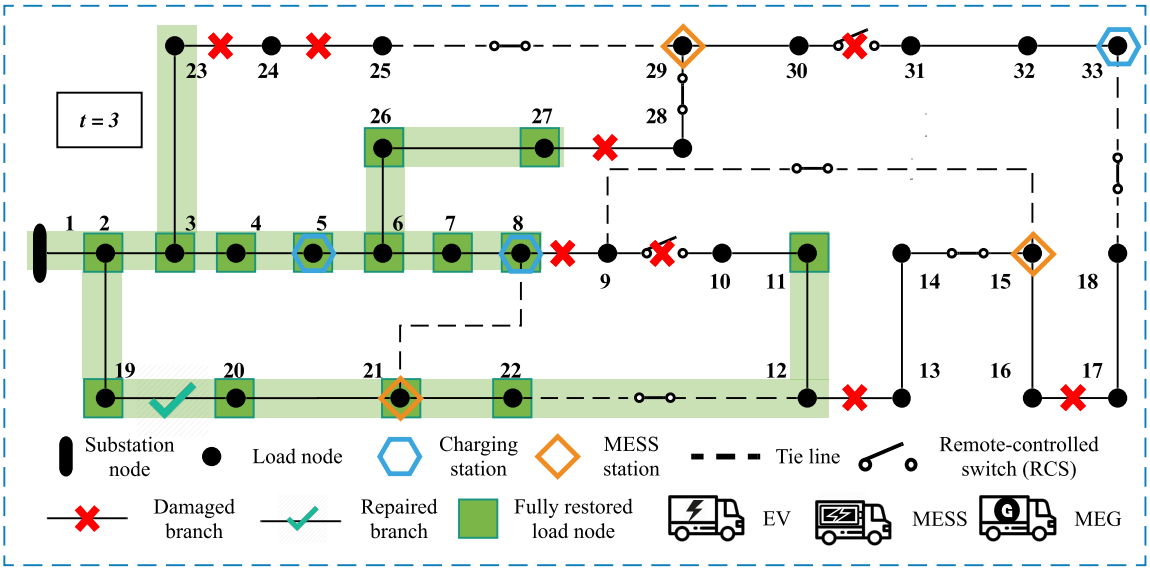

Figure 3.7: DS restoration process co-optimized with MPS dispatch and DS reconfiguration (Case Study 1, $t = 3$)

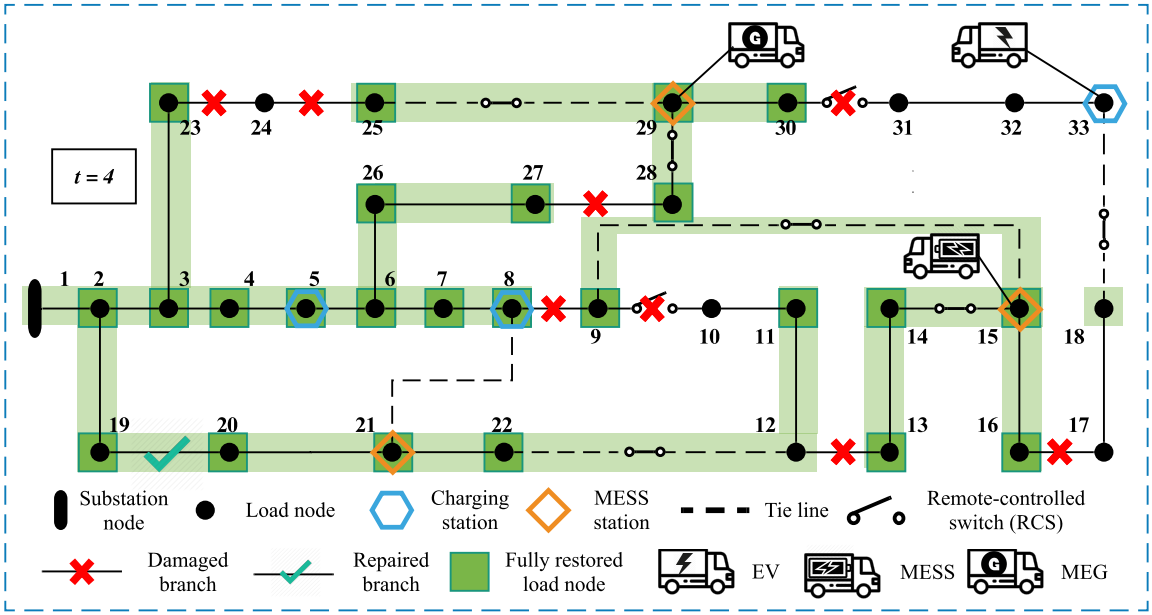

Figure 3.8: DS restoration process co-optimized with MPS dispatch and DS reconfiguration (Case Study 1, $t = 4$)

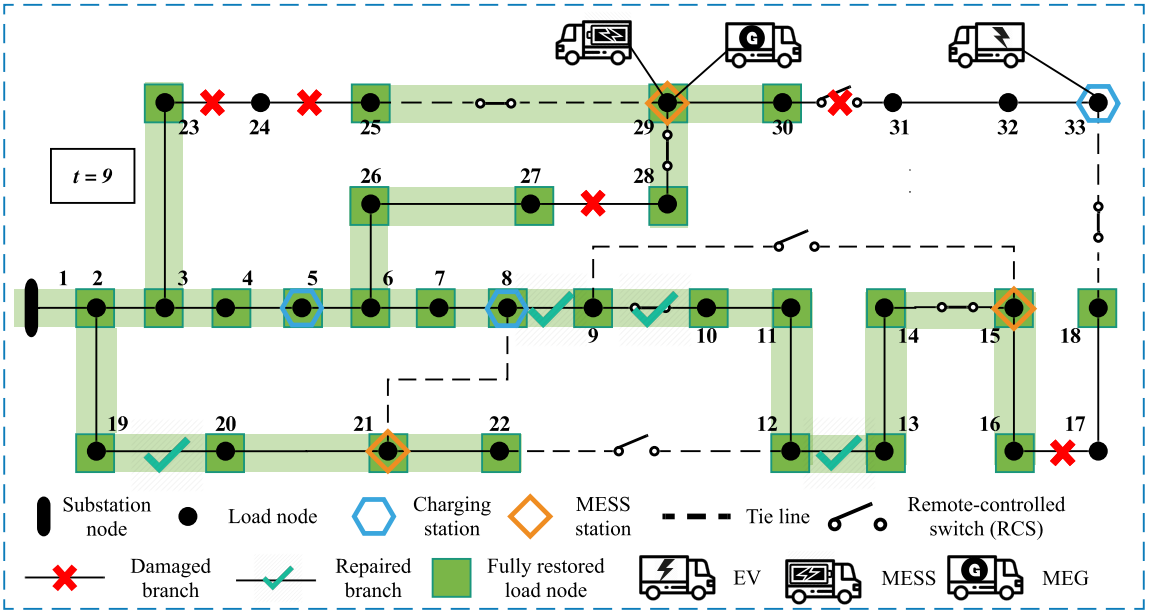

Figure 3.9: DS restoration process co-optimized with MPS dispatch and DS reconfiguration (Case Study 1, $t = 9$)

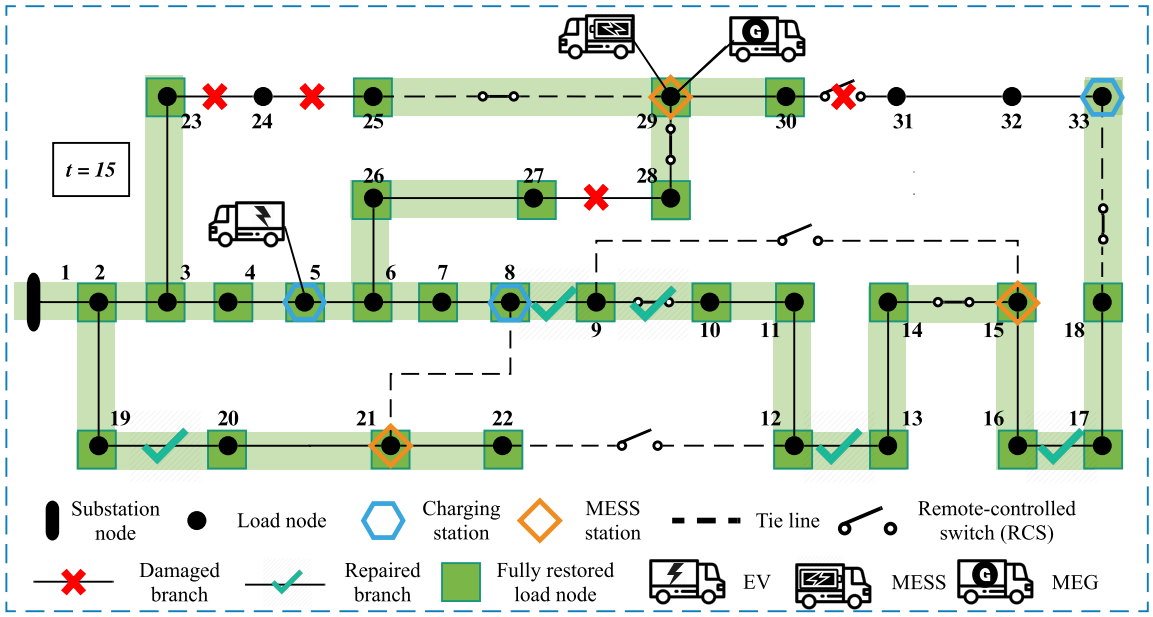

Figure 3.10: DS restoration process co-optimized with MPS dispatch and DS reconfiguration (Case Study 1, $t = 15$)

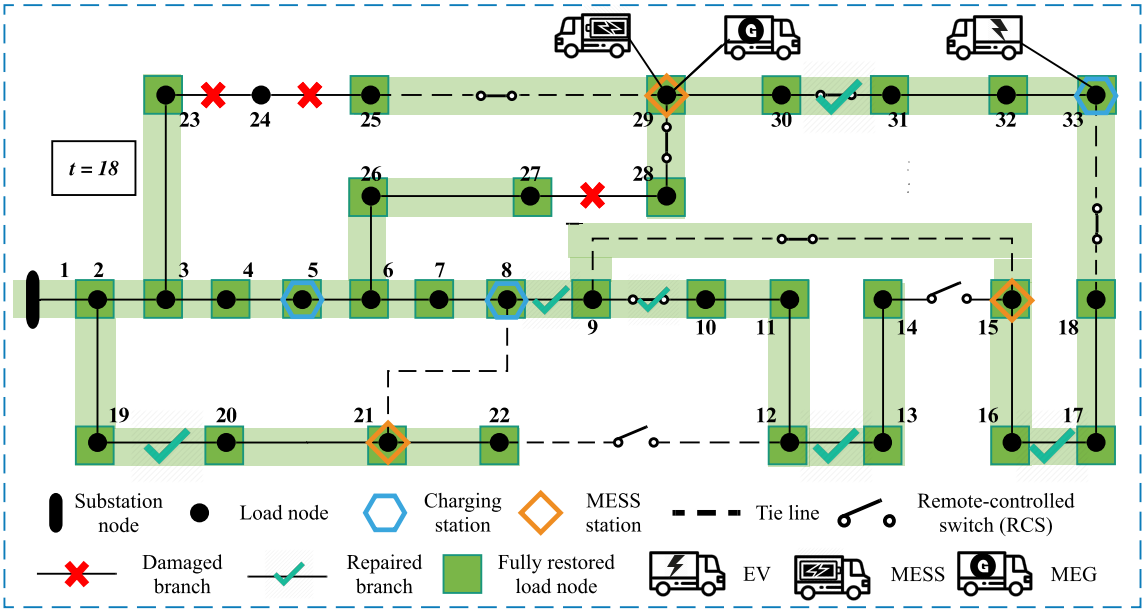

Figure 3.11: DS restoration process co-optimized with MPS dispatch and DS reconfiguration (Case Study 1, $t = 18$)

3.4.3 Case Study 2: Damage Scenario 2

Assume that 9 branches are damaged after the HILP hazard strikes as depicted in Figure 3.12, and the repair plan is adopted as shown in Table 3.4. According to the repair plan, the whole restoration process is set as $N_{\mathbf{T}} = 24$ time periods while each time period lasts $\Delta t = 0.5hr$.

Table 3.4: Repair Order of Damaged Branches in Case Study 2

Time period (t)	3	5	8	10	13	16	19	23	24
Repaired branch	1-2	19-20	5-6	7-8	26-27	25-29	32-33	12-13	11-12

The strategy of MPSs dynamic dispatch is obtained as presented in Table 3.5. The symbol "$\rightarrow$" denotes that the MPS is during transportation. The activity of the branches equipped with RCS is demonstrated in Table 3.6.

The recovery rate in each time period is depicted in Figure 3.13. Curves for the case only using DS reconfiguration method and the benchmark case without any MPS supply and DS reconfiguration are included for comparison. As can be seen in Figure 3.13, without

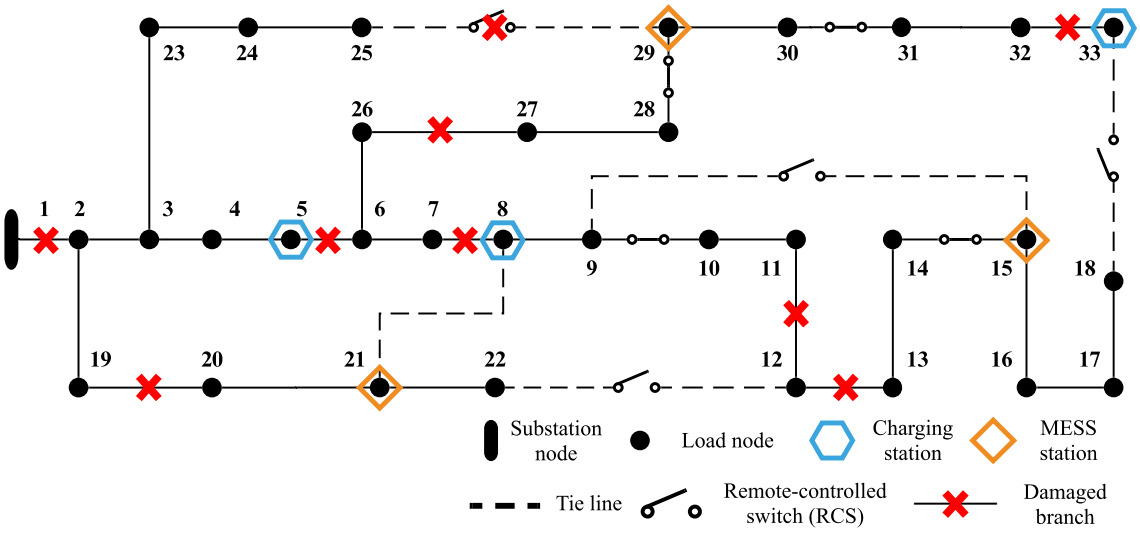

Figure 3.12: Damage scenario in Case Study 2

Table 3.5: Location of MPSs in Each Time Period in Case Study 2

---		Time Period										
		1	2	3	4	5	6~7	8	9	10	11~12	13~24
MPS	EV 1	node 1	→	node 8		→	node 5	→	node 8		→	node 33
	MESS 1	node 1	→		node 15				→	node 29		
	MEG 1	node 1	→		node 29							

Table 3.6: Distribution System (DS) Reconfiguration Actions in Case Study 2

Time period	Remote-controlled switch (RCS) actions
t = 1	close branch 9-15, 12-22, 18-33
t = 19	open branch 18-33
t = 23	open branch 12-22
t = 24	open branch 9-15

MPS and DS reconfiguration, the benchmark case has the lowest recovery rate over the restoration process. With MPS and DS reconfiguration employed, the proposed method restore the system to 98% at $t = 10$ and to 100% at $t = 24$. To be specific, with MPS and DS reconfiguration, the proposed method achieves a higher load outage recovery around 30% higher than the benchmark case at time period $t = 4 \sim 12$ and at least 20% higher than the case with DS reconfiguration alone at $t = 4 \sim 15$.

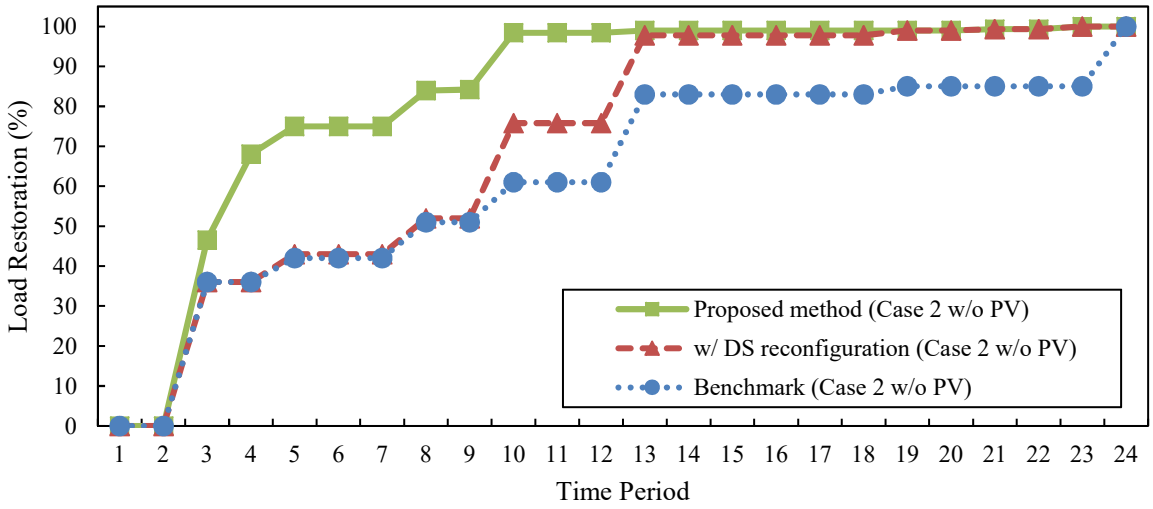

Figure 3.13: Load restoration in each time period using different strategies: Case Study 2

The curves for the system load demand, SOC of EV fleet 1, SOC of MESS 1, real power output of MEG 1 are demonstrated in Figure 3.14. Based on Tables 3.4 to 3.6 and Figures 3.12 and 3.14, the strategy of MPSs dispatch coordinated with the DS reconfiguration attains a better system restoration. Following a HILP event, tie lines 9-15, 12-22, and 18-33 which are normally open (i.e., offline) should be closed (i.e., online) in order to change the DS topology such that several PIs can be linked to facilitate the MPSs contribution in recovery of load outages in the subsequent time periods. Note that branch 9-10, 14-15, 28-29, and 30-31 are already online during the normal operating conditions, while branches 25-29 is offline due to post-event damages.

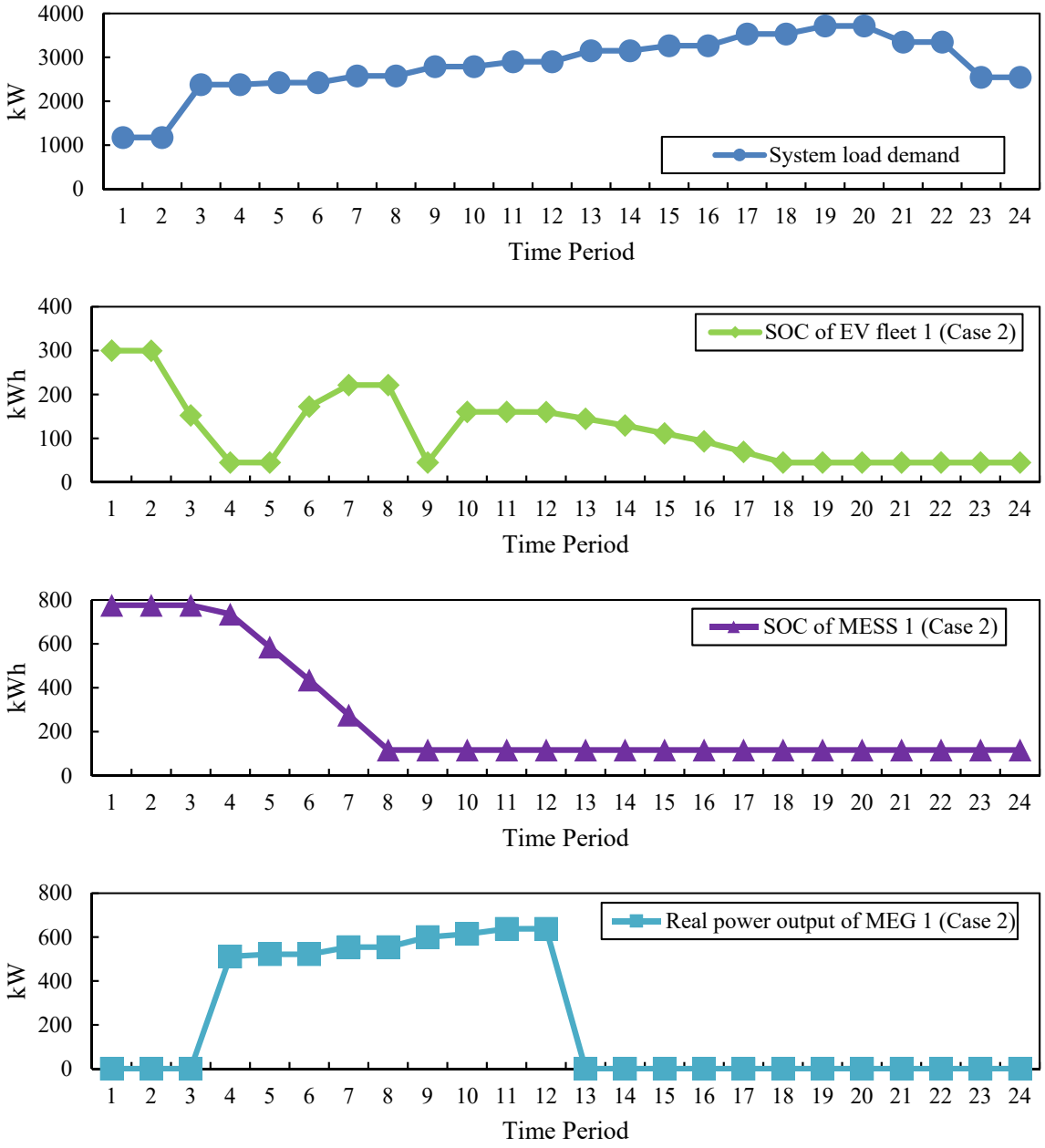

Figure 3.14: SOC of EV fleet 1, SOC of MESS 1, real power output of MEG 1 and system load demand in each time period: Case Study 2

3.4.4 Case Study 3: Damage Scenario 3

Assume that 8 branches are damaged after the hazard strikes as depicted in Figure 3.15, and the repair plan is adopted as shown in Table 3.7. According to the repair plan, the whole restoration process is set as $N_{\mathbf{T}} = 24$ time periods while each time period lasts $\Delta t = 0.5hr$.

Table 3.7: Repair Order of Damaged Branches in Case Study 3

Time period (t)	3	5	7	10	13	17	20	24
Repaired branch	4-5	6-7	6-26	27-28	29-30	16-17	11-12	21-22

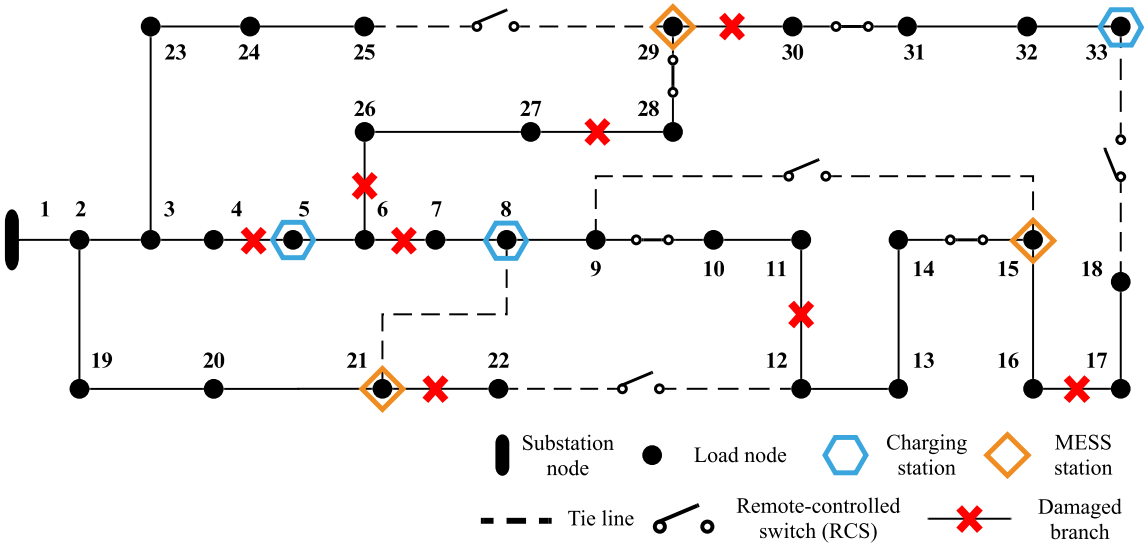

Figure 3.15: Damage scenario in Case Study 3

The strategy of MPSs dynamic dispatch is obtained as presented in Table 3.8. The symbol "$\rightarrow$" denotes that the MPS is during transportation. The activity of the branches equipped with RCS is demonstrated in Table 3.9.

The recovery rate in each time period is depicted in Figure 3.16. Curves for the case only using DS reconfiguration method and the benchmark case without any MPS supply and DS reconfiguration are included for comparison. As can be seen in Figure 3.16, without MPS and DS reconfiguration, the benchmark case has the lowest recovery rate over the restoration process. With MPS and DS reconfiguration, the proposed method restore the system to 99%

Table 3.8: Location of MPSs in Each Time Period in Case Study 3

---		Time Period					
		1	2	3	4~5	6~7	8~24
MPS	EV 1	node 1	→	node 8		→	node 33
	MESS 1	node 1					
	MEG 1	node 1	→		node 15		

Table 3.9: Distribution System (DS) Reconfiguration Actions in Case Study 3

Time period	Remote-controlled switch (RCS) actions
$t = 1$	close branch 9-15, 12-22, 18-33, 25-29
$t = 10$	open branch 25-29
$t = 17$	open branch 18-33
$t = 20$	open branch 9-15
$t = 24$	open branch 12-22

at $t = 17$ and to 100% at $t = 20$. To be specific, with MPS and DS reconfiguration employed, the proposed method achieves a higher recovery rate around 10% higher than the benchmark case at time period $t = 1 \sim 19$ and 10% higher than the case with DS reconfiguration alone at $t = 3 \sim 4$.

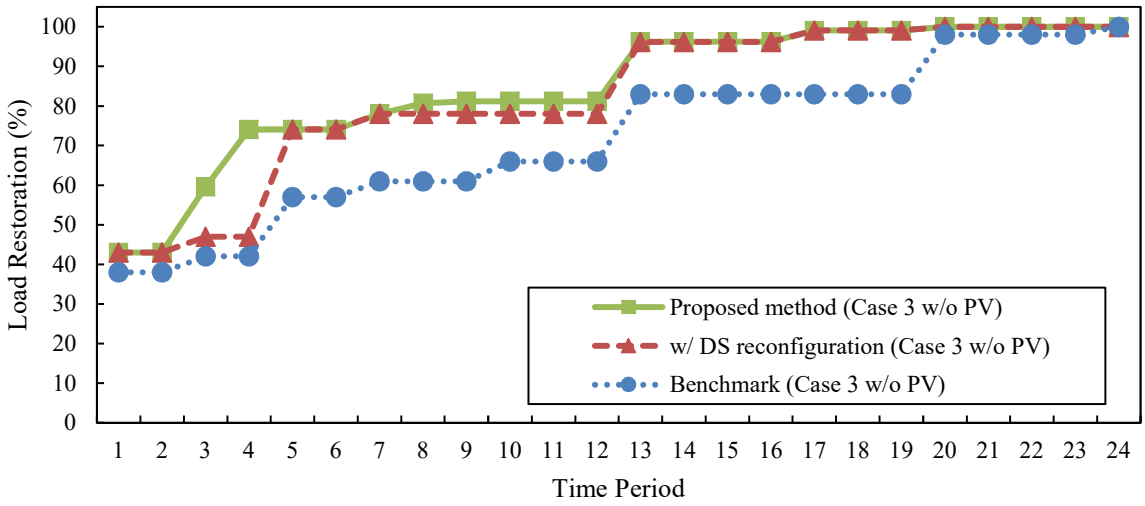

Figure 3.16: Load restoration in each time period using different strategies: Case Study 3

The curves for the system load demand, SOC of EV fleet 1, SOC of MESS 1, real power output of MEG 1 are demonstrated in Figure 3.17. Based on Tables 3.7 to 3.9 and Figures 3.15 and 3.17, the strategy of MPSs dispatch coordinated with the DS reconfiguration attains a better system restoration. Specifically, following a HILP event, tie lines 9-15, 12-22, 18-33, and 25-29 which are normally open (i.e., offline) should be closed (i.e., online) in order to change the DS topology such several PIs can be linked to facilitate the MPSs contribution in recovery of load outages in the subsequent time periods. Note that branch 9-10, 14-15, 28-29, and 30-31 are already online during the normal operating conditions.

3.5 Conclusion

In this chapter, the promising potential of mobile power sources (MPSs) on improving power system operational resilience is investigated. In the three case studies presented, it was demonstrated that the proposed MPS dispatch method improves the load outage recovery rate to a higher level at earlier time periods, compared with the benchmark system and the cases where only the DS reconfiguration method is employed. Cooperating with distribution system reconfiguration, the effectiveness of MPS dispatch to facilitate the restoration process and to enhance the system resilience is demonstrated and fully explained.

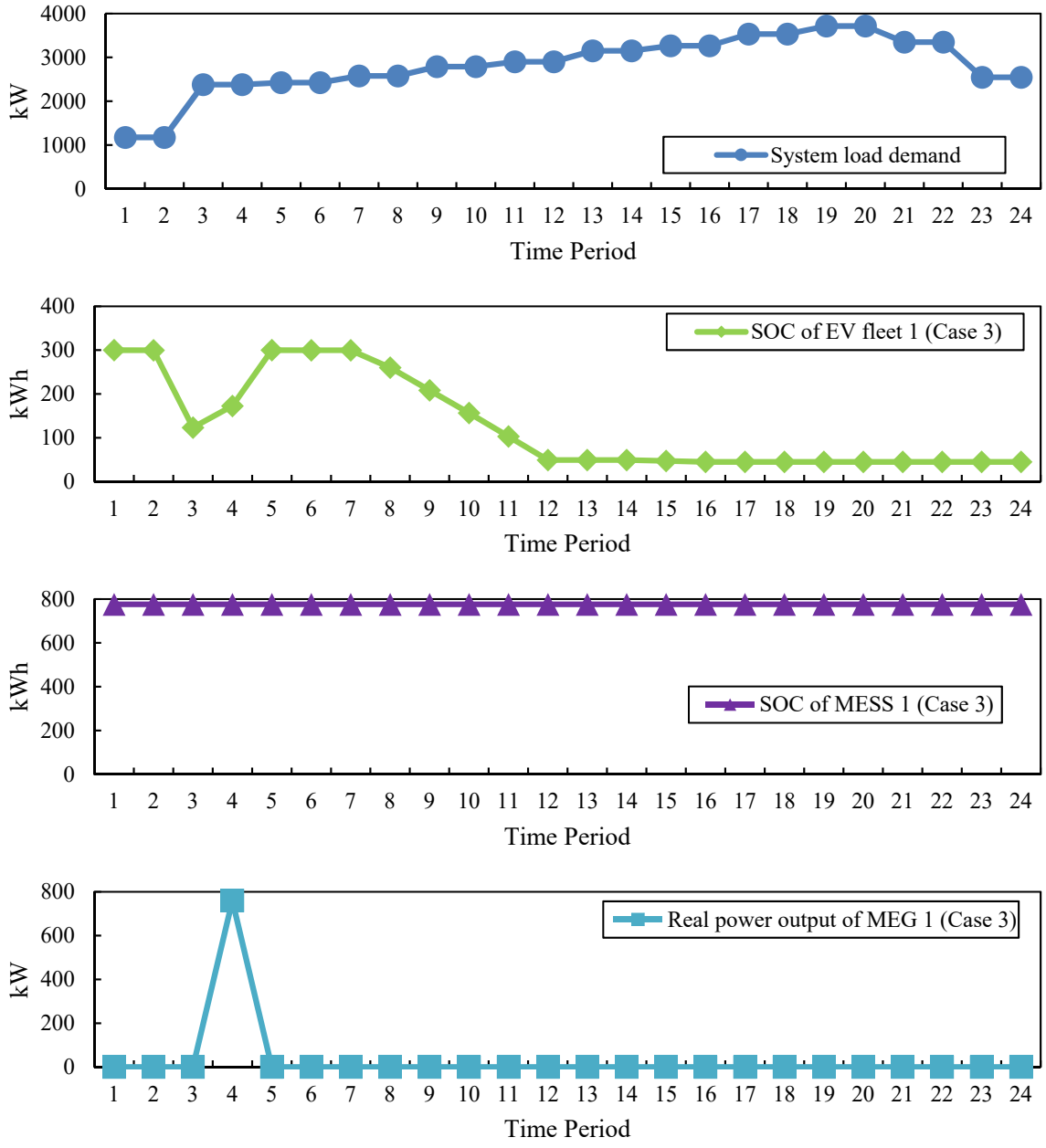

Figure 3.17: SOC of EV fleet 1, SOC of MESS 1, real power output of MEG 1 and system load demand in each time period: Case Study 3

Chapter 4: Mobile Power Sources Dispatch Coordinating With Distribution System Reconfiguration for Post-Disaster Restoration Considering the Presence of Photovoltaic Generation

4.1 Introduction

With the increasing interest in the renewable energy resources, this chapter investigates the coordination of photovoltaic (PV) generation with mobile power sources (MPSs) to improve the resilience of power systems, by assuming a PV farm located in the distribution system (DS). By introducing PV generation, the mathematical model presented in Section 3.3 in Chapter 3 is further extended. This chapter is organized as follows. Firstly, the model in Chapter 3 is extended. Afterward, three different damage scenarios are considered in the case studies to explore the impact of PV generation on the proposed method for DS restoration.

4.2 Extended Formulation

The objective function (3.1) is extended to include the terms associated with PV generation, as follows:

$$\begin{aligned}\max\Big(&\sum_{t\in\mathbf{T}}\sum_{i\in\mathbf{B}}\chi_i\cdot pd_{i,t}-\sum_{t\in\mathbf{T}}\sum_{m\in\mathbf{M}}C_m^{\mathrm{tr}}\cdot\varphi_{m,t}-\sum_{t\in\mathbf{T}}\sum_{m\in\{\mathbf{S},\mathbf{V}\}}C_m^{\mathrm{P}}\cdot(p_{m,t}^{\mathrm{ch}}+p_{m,t}^{\mathrm{dch}})-\\&\sum_{t\in\mathbf{T}}\sum_{m\in\mathbf{G}}\delta_m\cdot p_{m,t}-\sum_{t\in\mathbf{T}}\sum_{i\in\mathbf{B}}\mathrm{PVC}\cdot p_{i,t}^{\mathrm{SC}}\Big)\end{aligned}\tag{4.1}$$

In (4.1), an additional fifth term is represented by the value of loss of solar energy multiplied by the curtailed power of solar farm during the restoration process. This term is added to minimizing the cost produced by the curtailed power of solar farm so that the use of solar energy is maximized.

Additionally, some constraints need to be modified and several additional constraints

need to be included. The real power balance constraints (3.28) are modified as follows:

$$\sum_{(j,i)\in\mathbf{L}} pf_{ji,t} - \sum_{(i,j)\in\mathbf{L}} pf_{ij,t} = pd_{i,t} - pg_{i,t} - p_{i,t}^{\text{mps}} - p_{i,t}^{s}, \quad \forall i \in \mathbf{B}, \forall t \in \mathbf{T} \tag{4.2}$$

where $p_{i,t}^{s}$ denotes the real power generated by the solar farm on node i at time t. Note that it is assumed here that the power factor of the PV generation is 1, and thus the PV farm only inject real power into the distribution grid. The following constraints associated with the PV generation need to be added:

$$p_{i,t}^{\text{SC}} = \overline{P}_{i,t}^{s} - p_{i,t}^{s}, \quad \forall i \in \mathbf{B}, \forall t \in \mathbf{T} \tag{4.3}$$

$$0 \leq p_{i,t}^{s} \leq \overline{P}_{i,t}^{s}, \quad \forall i \in \mathbf{B}, \forall t \in \mathbf{T} \tag{4.4}$$

The solar power curtailment is formulated in constraint (4.3). At any node hosting the solar farm, the amount of solar power generation depends on solar power availability and solar power capacity as demonstrated in constraint (4.4).

4.3 Case Study: Modified IEEE 33-Node Test System Considering PV Generation

4.3.1 System Characteristics, Assumption, and Data

In this chapter, the modified IEEE 33-node test system is adopted for case studies. The system characteristics, assumption and data in Section 3.4 are continued to be used in this section. Furthermore, it is assumed that a PV farm of 500 kW capacity is located at node 10 in the DS as Figure 4.1 demonstrates. The maximum available real power from the PV farm, $\overline{P}_{i,t}^{s}$, depends on the weather conditions and it is typically predicted based on the historical data. In the case studies, it is assumed that the predicted data of $\overline{P}_{i,t}^{s}$ is available. The three damage scenarios and the corresponding repair plans used in Section 3.4 are employed in this section for case studies to compare the effectiveness of the proposed method in the case

with PV generation against that in the case without PV generation.

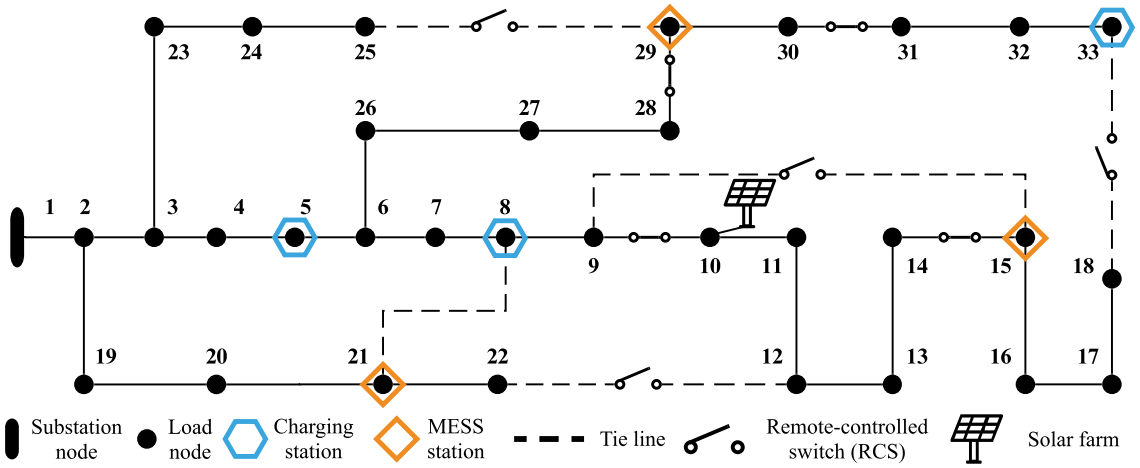

Figure 4.1: The modified IEEE 33-node test system with solar farm

4.3.2 Case Study 1b: Damage Scenario 1 with PV Generation

The same damage scenario (Figure 3.4) and the same repair plan (Table 3.1) in Section 3.4.2 are adopted here. The strategy of MPSs dynamic dispatch is obtained the same as the strategy in the case without the solar farm, as shown in Table 3.2. The activity of the branches equipped with the RCS is the same as those taken in the case without the solar farm, as demonstrated in Table 3.3. The recovery rate in each time period is depicted in Figure 4.2. Curves for the case only using DS reconfiguration method and the benchmark case without any MPS supply and DS reconfiguration are included for comparison. Figure 4.2 demonstrates that the proposed method remains effective to facilitate the restoration speed.

With the proposed method, the recovery rate in the case 1 with and without PV generation is shown in Figure 4.3. Specifically, compared with the case without PV generation, the proposed method in the case with PV generation has 2% higher recovery rate at $t = 3 \sim 5$ while the other time periods have the same recovery rate.

The curves for the system load demand, SOC of EV fleet 1, SOC of MESS 1, the real power output of MEG 1 as well as the utilized real power output from the solar farm are

demonstrated in Figure 4.4. The PV real power output is utilized since $t = 3$. The PV real power output is not utilized at the beginning which is because of the non-decreasing recovery constraint (Equation (3.31)). The system load increases significantly at $t = 3$ and at $t = 1 \sim 2$ PV real power output just slightly increase. Since the PV generation cannot maintain the recovery rate of the surrounding load node at the subsequent time period if its real power output is utilized since $t = 1$, thus the PV real power output at $t = 1 \sim 2$ is curtailed (wasted). Compared with the case without PV generation, the SOC of EV fleet 1 and MESS 1 and the real power output of MEG 1 remain the same in the case with PV generation. Therefore, in case 1, the PV generation further improves the recovery rate at some time periods, though the increase is not significant.

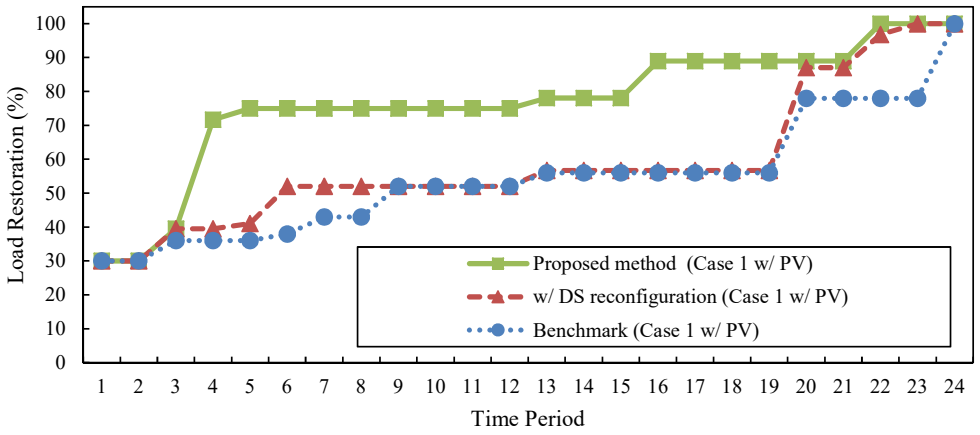

Figure 4.2: Load restoration in each time period using different strategies: Case Study 1 with PV

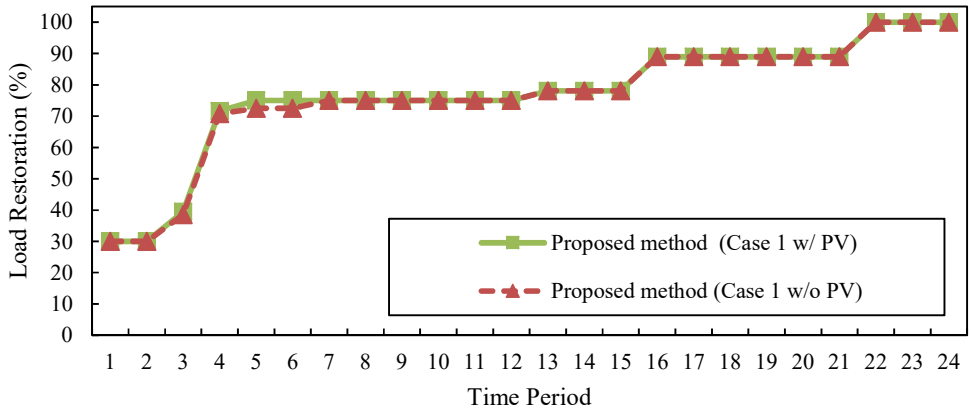

Figure 4.3: Load recovery rate: Case Study 1 with and without PV

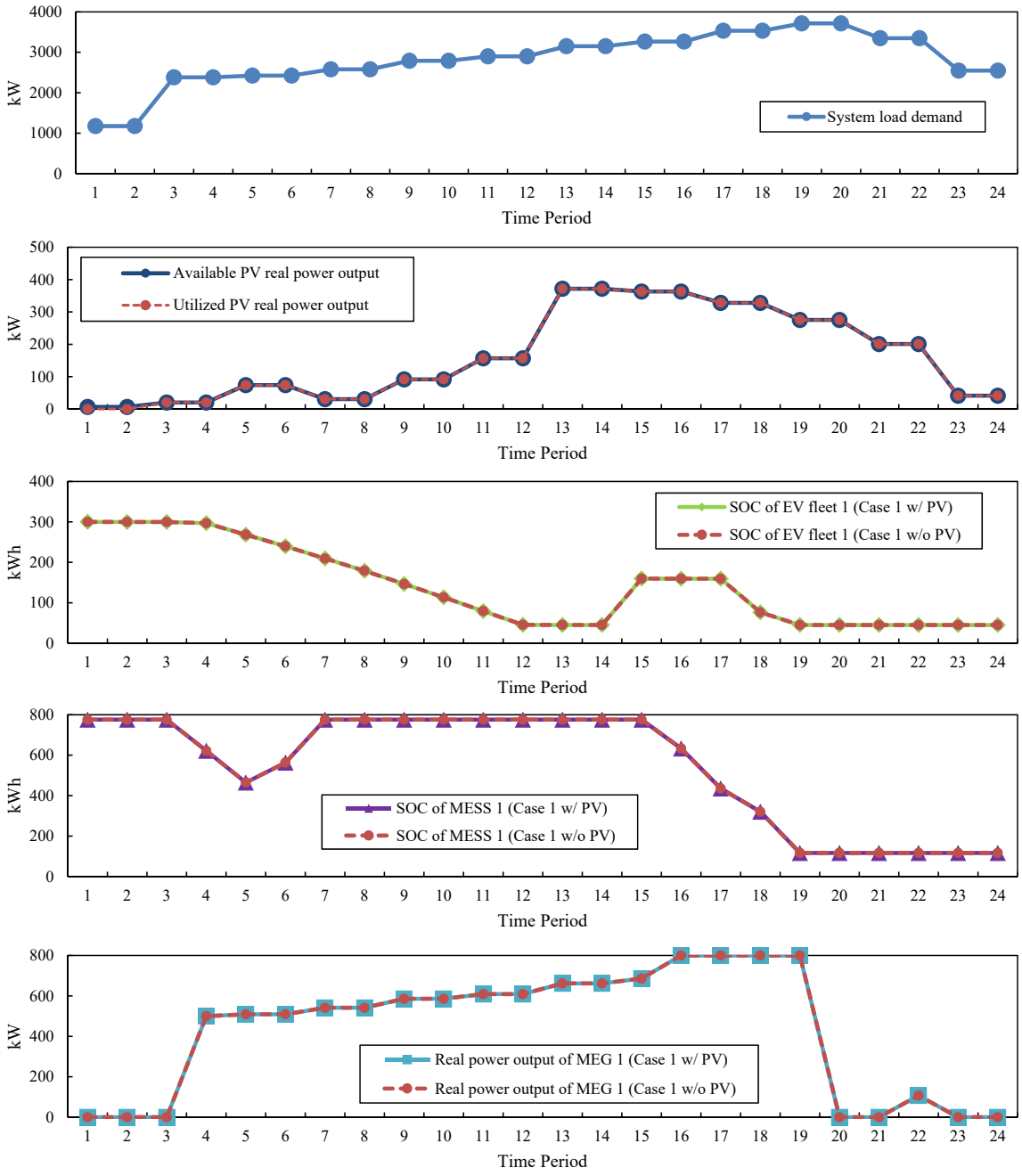

Figure 4.4: SOC of EV fleet 1, SOC of MESS 1, real power output of MEG 1, system load demand and PV real power output in each time period: Case Study 1 with PV

4.3.3 Case Study 2b: Damage Scenario 2 with PV Generation

The same damage scenario (Figure 3.12) and the same repair plan (Table 3.4) in Section 3.4.3 are adopted here. The strategy of MPSs dynamic dispatch is obtained the same as the strategy in the case without the solar farm, as shown in Table 3.5. The activity of the branches equipped with RCS is the same as the action taken in the case without the solar farm, as demonstrated in Table 3.6. The recovery rate in each time period is depicted in Figure 4.5. Curves for the case only using DS reconfiguration method and the benchmark case without any MPS supply and DS reconfiguration are included for comparison. Figure 4.5 demonstrates that the proposed method remains effective to facilitate the restoration speed.

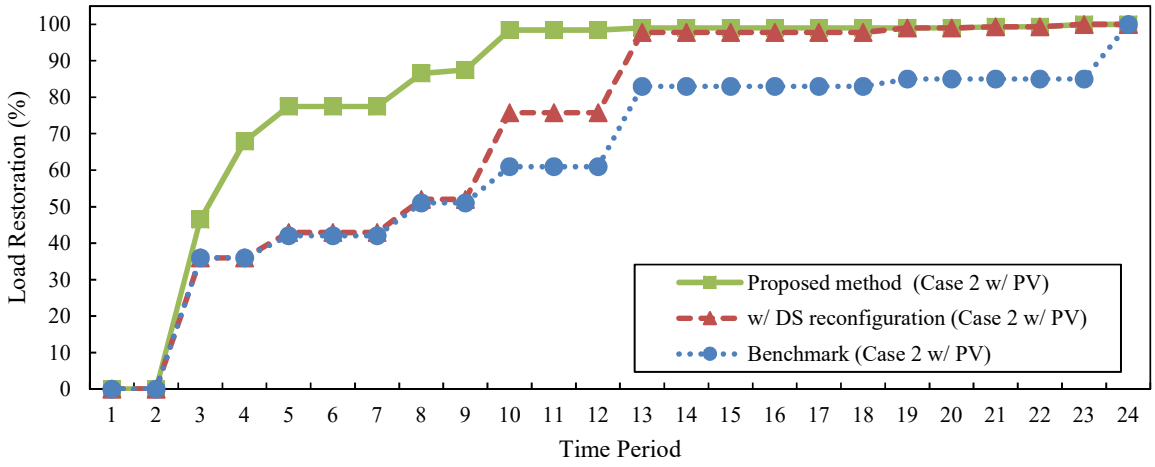

Figure 4.5: Load restoration in each time period using different strategies: Case Study 2 with PV

With the proposed method, the recovery rate in the Case Study 2 with and without PV generation is shown in Figure 4.6. Specifically, compared with the case without PV generation, the proposed method in the case with PV generation has 3% higher recovery rate at $t = 5 \sim 9$ while the other time periods have the same recovery rate.

The curves for the system load demand, SOC of EV fleet 1, SOC of MESS 1, the real power output of MEG 1 as well as the utilized real power output from the solar farm are demonstrated in Figure 4.7. The PV real power output is utilized since $t = 3$. Similar to

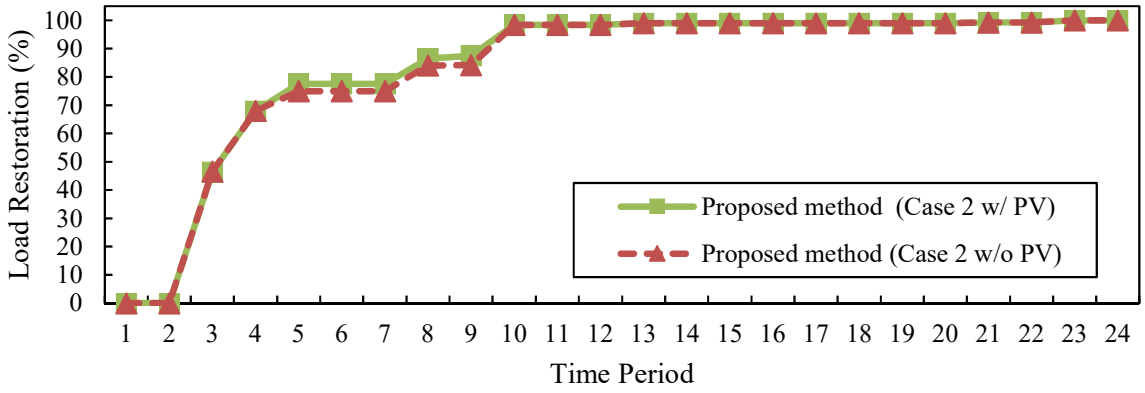

Figure 4.6: Load recovery rate: Case Study 2 with and without PV

case 1, the PV real power output is not utilized at the beginning which is because of the non-decreasing recovery constraint (Equation (3.31)). Compared with the case without PV generation, the SOC of EV fleet 1 and the real power output of MEG 1 remain the same in the case with PV generation. When MESS 1 connects to node 15, PV generation also supply some surrounding loads, thus the SOC of MESS 1 is higher than that in the case without PV generation at $t = 4 \sim 7$.

Therefore, in Case Study 2, the PV generation further improves the recovery rate at some time periods, though the increase is not significant.

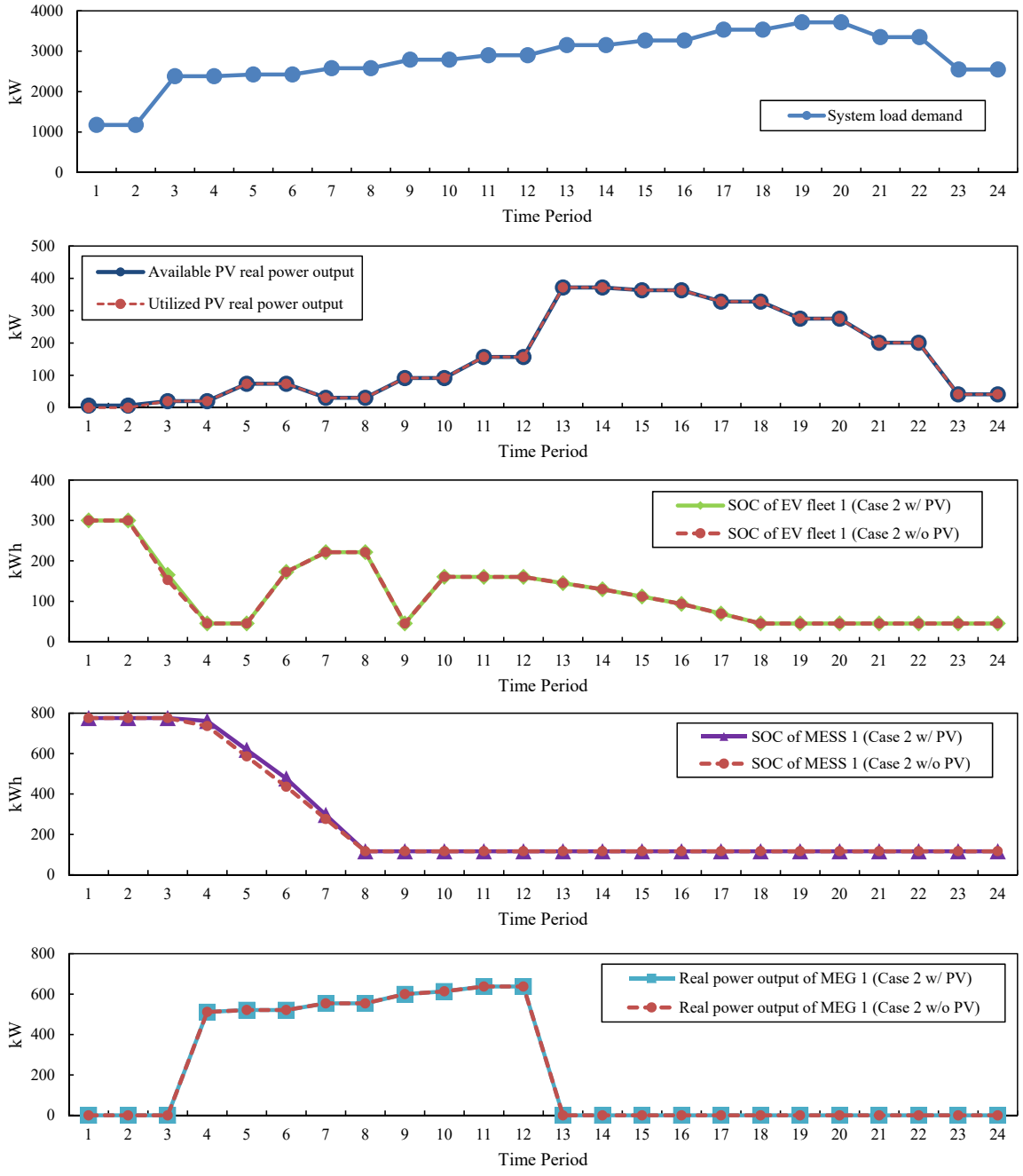

Figure 4.7: SOC of EV fleet 1, SOC of MESS 1, real power output of MEG 1, system load demand and PV real power output in each time period: Case Study 2 with PV

4.3.4 Case Study 3b: Damage Scenario 3 with PV Generation

The same damage scenario (Figure 3.15) and the same repair plan (Table 3.7) in Section 3.4.4 are adopted here. The strategy of MPSs dynamic dispatch is obtained the same as the strategy in the case without the solar farm, as shown in Table 3.8. The activity of the branches equipped with RCS is the same as the action taken in the case without the solar farm, as demonstrated in Table 3.9. The recovery rate in each time period is depicted in Figure 4.8. Curves for the case only using DS reconfiguration method and the benchmark case without any MPS supply and DS reconfiguration are included for comparison. Figure 4.8 demonstrates that the proposed method remains effective to facilitate the restoration speed.

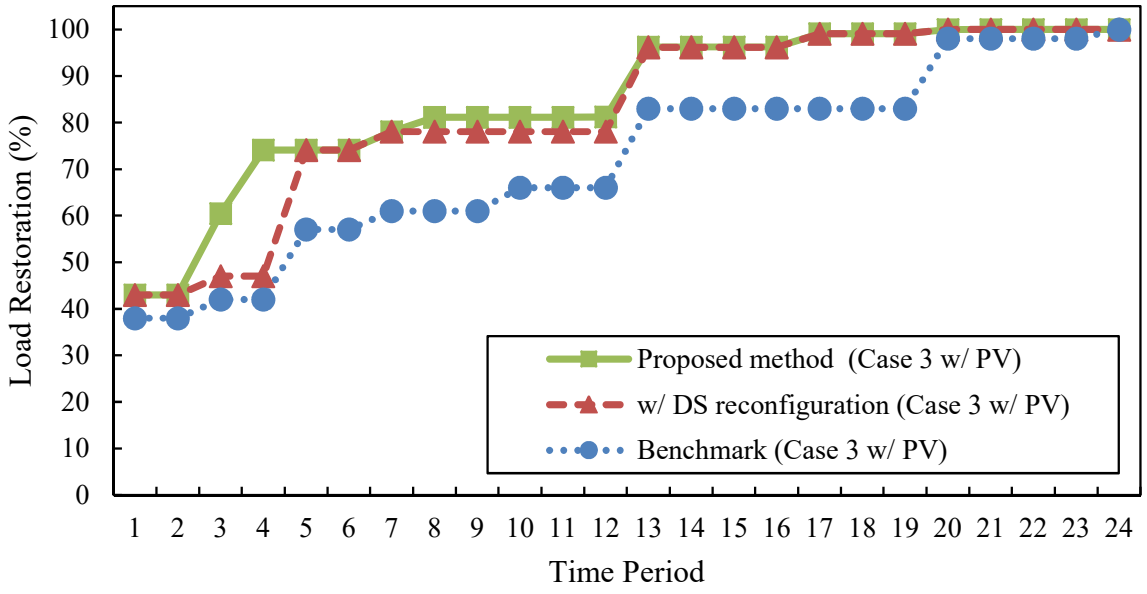

Figure 4.8: Load restoration in each time period using different strategies: Case Study 3 with PV

With the proposed method, the recovery rate in the Case Study 3 with and without PV generation is shown in Figure 4.9. Specifically, compared with the case without PV generation, the proposed method in the case with PV generation has the same recovery rate during the restoration.

The curves for the system load demand, SOC of EV fleet 1, SOC of MESS 1, the real

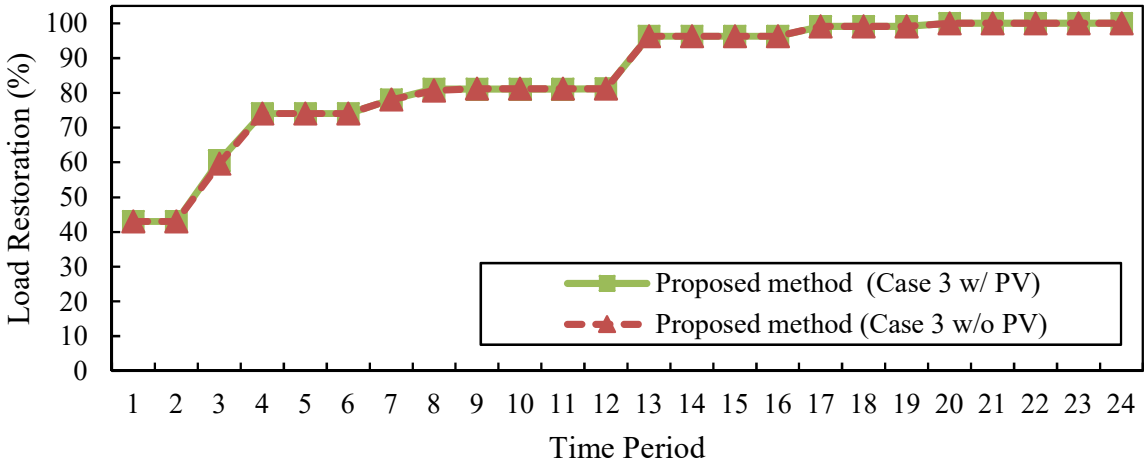

Figure 4.9: Load recovery rate: Case Study 3 with and without PV

power output of MEG 1 as well as the utilized real power output from the solar farm are demonstrated in Figure 4.10. The PV real power output is utilized since $t = 3$. Similar to Case Study 1, the PV real power output is not utilized at the beginning which is because of the non-decreasing recovery constraint (Equation (3.31)). Compared with the case without PV generation, the SOC of EV fleet 1 and MESS 1 and the real power output of MEG 1 remain the same in the case with PV generation.

Therefore, in Case Study 3, the PV generation does not help to facilitate the restoration.

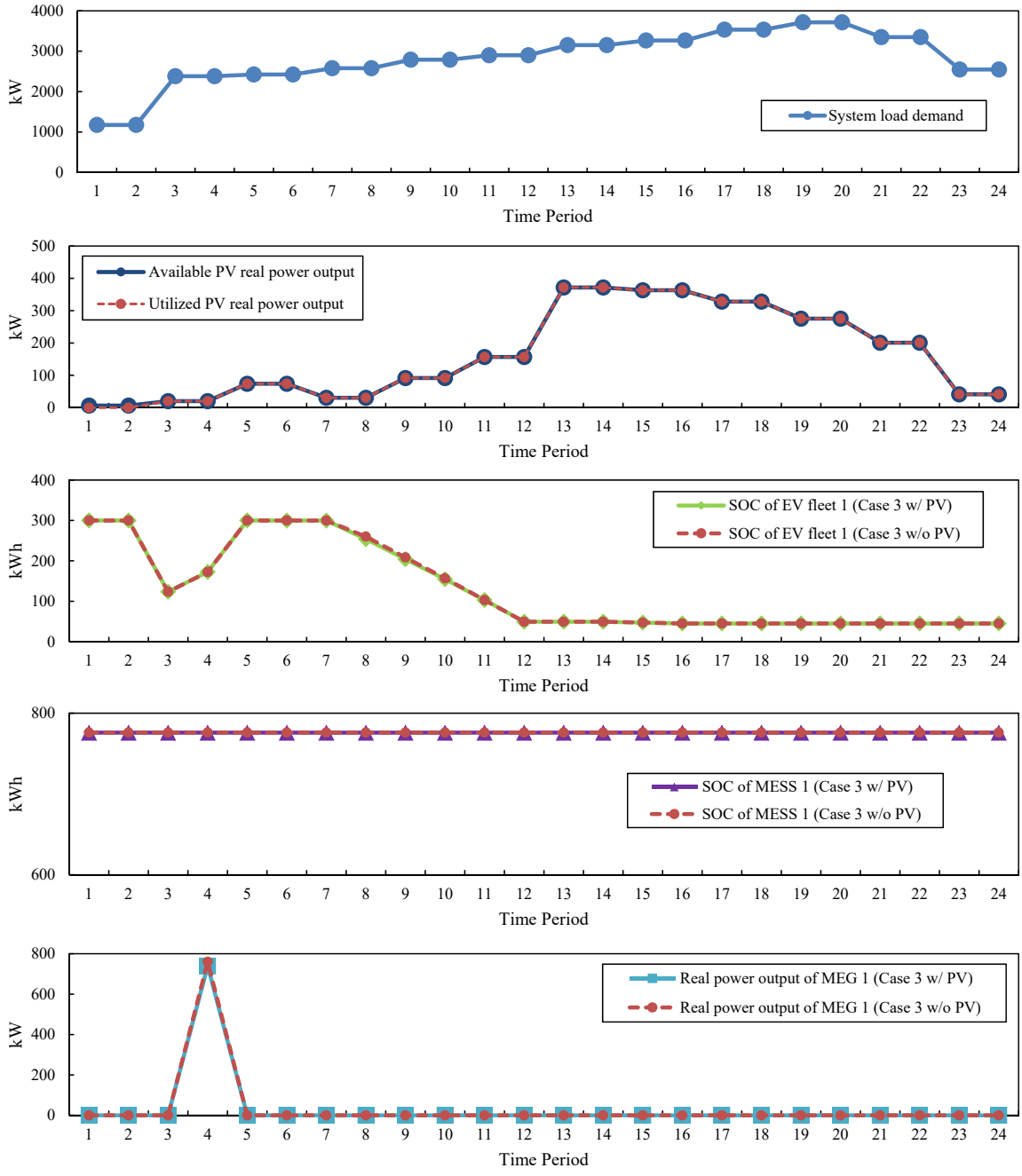

Figure 4.10: SOC of EV fleet 1, SOC of MESS 1, real power output of MEG 1, system load demand and PV real power output in each time period: Case Study 3 with PV

4.4 Conclusion

This chapter investigates the impact of PV generation in the DS on the effectiveness of the proposed MPS dispatch method in facilitating the restoration process. According to Figures 4.2, 4.5 and 4.8, the proposed MPS dispatch method remains effective when considering a PV farm in the DS. However, compared with the cases without PV generation, the cases with PV generation have no significant change in the load recovery rates in the three case studies, as Figures 4.3, 4.6 and 4.9 showed. Similarly, PV generation does not affect the strategies of MPS dispatch and DS reconfiguration actions in these three case studies. In order to investigate how much contribution PV generation makes to the DS restoration agility and effectiveness, with only the DS reconfiguration method, the recovery rates of the cases with PV generation are compared with those without PV generation as demonstrated in Figure 4.11. As can be seen, even in the cases that the DS has PV generation as the only emergency energy source, the contribution of PV generation to the DS restoration is insignificant.

By analyzing the recovery rate of each individual load node and the damaged branch repair plan, it is found that the PV farm and its surrounding load nodes are reconnected to the main grid at relatively early time periods (i.e., t = 7, 10 and 5, respectively). Additionally, due to the relatively small available PV real power output at the early time periods (i.e. $t = 1 \sim 10$), even though the PV real power output is 100% utilized since $t = 3$, it does not make significant contribution to the DS restoration. As a result, under the given damaged branch repair plan, PV generation make no significant contribution in facilitating the DS restoration. We concluded that the PV effectiveness in the restoration process highly depends on the location of such resources and the repair plan strategy taken during the restoration process. In the next chapter, the impact of different damaged branch repair plan on the contribution of MPS dispatch and PV generation to the DS restoration is investigated.

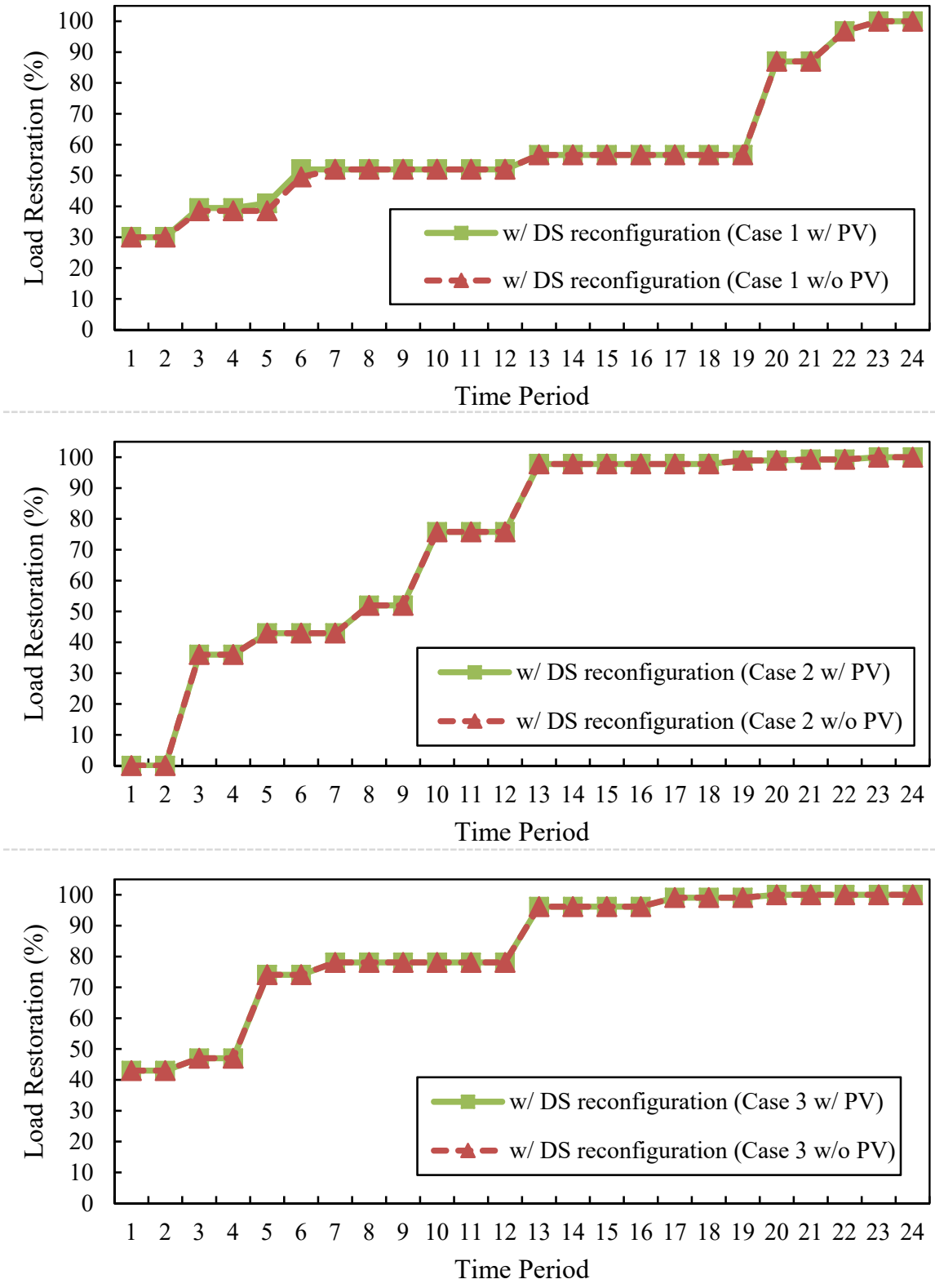

Figure 4.11: Load recovery rate: Case Study 1 $\sim$ 3 with and without PV

Chapter 5: The Contribution of MPS Dispatch, PV Generation and Repair Plan on Post-Disaster Restoration

5.1 Introduction

In this chapter, according to the results achieved in case studies in Section 4.3, the impact of the damaged branch repair plan on the contribution of MPS dispatch and PV generation to the distribution system (DS) restoration needs to be investigated. In order to study the impact of the repair plan, the case study continue to use the system characteristics, assumption and data in Section 3.4 and Section 4.3, but only the repair plans are changed.

5.2 Case Study: Modified IEEE 33-Node Test System with Different Repair Plans

5.2.1 System Characteristics, Assumptions, and Data

In this section, the three damage scenarios in Section 3.4 and Section 4.3 continue to be used here. In order to investigate the impact of the repair plan, it is assumed that due to several reasons (e.g., traffic issues, insufficient repair crews, etc.), the repair plans used in Section 3.4 and Section 4.3 are changed. The system with and without PV farm are both studied in this section, and the system characteristics, the other assumptions, and data in Section 3.4 and Section 4.3 continue to be used here. Thus, the result of the proposed MPS dispatch method and the PV generation in the same systems with the same damage scenarios but different repair plans can be compared.

5.2.2 Case Study 4: Damage Scenario 1 with Different Repair Plans

The damage scenario is the same as that in Case Study 1 (Figure 3.4) is adopted here, but the repair strategy is changed as presented in Table 5.1. According to the repair plan, the whole restoration process is set as $\mathbf{T}$ = 24 time periods while each time period lasts $\Delta t = 0.5hr$.

Table 5.1: Repair Order of Damaged Branches in Case Study 4

Time period (t)	3	4	7	9	13	16	19	20	24
Repaired branch	23-24	24-25	27-28	30-31	16-17	12-13	9-10	8-9	19-20

The proposed MPS dispatch method is exploited to both systems with and without PV farm. The MPS dispatch strategy for the DS without PV farm is obtained as demonstrated in Table 5.2. The MPS dispatch strategy for the DS with PV farm is obtained as presented in Table 5.3. The obtained remote-controlled switch (RCS) actions for both systems with and without PV generation are the same, as shown in Table 5.4.

The recovery rate achieved in Case Study 4 in both systems (with and without PV generation) in each time period is depicted in Figure 5.1. As can be seen, with different repair plans adopted, the proposed MPS dispatch method remains effective in facilitating the DS restoration. In the case without PV generation, the proposed MPS method improves the recovery rate $10 \sim 20\%$ higher than the DS reconfiguration method alone and reach 100% recovery at $t = 19$. Compared with the case without PV generation, coordinated with the PV generation, the proposed MPS method further enhances the recovery rate 7% at $t = 13 \sim 18$ and reach the 100% recovery rate at $t = 16$.

Table 5.2: Location of MPSs in Each Time Period in Case Study 4 without PV Generation

---		**Time Period**							
		1	**2**	**3**	**4~15**	**16**	**17**	**18**	**19~24**
MPS	**EV 1**	**node 1**	→		**node 33**				
	MESS 1	**node 1**	→	**node 21**		→	**node 29**	→	**node 21**
	MEG 1	**node 1**	→		**node 15**				

Table 5.3: Location of MPSs in Each Time Period in Case Study 4 with PV Generation

---		**Time Period**					
		1	**2**	**3**	**4~19**	**20~21**	**22~24**
MPS	**EV 1**	**node 1**	→		**node 33**		
	MESS 1	**node 1**	→	**node 21**			
	MEG 1	**node 1**	→		**node 15**	→	**node 21**

The curves for the system load demand, SOC of EV fleet 1, SOC of MESS 1, the real power output of MEG 1 as well as the utilized real power output from the solar farm are demonstrated in Figure 5.2. The PV real power output is utilized since $t = 3$. The PV real power output is not utilized at the beginning which is because of the non-decreasing recovery constraint (Equation (3.31)).

Table 5.4: Distribution System (DS) Reconfiguration Actions in Case Study 4

Time period	Remote-controlled switch (RCS) actions
$t = 1$	close branch 9-15, 12-22, 18-33, 25-29
$t = 7$	open branch 25-29
$t = 9$	close branch 30-31 (repaired)
$t = 19$	close branch 9-10 (repaired), open branch 14-15
$t = 20$	close branch 14-15, open branch 9-15, 18-33
$t = 24$	open branch 12-22

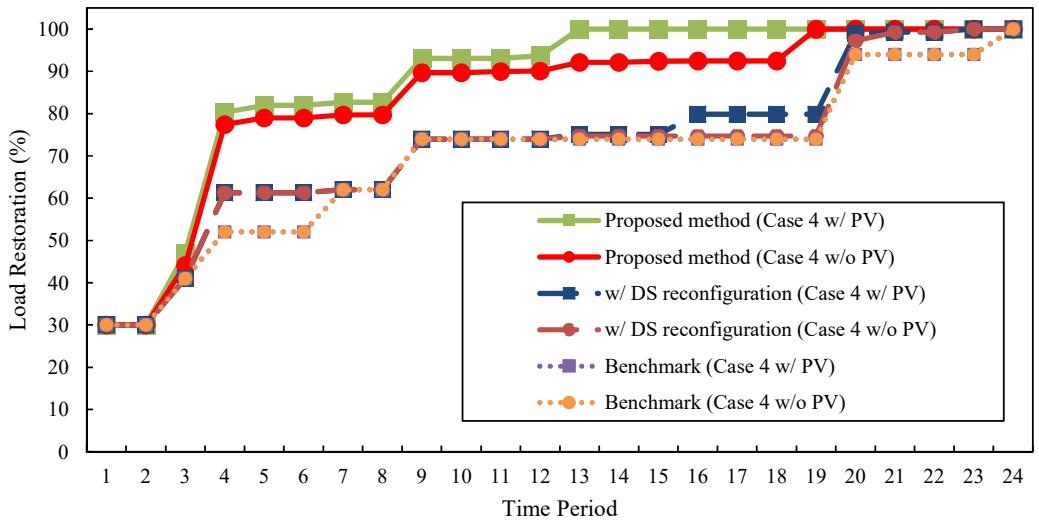

Figure 5.1: Load restoration in each time period using different strategies: Case Study 4

Case Study 4 reveals that the proposed MPS dispatch method remains valid in different repair strategies. Additionally, the coordination of PV generation in the DS with the proposed MPS dispatch method can make a significant contribution to DS restoration when particular repair plans are implemented.

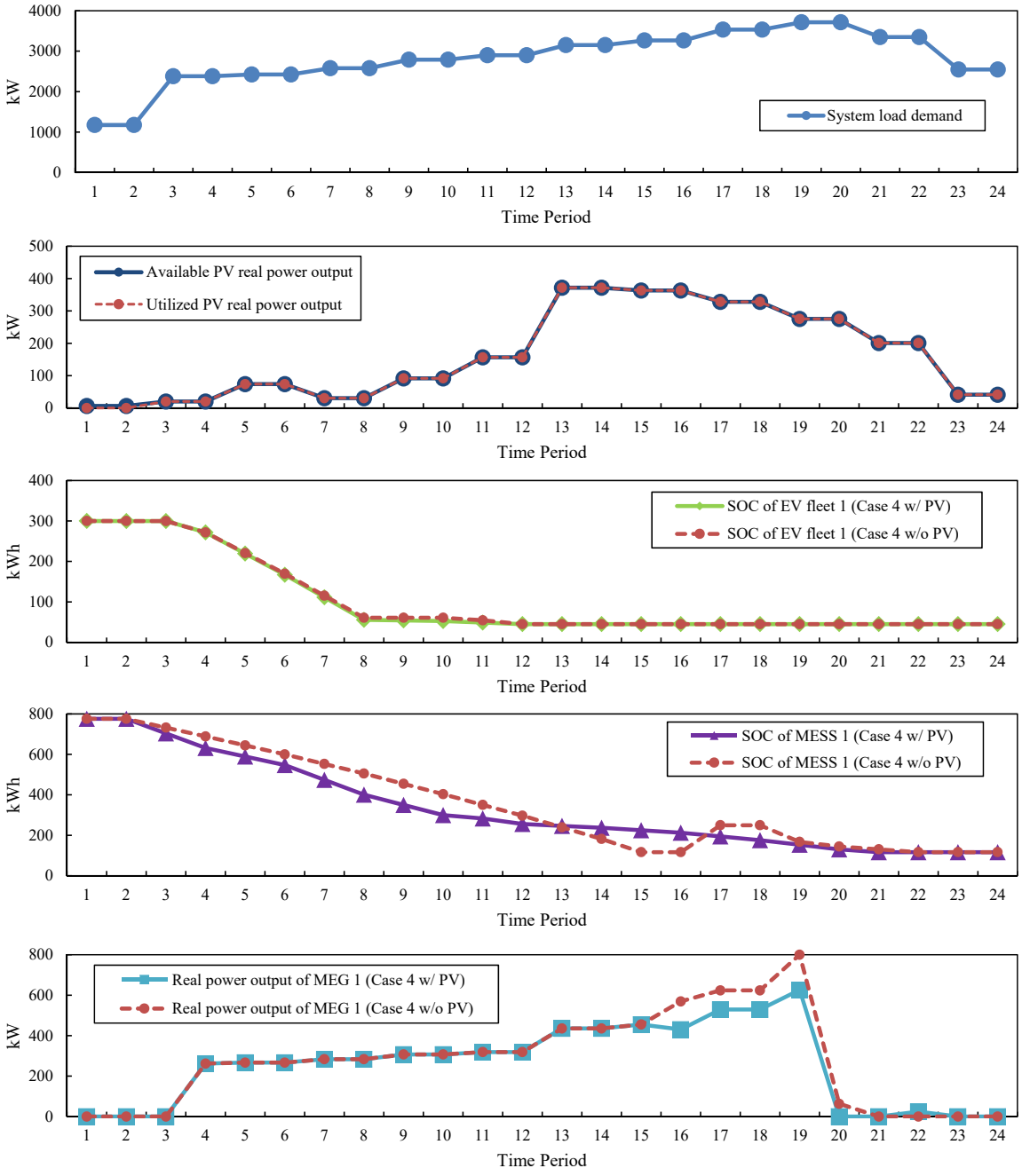

Figure 5.2: SOC of EV fleet 1, SOC of MESS 1, real power output of MEG 1, system load demand and PV real power output in each time period: Case Study 4 with PV

5.2.3 Case Study 5: Damage Scenario 2 with Different Repair Plans

The damage scenario, the same as that in Case Study 2 (Figure 3.12), is adopted here, but the repair strategy is changed as presented in Table 5.5. According to the repair plan, the whole restoration process is set as **T** = 24 time periods while each time period lasts $\Delta t = 0.5hr$. The proposed MPS dispatch method is exploited to both systems with and without PV farm.

Table 5.5: Repair Order of Damaged Branches in Case Study 5

Time period (t)	3	6	8	10	14	18	19	21	24
Repaired branch	1-2	5-6	26-27	25-29	32-33	12-13	11-12	7-8	19-20

The MPS dispatch strategy for the DS without PV farm is obtained as demonstrated in Table 5.6. The MPS dispatch strategy for the DS with PV farm is obtained as presented in Table 5.7. The obtained remote-controlled switch (RCS) actions for both systems with and

Table 5.6: Location of MPSs in Each Time Period in Case Study 5 without PV Generation

---		Time Period											
		1	2	3	4	5~6	7~10	11	12~13	14~15	16	17	18~24
MPS	EV 1	node 1	→	node 8		→	node 33			→	node 5	→	node 8
	MESS 1	node 1	→		node 29			→	node 21				
	MEG 1	node 1	→		node 15								

Table 5.7: Location of MPSs in Each Time Period in Case Study 5 with PV Generation

---		Time Period							
		1	2	3	4	5~6	7~10	11	12~24
MPS	EV 1	node 1	→	node 8		→	node 33		
	MESS 1	node 1	→	node 29				→	node 21
	MEG 1	node 1	→	node 15					

without PV generation are the same, as shown in Table 5.8.

The recovery rate achieved in Case Study 5 in both systems (with and without PV generation) in each time period is depicted in Figure 5.3. The curves for the system load demand, SOC of EV fleet 1, SOC of MESS 1, the real power output of MEG 1 as well as the utilized real power output from the solar farm are demonstrated in Figure 5.4. The PV

Table 5.8: Distribution System (DS) Reconfiguration Actions in Case Study 5

Time period	Remote-controlled switch (RCS) actions
$t = 1$	close branch 9-15, 12-22, 18-33
$t = 19$	open branch 14-15
$t = 21$	close branch 14-15, open branch 9-15, 18-33
$t = 24$	open branch 12-22

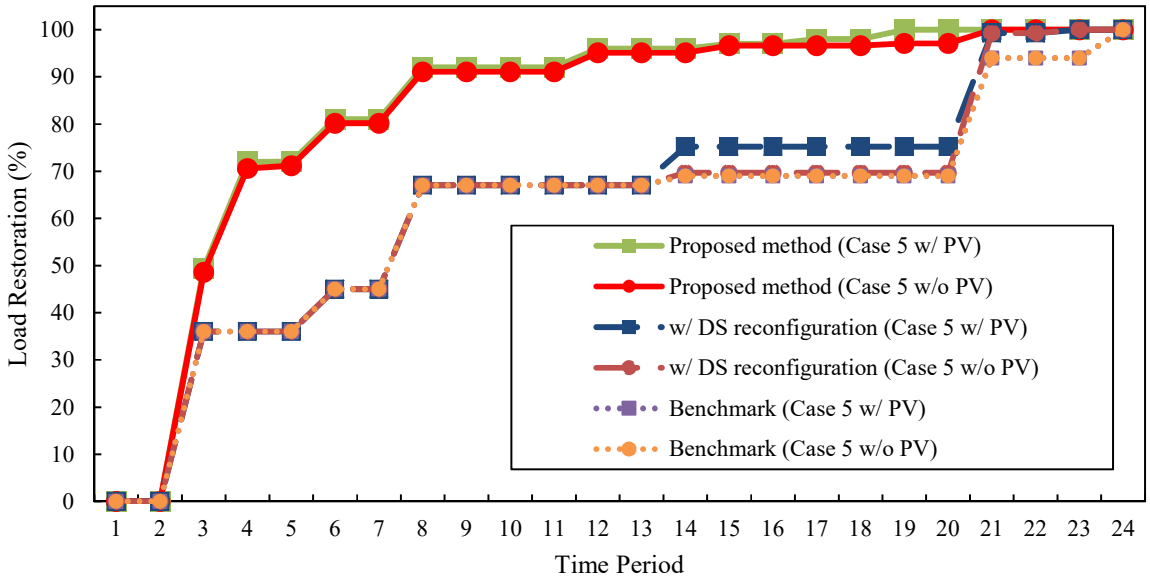

Figure 5.3: Load restoration in each time period using different strategies: Case Study 5

real power output is utilized since $t = 3$. The PV real power output is not utilized at the beginning which is because of the non-decreasing recovery constraint (Equation (3.31)). In this case, the proposed method remains effective. The contribution from PV generation on improving the recovery rate is not significant even though the available PV real power output is fully utilized, as shown in Figures 5.3 and 5.4. In contrast, Figure 5.4 demonstrates that the real power output of MEG 1 has significantly decreased, which means that the restored loads more rely on the supply from PV generation and thus the energy from MEG 1 is saved.

Case Study 5 demonstrates that the PV generation in the DS can help save the energy from MPSs during the DS restoration process.

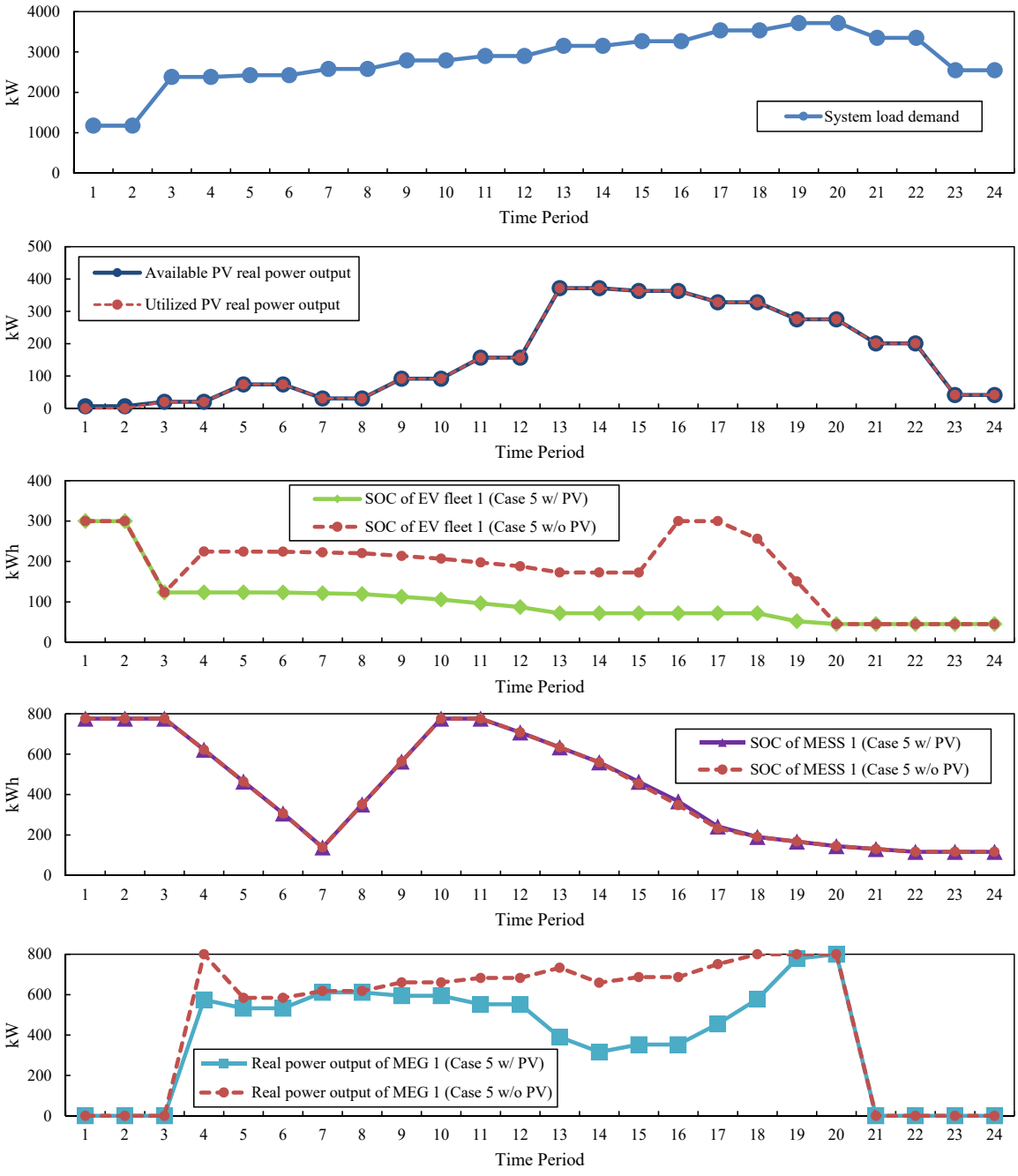

Figure 5.4: SOC of EV fleet 1, SOC of MESS 1, real power output of MEG 1, system load demand and PV real power output in each time period: Case Study 5 with PV

5.2.4 Case Study 6: Damage Scenario 3 with Different Repair Plans

The damage scenario, the same as that in case study 3 (Figure 3.15), is adopted here, but the repair strategy is changed as presented in Table 5.9. According to the repair plan, the whole restoration process is set as **T** = 24 time periods while each time period lasts $\Delta t = 0.5hr$.

Table 5.9: Repair Order of Damaged Branches in Case Study 6

Time period (t)	3	7	12	14	16	18	20	24
Repaired branch	16-17	11-12	29-30	27-28	6-26	6-7	4-5	21-22

The proposed MPS dispatch method is exploited to both systems with and without PV farm. The MPS dispatch strategy for the DS without PV farm is obtained as demonstrated in Table 5.10. The MPS dispatch strategy for the DS with PV farm is obtained as presented in Table 5.11. The obtained remote-controlled switch (RCS) actions for both systems with and without PV generation are the same, as shown in Table 5.12.

Table 5.10: Location of MPSs in Each Time Period in Case Study 6 without PV Generation

---		Time Period												
		1	2	3	4	5	6	7	8	9~13	14	15	16	17~24
MPS	EV 1	node 1	→	node 8				→		node 33				
	MESS 1	node 1	→		node 15			→	node 29		→	node 21	→	node 29
	MEG 1	node 1	→		node 15									

Table 5.11: Location of MPSs in Each Time Period in Case Study 6 with PV Generation

---		Time Period								
		1	2	3	4~5	6	7	8~12	13~14	15~24
MPS	EV 1	node 1	→		node 8	→		node 33	→	node 8
	MESS 1	node 1	→		node 15		→	node 29		
	MEG 1	node 1	→		node 15					

The recovery rate achieved in the Case Study 6 in both systems (with and without PV generation) in each time period is depicted in Figure 5.5. The proposed MPS dispatch method coordinated with PV generation improve the recovery rate around 7% higher than that in the case without PV generation at $t = 12 \sim 16$.

Table 5.12: Distribution System (DS) Reconfiguration Actions in Case Study 6

Time period	Remote-controlled switch (RCS) actions
t = 1	close branch 9-15, 12-22, 18-33, 25-29
t = 7	open branch 14-15
t = 18	open branch 18-33
t = 20	close branch 14-15, open branch 9-15, 25-29
t = 24	open branch 12-22

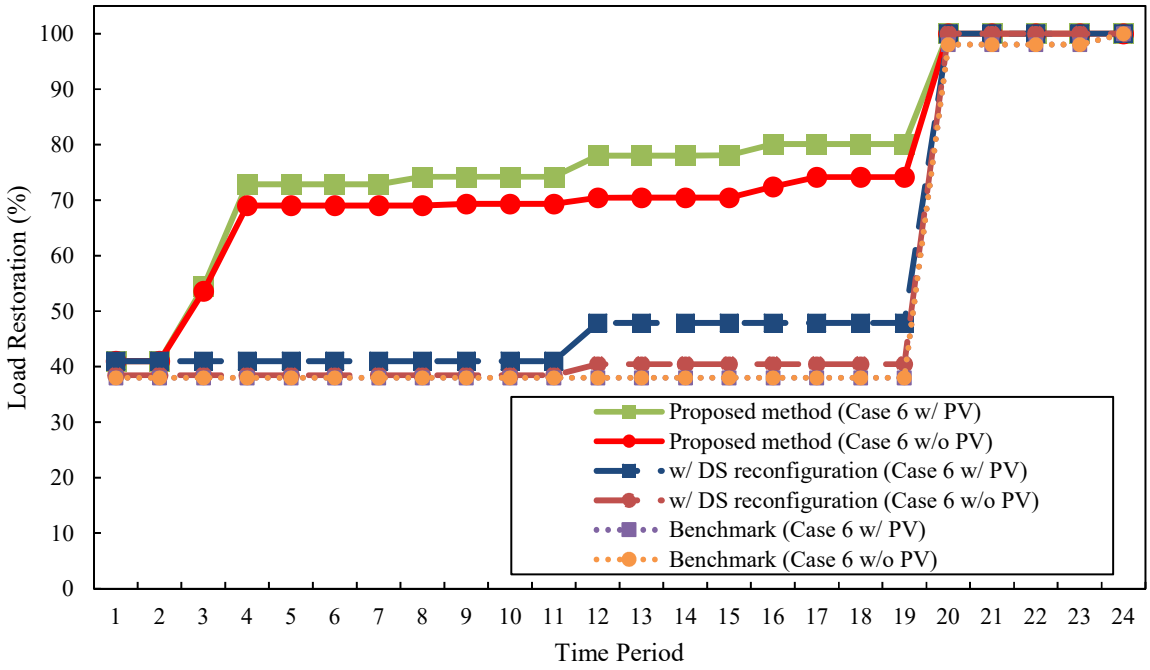

Figure 5.5: Load restoration in each time period using different strategies: Case Study 6

The curves for the system load demand, SOC of EV fleet 1, SOC of MESS 1, the real power output of MEG 1 as well as the utilized real power output from the solar farm are demonstrated in Figure 5.6. The PV real power output is utilized since $t = 3$. The PV real power output is not utilized at the beginning which is because of the non-decreasing recovery constraint (Equation (3.31)).

Case Study 6 indicates that the proposed MPS dispatch method remains valid under different repair strategies. Moreover, the coordination of PV generation in DS with the proposed method can make a significant contribution to DS restoration in the case where certain repair plans are applied.

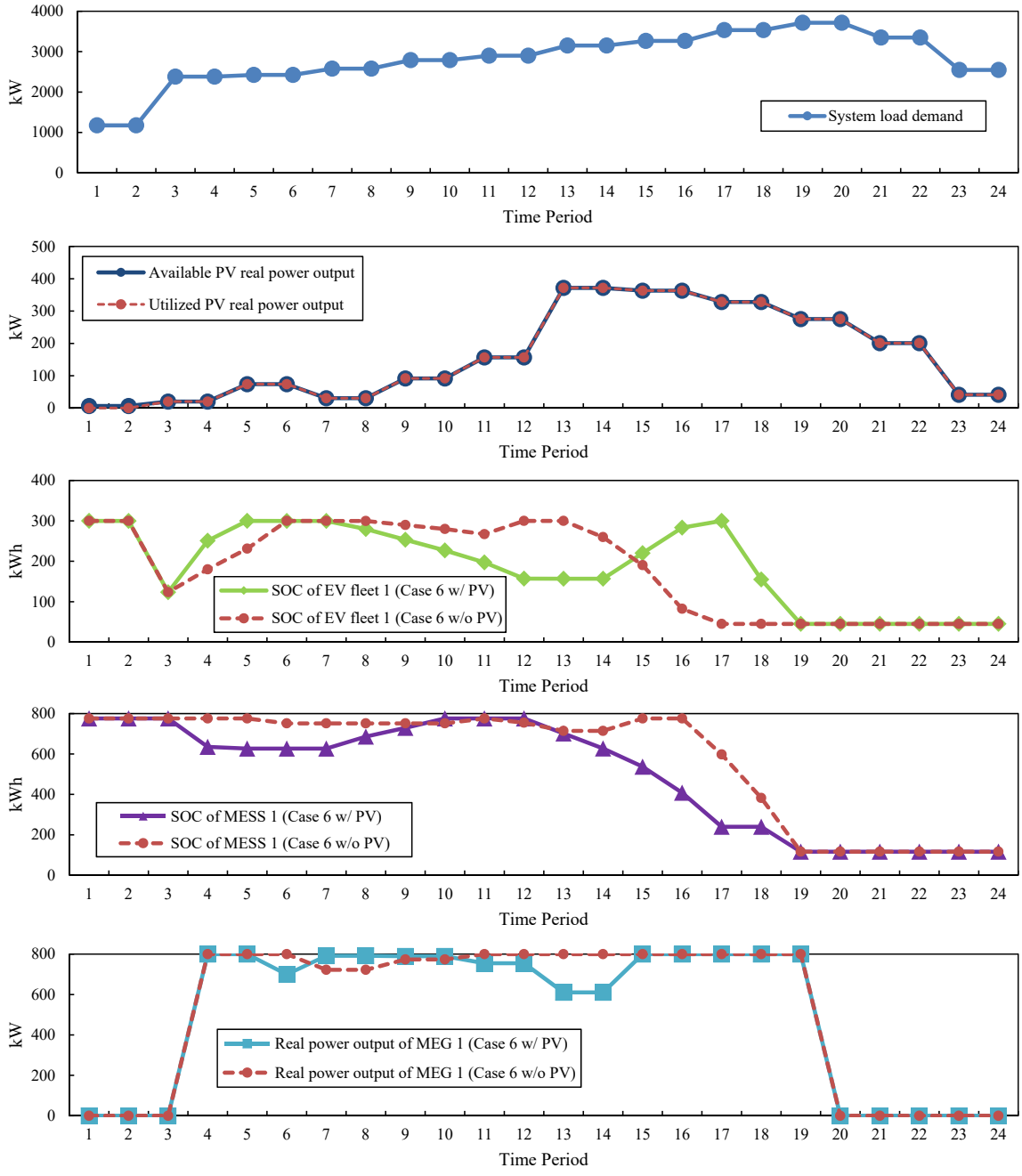

Figure 5.6: SOC of EV fleet 1, SOC of MESS 1, real power output of MEG 1, system load demand and PV real power output in each time period: Case Study 6 with PV

5.3 The Impact of Different Repair Plans on the Proposed MPS Dispatch Method in Improving the DS Resilience

The load restoration in Case Study 2 and Case Study 5 is presented in Tables 5.13 and 5.14. Table 5.13 reveals that the repair plan in Case Study 5 is worse than that in Case Study 2 since the recovery rate is quite low in the majority of time intervals during the DS restoration without the supply from MPSs. However, with the MPS dispatch method and the supply of MPSs, the recovery rate in Case Study 5 significantly improves and it reaches to 100% earlier than that in Case Study 2. Similarly, Table 5.14 demonstrates that with PV generation and MPS dispatch, the "worse" repair plan in Case Study 5 obtain a higher recovery rate than that in Case Study 2 and fully restore the entire system earlier. This finding reveals that the MPS dispatch and PV generation can make a significant contribution to DS restoration when the repair plan is poor. Furthermore, different repair strategy coordinated with the proposed MPS dispatch method and PV generation may further facilitate the DS restoration and improve the DS resilience in the face of alarming HILP events.

5.4 Conclusion

In this chapter, the impact of the repair strategy on the effectiveness of the proposed MPS dispatch method and PV generation in facilitating the DS restoration is investigated. The three case studies reveal that the proposed MPS dispatch method remains effective when different repair strategies are exploited. When different repair strategies are applied, the routing and scheduling of MPSs change. In addition, Case Study 5 reveals that when an appropriate repair strategy is employed, the proposed method can further facilitate the recovery speed and PV generation can help save the energy of the MPSs during the restoration process.

Table 5.13: Load Restoration Comparison Between Case Study 2 and Case Study 5 without PV Generation

Time Period (t)	No PV Generation			
	Case 2		Case 5	
	w/ DS reconfiguration	Proposed method	w/ DS reconfiguration	Proposed method
1	0	0	0	0
2	0	0	0	0
3	36	46.52643876	36	48.60456537
4	36	68.02694643	36	70.62256052
5	42.96094513	74.98789156	36	71.1597458
6	42.96094513	74.98789156	45	80.1597458
7	42.96094513	74.98789156	45	80.1597458
8	51.96094513	83.98789156	67	91.09445041
9	51.96094513	84.21221432	67	91.09445041
10	75.7920419	98.4101963	67	91.09445041
11	75.7920419	98.4101963	67	91.09445041
12	75.7920419	98.4101963	67	95.09445041
13	97.7920419	98.96094513	67	95.09445041
14	97.7920419	98.96094513	69.6917683	95.09445041
15	97.7920419	98.96094513	69.6917683	96.62268222
16	97.7920419	98.96094513	69.6917683	96.62268222
17	97.7920419	98.96094513	69.6917683	96.62268222
18	97.7920419	98.96094513	69.6917683	96.62268222
19	98.96094513	98.96094513	69.6917683	97.09445041
20	98.96094513	98.96094513	69.6917683	97.09445041
21	99.28507263	99.28507263	99.28507263	100
22	99.28507263	99.28507263	99.28507263	100
23	100	100	100	100
24	100	100	100	100

Table 5.14: Load Restoration Comparison Between Case Study 2 and Case Study 5 with PV Generation

Time Period (t)	PV Generation			
	Case 2		Case 5	
	w/ DS reconfiguration	Proposed method	w/ DS reconfiguration	Proposed method
1	0	0	0	0
2	0	0	0	0
3	36	46.44925117	36	49.44834439
4	36	67.94975884	36	72
5	42.96094513	77.50616255	36	72.06529539
6	42.96094513	77.50616255	45	81.06529539
7	42.96094513	77.50616255	45	81.06529539
8	51.96094513	86.50616255	67	92
9	51.96094513	87.49705575	67	92
10	75.7920419	98.4101963	67	92
11	75.7920419	98.4101963	67	92
12	75.7920419	98.4101963	67	96
13	97.7920419	98.96094513	67	96
14	97.7920419	98.96094513	75.22651986	96
15	97.7920419	98.96094513	75.22651986	97.01795366
16	97.7920419	98.96094513	75.22651986	97.01795366
17	97.7920419	98.96094513	75.22651986	98
18	97.7920419	98.96094513	75.22651986	98
19	98.96094513	98.96094513	75.22651986	100
20	98.96094513	98.96094513	75.22651986	100
21	99.28507263	99.28507263	99.28507263	100
22	99.28507263	99.28507263	99.28507263	100
23	100	100	100	100
24	100	100	100	100

Chapter 6: Conclusion

6.1 Conclusion

As the increasing trend of the occurrence of natural hazards is realized, the high-impact low-probability (HILP) events challenge the power system more frequently. When the prolonged electric outages caused by HILP events severely influence society and economics, the conventional reliability view is not sufficient. It is significant to efficiently and smartly exploit the existing resources to maintain the continuous supply of electricity to the critical loads. While the stationary storage systems and the distributed energy resources (DERs) in the power system can be the emergency energy source during the long-duration outages, only the surrounding loads can be supplied. In order to shorten the prolonged outages and improve the grid resilience, this research investigated the potential of utilizing the flexibility of mobile power sources (MPSs) to supply critical loads in multiple areas during the outages. When MPSs are exhausted due to the disadvantage of the limited capacity, the DERs, e.g. photovoltaic generation (PV), in the system can be the supplement of the energy. Hence, the cooperation and coordination of the MPSs with PV generation is also studied in this research. Besides, the repair plan considerably affects the recovery speed and the recovery level of the system after HILP events. The impact of different repair strategies on the contribution of the proposed MPS dispatch method and the PV generation to promoting the restoration is investigated in this thesis.

In Chapter 3, the dispatch of MPSs coordinated with the distribution system (DS) reconfiguration during the restoration process is formulated as a mixed-integer linear programming (MILP) model to derive the optimal MPS dispatch strategy during the system restoration. Three case studies with different damage scenarios verified the effectiveness of the proposed MPS dispatch, using the modified IEEE 33-node test system, and considering the dynamic load variations over time.

In Chapter 4, in order to explore the effectiveness of the proposed method in a DS that incorporates solar farms, the coordination of the MPS dispatch and PV generation is also formulated as a MILP model to derive the optimal MPS dispatch strategy. Taking PV generation into account, case studies with different damage scenarios demonstrated the effectiveness of the proposed method. The numerical results in the case with and without PV generation were compared. It demonstrated that when exploiting the proposed method, the PV generation may not have a significant contribution to the DS restoration under some given repair strategies.

In Chapter 5, the impact of the repair strategy on the proposed MPS dispatch method was studied. The same test system and damage scenarios were applied in the case studies with different repair strategies. The proposed method remains effective under different repair strategies. The numerical results revealed the contribution of PV generation and MPS dispatch to facilitating the system restoration which was concluded dependent on the choice of the repair strategy.

6.2 Future Research

The future work may include investigating the co-optimization of the MPS dispatch, PV generation, and the repair strategy in facilitating the power system restoration during the post-disaster outage scenarios.

Future research may also include incorporating the formulation for predicting the uncertainty of the PV generation based on historical data when applying the proposed MPS dispatch method.

Bibliography

[1] B. Zhang, P. Dehghanian, and M. Kezunovic, "Optimal allocation of pv generation and battery storage for enhanced resilience," *IEEE Transactions on Smart Grid*, vol. 10, no. 1, pp. 535–545, 2017.

[2] P. Dehghanian, S. Aslan, and P. Dehghanian, "Maintaining electric system safety through an enhanced network resilience," *IEEE Transactions on Industry Applications*, vol. 54, no. 5, pp. 4927–4937, 2018.

[3] R. J. Campbell, "Weather-related power outages and electric system resiliency," Congressional Research Service, Library of Congress Washington, DC, 2012.

[4] A. T. Crane, "Physical vulnerability of electric systems to natural disaster and sabotage," 1990.

[5] Major California earthquakes, [Online] Available: `https://cnico.com/pgs/earthquake/earth3.aspx`.

[6] X. Dong, M. Shinozuka, and S. Chang, "Utility power network systems," in *Proc. of 13th World Conference on Earthquake Engineering*, 2004.

[7] Y. Kitagawa and H. Hiraishi, "Overview of the 1995 hyogo-ken nanbu earthquake and proposals for earthquake mitigation measures," *Journal of Japan association for earthquake engineering*, vol. 4, no. 3, pp. 1–29, 2004.

[8] M. Ghafory-Ashtiany and M. Hosseini, "Post-bam earthquake: recovery and reconstruction," *Natural Hazards*, vol. 44, no. 2, pp. 229–241, 2008.

[9] J. Eidinger, "Wenchuan earthquake impact to power systems," in *TCLEE 2009: Lifeline Earthquake Engineering in a Multihazard Environment*, pp. 1–12, 2009.

[10] Y. Kuwata and Y. Ohnishi, "Emergency-response capacity of lifelines after wide-area earthquake disasters," in *Proc. Int. Symp. Eng. Lessons Learned Great East Jpn. Earthquake*, pp. 1475–1486, 2011.

[11] M. Zare, F. Kamranzad, I. Parcharidis, and V. Tsironi, "Preliminary report of mw7. 3 sarpol-e zahab, iran earthquake on november 12, 2017," *Tehran, Iran: International Institute of Earthquake Engineering and Seismology (IIEES)*, 2017.

[12] P. Hines, J. Apt, and S. Talukdar, "Large blackouts in north america: Historical trends and policy implications," *Energy Policy*, vol. 37, no. 12, pp. 5249–5259, 2009.

[13] E. National Academies of Sciences, Medicine, *et al.*, *Enhancing the resilience of the Nation's electricity system*. National Academies Press, 2017.

[14] P. Hoffman, W. Bryan, and A. Lippert, "Comparing the impacts of the 2005 and 2008 hurricanes on us energy infrastructure," *US Department of Energy*, 2009.

[15] B. Ball, "Rebuilding electrical infrastructure along the gulf coast: A case study," *BRIDGE-WASHINGTON-NATIONAL ACADEMY OF ENGINEERING-*, vol. 36, no. 1, p. 21, 2006.

[16] M.-B. Hart, "Tropical storm irene delivered a sunday punch to connecticut," 2011.

[17] E. S. Blake, T. B. Kimberlain, R. J. Berg, J. P. Cangialosi, and J. L. Beven Ii, "Tropical cyclone report: Hurricane sandy," *National Hurricane Center*, vol. 12, pp. 1–10, 2013.

[18] M. Panteli and P. Mancarella, "The grid: Stronger bigger smarter?: Presenting a conceptual framework of power system resilience," *IEEE Power Energy Mag*, vol. 13, no. 3, pp. 58–66, 2015.

[19] D. Sandalow, "Hurricane sandy and our energy infrastructure," *US Department of Energy*, November 2012.

[20] Z. Bie, Y. Lin, G. Li, and F. Li, "Battling the extreme: A study on the power system resilience," *Proceedings of the IEEE*, vol. 105, no. 7, pp. 1253–1266, 2017.

[21] "The 1998 ice storm: 10-year retrospective," *Risk management Solutions (RMS)*, 2008.

[22] "Service assessment: The ice storm and flood of january 1998," *National Weather Service*, 1998.

[23] D. U. Case, "Analysis of the cyber attack on the ukrainian power grid," *Electricity Information Sharing and Analysis Center (E-ISAC)*, 2016.

[24] E. O. of the President. Council of Economic Advisers, *Economic Benefits of Increasing Electric Grid Resilience to Weather Outages*. The Council, 2013.

[25] P. Dehghanian, B. Zhang, T. Dokic, and M. Kezunovic, "Predictive risk analytics for weather-resilient operation of electric power systems," *IEEE Transactions on Sustainable Energy*, vol. 10, no. 1, pp. 3–15, 2019.

[26] N. R. Council *et al.*, *The resilience of the electric power delivery system in response to terrorism and natural disasters: summary of a workshop*. National Academies Press, 2013.

[27] P. Interconnection, "Pjm's evolving resource mix and system reliability," *March*, vol. 30, p. 2017, 2017.

[28] B. H. Obama, "Critical infrastructure security and resilience," *Presidential Policy Directive/PPD-21*, 2013.

[29] M. Chaudry, P. Ekins, K. Ramachandran, A. Shakoor, J. Skea, G. Strbac, X. Wang, and J. Whitaker, "Building a resilient uk energy system," 2011.

[30] H. H. Willis and K. Loa, "Measuring the resilience of energy distribution systems," *RAND Corporation: Santa Monica, CA, USA*, 2015.

[31] A. Berkeley, M. Wallace, and C. COO, "A framework for establishing critical infrastructure resilience goals," *Final Report and Recommendations by the Council, National Infrastructure Advisory Council*, 2010.

[32] C. Office, "Keeping the country running: natural hazards and infrastructure," 2011.

[33] M. McGranaghan, M. Olearczyk, and C. Gellings, "Enhancing distribution resiliency: Opportunities for applying innovative technologies," *EPRI: Palo Alto, CA, USA*, 2013.

[34] M. Panteli, D. N. Trakas, P. Mancarella, and N. D. Hatziargyriou, "Power systems resilience assessment: Hardening and smart operational enhancement strategies," *Proceedings of the IEEE*, vol. 105, no. 7, pp. 1202–1213, 2017.

[35] B. Zhang, P. Dehghanian, and M. Kezunovic, "Simulation of weather impacts on the wholesale electricity market," in *10th International Conference on Deregulated Electricity Market Issues in South Eastern Europe (DEMSEE)*, pp. 1–6, 2015.

[36] T. Dokic, P. Dehghanian, P.-C. Chen, M. Kezunovic, Z. Medina-Cetina, J. Stojanovic, and Z. Obradovic, "Risk assessment of a transmission line insulation breakdown due to lightning and severe weather," in *The 49th Hawaii International Conference on System Science (HICSS)*, pp. 1–8, 2016.

[37] B. Zhang, P. Dehghanian, and M. Kezunovic, "Spatial-temporal solar power forecast through gaussian conditional random fields," in *IEEE Power and Energy Society (PES) General Meeting*, pp. 1–5, 2016.

[38] P. Dehghanian, S. Aslan, and P. Dehghanian, "Quantifying power system resiliency improvement using network reconfiguration," in *IEEE 60th International Midwest Symposium on Circuits and Systems (MWSCAS)*, pp. 1–5, IEEE, 2017.

[39] *Disaster Resilience: A National Imperative*. Washington, DC: The National Academies Press, 2012.

[40] Z. Tayebi and M. Bakhshoodeh, "Factors affecting procrastination of rural women's decision making to participate in micro credit funds and self-financed groups in fars," *Iranian Journal of Rural Economics*, vol. 2, no. 4, pp. 1–14, 2015.

[41] Z. Tayebi and B. Najafi, "Determination of vulnerability and risk management in microcredit programs: applying risk sharing model and panel data approach," *Iranian Journal of Agricultural Economics*, vol. 5, no. 4, pp. 25–49, 2012.

[42] Z. Tayebi and L. E. Fulginiti, "Agricultural productivity and climate change in the greater middle east," 2016.

[43] Z. Tayebi and G. Onel, "Revisiting the neoclassical model of out-farm migration: Evidence from nonlinear panel time series data," *Agricultural and Applied Economics Association Annual Meeting*, 2017.

[44] Z. Tayebi and G. Onel, "Microcredit programs, poverty and vulnerability in rural iran," *Southern Agricultural Economics Association Annual Meeting*, 2016.

[45] J.-P. Watson, R. Guttromson, C. Silva-Monroy, R. Jeffers, K. Jones, J. Ellison, C. Rath, J. Gearhart, D. Jones, T. Corbet, *et al.*, "Conceptual framework for developing resilience metrics for the electricity oil and gas sectors in the united states," *Sandia National Laboratories, Albuquerque, NM (United States), Tech. Rep*, 2014.

[46] F. Pourahmadi, H. Heidarabadi, S. H. Hosseini, and P. Dehghanian, "Dynamic uncertainty set characterization for bulk power grid flexibility assessment," *IEEE Systems Journal*, 2019.

[47] J. C. Whitson and J. E. Ramirez-Marquez, "Resiliency as a component importance measure in network reliability," *Reliability Engineering & System Safety*, vol. 94, no. 10, pp. 1685 – 1693, 2009.

[48] M. Shinozuka, S. E. Chang, T.-C. Cheng, M. Feng, T. D. O'rourke, M. A. Saadeghvaziri, X. Dong, X. Jin, Y. Wang, and P. Shi, "Resilience of integrated power and water systems," *Seismic Evaluation and Retrofit of Lifeline Systems, Articles from MCEER's Research Progress and Accomplishments Volumes*, pp. 65–86, 2004.

[49] M. Panteli and P. Mancarella, "Operational resilience assessment of power systems under extreme weather and loading conditions," in *2015 IEEE Power Energy Society General Meeting*, pp. 1–5, July 2015.

[50] P. J. Maliszewski and C. Perrings, "Factors in the resilience of electrical power distribution infrastructures," *Applied Geography*, vol. 32, no. 2, pp. 668 – 679, 2012.

[51] D. A. Reed, K. C. Kapur, and R. D. Christie, "Methodology for assessing the resilience of networked infrastructure," *IEEE Systems Journal*, vol. 3, pp. 174–180, June 2009.

[52] R. Francis and B. Bekera, "A metric and frameworks for resilience analysis of engineered and infrastructure systems," *Reliability Engineering & System Safety*, vol. 121, pp. 90 – 103, 2014.

[53] M. Panteli and P. Mancarella, "Modeling and evaluating the resilience of critical electrical power infrastructure to extreme weather events," *IEEE Systems Journal*, vol. 11, pp. 1733–1742, Sep. 2017.

[54] A. Kwasinski, "Quantitative model and metrics of electrical grids' resilience evaluated at a power distribution level," *Energies*, vol. 9, no. 2, p. 93, 2016.

[55] *Foundational Metrics Analysis*. Grid Modernization Laboratory Consortium (GMLC), May 2017.

[56] F. Pourahmadi and P. Dehghanian, "A game-theoretic loss allocation approach in power distribution systems with high penetration of distributed generations," *Mathematics*, vol. 6, no. 9, pp. 1–14, 2018.

[57] P. Dehghanian, M. Fotuhi-Firuzabad, F. Aminifar, and R. Billinton, "A comprehensive scheme for reliability centered maintenance implementation in power distribution systems- part ii: Numerical analysis," *IEEE Transactions on Power Delivery*, vol. 28, no. 2, pp. 771–778, 2013.

[58] S. Moradi, V. vahidinasab, M. Kia, and P. Dehghanian, "A mathematical framework for reliability-centered asset management implementation in microgrids," *International Transactions on Electrical Energy Systems*, 2018.

[59] H. Mirsaeedi, A. Fereidunian, S. M. Mohammadi-Hosseininejad, P. Dehghanian, and H. Lesani, "Long-term maintenance scheduling and budgeting in electricity distribution systems equipped with automatic switches," *IEEE Transactions on Industrial Informatics*, vol. 14, no. 5, pp. 1909–1919, 2018.

[60] M. Asghari Gharakheili, M. Fotuhi-Firuzabad, and P. Dehghanian, "A new multi-attribute support tool for identifying critical components in power transmission systems," *IEEE Systems Journal*, vol. 12, no. 1, pp. 316–327, 2018.

[61] F. Pourahmadi, M. Fotuhi-Firuzabad, and P. Dehghanian, "Application of game theory in reliability centered maintenance of electric power systems," *IEEE Transactions on Industry Applications*, vol. 53, no. 2, pp. 936–946, 2017.

[62] F. Pourahmadi, M. Fotuhi-Firuzabad, and P. Dehghanian, "Identification of critical generating units for maintenance: A game theory approach," *IET Generation, Transmission & Distribution*, vol. 10, no. 12, pp. 2942–2952, 2016.

[63] H. Sabouhi, A. Abbaspour, M. Fotuhi-Firuzabad, and P. Dehghanian, "Identifying critical components of combined cycle power plants for implementation of reliability centered maintenance," *IEEE CSEE Journal of Power and Energy Systems*, vol. 2, no. 2, pp. 87–97, 2016.

[64] H. Sabouhi, A. Abbaspour, M. Fotuhi-Firuzabad, and P. Dehghanian, "Reliability modeling and availability analysis of combined cycle power plants," *International Journal of Electrical Power and Energy Systems*, vol. 79, pp. 108–119, 2016.

[65] R. Ghorani, M. Fotuhi-Firuzabad, P. Dehghanian, and W. Li, "Identifying critical component for reliability centered maintenance management of deregulated power systems," *IET Generation, Transmission, and Distribution*, vol. 9, no. 9, pp. 828–837, 2015.

[66] P. Dehghanian, M. Fotuhi-Firuzabad, S. Bagheri-Shoraki, and A. Razi-Kazemi, "Critical component identification in reliability centered asset management of distribution power systems via fuzzy ahp," *IEEE Systems Journal*, vol. 6, no. 4, pp. 593–602, 2012.

[67] P. Dehghanian, M. Fotuhi-Firuzabad, F. Aminifar, and R. Billinton, "A comprehensive scheme for reliability centered maintenance implementation in power distribution systems- part i: Methodology," *IEEE Transactions on Power Delivery*, vol. 28, no. 2, pp. 761–770, 2013.

[68] P. Dehghanian, M. Fotuhi-Firuzabad, and A. Razi-Kazemi, "An approach for critical component identification in reliability-centered maintenance of power distribution systems based on analytical hierarchical process," in *The 21st International Conference and Exhibition on Electricity Distribution (CIRED)*, pp. 1–4, 2011.

[69] P. Dehghanian and M. Fotuhi-Firuzabad, "A reliability-oriented outlook on the critical components of power distribution systems," in *The 9th IET International Conference on Advances in Power System Control, Operation, and Management (APSCOM)*, pp. 1–6, 2011.

[70] P. Dehghanian, M. Kezunovic, G. Gurrala, and Y. Guan, "Security-based circuit breaker maintenance management," in *IEEE Power and Energy Society (PES) General Meeting*, pp. 1–5, 2013.

[71] K. M. Guan, Yufan, P. Dehghanian, and G. Gurrala, "Assessing circuit breaker life cycle using condition-based data," in *IEEE Power and Energy Society (PES) General Meeting*, pp. 1–5, 2013.

[72] P. Dehghanian, Y. Guan, and M. Kezunovic, "Real-time life-cycle assessment of circuit breakers for maintenance using online condition monitoring data," in *IEEE/IAS 54th Industrial and Commercial Power Systems (I&CPS) Technical Conference*, pp. 1–8, IEEE, 2018.

[73] F. Pourahmadi, M. Fotuhi-Firuzabad, and P. Dehghanian, "Identification of critical components in power systems: A game theory application," in *IEEE Industry Application Society (IAS) Annual Meeting*, pp. 1–6, 2016.

[74] P. Dehghanian, T. Popovic, and M. Kezunovic, "Circuit breaker operational health assessment via condition monitoring data," in *The 46th North American Power Symposium*, pp. 1–6, 2014.

[75] P. Dehghanian, M. Moeini-Aghtaie, M. Fotuhi-Firuzabad, and R. Billinton, "A practical application of the delphi method in maintenance-targeted resource allocation of distribution utilities," in *The 13th International Conference on Probabilistic Methods Applied to Power Systems (PMAPS)*, pp. 1–6, 2014.

[76] P. Dehghanian and M. Kezunovic, "Cost/benefit analysis for circuit breaker maintenance planning and scheduling," in *The 45th North American Power Symposium (NAPS)*, pp. 1–6, 2013.

[77] P. Dehghanian, Y. Guan, and M. Kezunovic, "Real-time life-cycle assessment of high voltage circuit breakers for maintenance using online condition monitoring data," *IEEE Transactions on Industry Applications*, vol. 55, no. 2, pp. 1135–1146, 2019.

[78] P. Dehghanian and M. Kezunovic, "Probabilistic decision making for the bulk power system optimal topology control," *IEEE Transactions on Smart Grid*, vol. 7, no. 4, pp. 2071–2081, 2016.

[79] P. Dehghanian, Y. Wang, G. Gurrala, E. Moreno-Centeno, and P. Kezunovic, "Flexible implementation of power system corrective topology control," *Electric Power System Research*, vol. 128, pp. 79–89, 2015.

[80] M. Alhazmi, P. Dehghanian, S. Wang, and B. Shinde, "Power grid optimal topology control considering correlations of system uncertainties," in *2014 IEEE Conference and Expo Transportation Electrification Asia-Pacific (ITEC Asia-Pacific)IEEE/IAS 55th Industrial and Commercial Power Systems (I&CPS) Technical Conference*, pp. 1–7, IEEE, 2019.

[81] M. Kezunovic, T. Popovic, G. Gurrala, P. Dehghanian, A. Esmaeilian, and M. Tasdighi, "Reliable implementation of robust adaptive topology control," in *The 47th Hawaii International Conference on System Science (HICSS)*, pp. 1–10, 2014.

[82] P. Dehghanian and M. Kezunovic, "Impact assessment of power system topology control on system reliability," in *IEEE Conference on Intelligent Systems Applications to Power Systems (ISAP)*, pp. 1–6, 2015.

[83] P. Dehghanian and M. Kezunovic, "Probabilistic impact of transmission line switching on power system operating states," in *IEEE Power and Energy Society (PES) Transmission and Distribution (T&D) Conference and Exposition*, pp. 1–6, 2016.

[84] M. Nazemi, M. Moeini-Aghtaie, M. Fotuhi-Firuzabad, and P. Dehghanian, "Energy storage planning for enhanced resilience of power distribution networks against earthquakes," *IEEE Transactions on Sustainable Energy*, pp. 1–1, 2019.

[85] B. Zhang, P. Dehghanian, and M. Kezunovic, "Optimal allocation of pv generation and battery storage for enhanced resilience," *IEEE Transactions on Smart Grid*, vol. 10, pp. 535–545, Jan 2019.

[86] *A Smarter Electric Circuit: Electric Power Board of Chattanooga Makes the Switch*. Department of Energy, 2011.

[87] A. Razi-Kazemi and P. Dehghanian, "A practical approach to optimal rtu placement in power distribution systems incorporating fuzzy sets theory," *International Journal of Electrical Power and Energy Systems*, vol. 37, no. 1, pp. 31–42, 2012.

[88] P. Dehghanian, A. Razi-Kazemi, and M. Fotuhi-Firuzabad, "Optimal rtu placement in power distribution systems using a novel method based on analytical hierarchical process (ahp)," in *The 10th International IEEE Conference on Environmental and Electrical Engineering (EEEIC)*, pp. 1–6, 2011.

[89] M. Moeini-Aghtaie, P. Dehghanian, and S. H. Hosseini, "Optimal distributed generation placement in a restructured environment via a multi-objective optimization

approach," in *16th Conference on Electric Power Distribution Networks (EPDC)*, pp. 1–6, 2011.

[90] A. Razi-Kazemi, P. Dehghanian, and G. Karami, "A probabilistic approach for remote terminal unit placement in power distribution systems," in *The 33rd IEEE International Telecommunications Energy Conference (INTELEC)*, pp. 1–6, 2011.

[91] P. Dehghanian, A. Razi-Kazemi, and G. Karami, "Incorporating experts knowledge in rtu placement procedure using fuzzy sets theory- a practical approach," in *The 33rd IEEE International Telecommunications Energy Conference (INTELEC)*, pp. 1–6, 2011.

[92] M. Shojaei, V. Rastegar-Moghaddam, A. Razi-Kazemi, P. Dehghanian, and G. Karami, "A new look on the automation of medium voltage substations in power distribution systems," in *17th Conference on Electric Power Distribution Networks (EPDC)*, pp. 1–6, 2012.

[93] T. Becejac and P. Dehghanian, "Pmu multilevel end-to-end testing to assess synchrophasor measurements during faults," *IEEE Power and Energy Technology Systems Journal*, vol. 6, no. 1, pp. 71–80, 2019.

[94] S. Wang, P. Dehghanian, and B. Zhang, "A data-driven algorithm for online power grid topology change identification with pmus," in *IEEE Power and Energy Society (PES) General Meeting*, pp. 1–5, IEEE, 2019.

[95] S. Wang, P. Dehghanian, and Y. Gu, "A novel multi-resolution wavelet transform for online power grid waveform classification," in *The 1st IEEE International Conference on Smart Grid Synchronized Measurements and Analytics (SGSMA)*, pp. 1–6, IEEE, 2019.

[96] M. Kezunovic, A. Esmaeilian, T. Becejac, P. Dehghanian, and C. Qian, "Life-cycle management tools for synchrophasor systems: Why we need them and what they should entail," in *The 2016 IFAC CIGRE/CIRED Workshop on Control of Transmission and Distribution Smart Grids*, pp. 1–6, CIGRE, 2016.

[97] T. Becejac, P. Dehghanian, and M. Kezunovic, "Analysis of pmu algorithm errors during fault transients and out-of-step disturbances," in *IEEE Power and Energy Society (PES) Transmission & Distribution (T&D) Conference and Exposition Latin America*, pp. 1–6, IEEE, 2016.

[98] T. Becejac, P. Dehghanian, and M. Kezunovic, "Probabilistic assessment of pmu integrity for planning of periodic maintenance and testing," in *International Conference on Probabilistic Methods Applied to Power Systems (PMAPS)*, pp. 1–6, IEEE, 2016.

[99] T. Becejac, P. Dehghanian, and M. Kezunovic, "Impact of pmu errors on the synchrophasor-based fault location algorithms," in *48th North American Power Symposium (NAPS)*, pp. 1–6, IEEE, 2016.

[100] M. Kezunovic, P. Dehghanian, and J. Sztipanovits, "An incremental system-of-systems integration modelling of cyber-physical electric power systems," in *Grid of the Future Symposium, CIGRE US National Committee*, pp. 1–6, CIGRE, 2016.

[101] M. H. Rezaeian Koochi, P. Dehghanian, S. Esmaeili, P. Dehghanian, and S. Wang, "A synchrophasor-based decision tree approach for identification of most coherent generating units," in *The 44th Annual Conference of the IEEE Industrial Electronics Society (IECON)*, pp. 1–6, IEEE, 2018.

[102] K. P. Schneider, F. K. Tuffner, M. A. Elizondo, C.-C. Liu, Y. Xu, and D. Ton, "Evaluating the feasibility to use microgrids as a resiliency resource," *IEEE Transactions on Smart Grid*, vol. 8, no. 2, pp. 687–696, 2017.

[103] J. Lai, X. Lu, F. Wang, P. Dehghanian, and R. Tang, "Broadcast gossip algorithms for distributed peer-to-peer control in ac microgrids," *IEEE Transactions on Industry Applications*, 2019.

[104] C. Chen, J. Wang, F. Qiu, and D. Zhao, "Resilient distribution system by microgrids formation after natural disasters," *IEEE Transactions on Smart Grid*, vol. 7, pp. 958–966, March 2016.

[105] P. M. de Quevedo, J. Contreras, A. Mazza, G. Chicco, and R. Porumb, "Reliability assessment of microgrids with local and mobile generation, time-dependent profiles, and intraday reconfiguration," *IEEE Transactions on Industry Applications*, vol. 54, pp. 61–72, Jan 2018.

[106] Z. Wang and J. Wang, "Self-healing resilient distribution systems based on sectionalization into microgrids," *IEEE Transactions on Power Systems*, vol. 30, no. 6, pp. 3139–3149, 2015.

[107] L. Che and M. Shahidehpour, "Dc microgrids: Economic operation and enhancement of resilience by hierarchical control," *IEEE Transactions on Smart Grid*, vol. 5, no. 5, pp. 2517–2526, 2014.

[108] A. Khodaei, "Resiliency-oriented microgrid optimal scheduling," *IEEE Transactions on Smart Grid*, vol. 5, no. 4, pp. 1584–1591, 2014.

[109] Y. Xu, C.-C. Liu, K. P. Schneider, F. K. Tuffner, and D. T. Ton, "Microgrids for service restoration to critical load in a resilient distribution system," *IEEE Transactions on Smart Grid*, vol. 9, no. 1, pp. 426–437, 2018.

[110] R. Azizpanah-Abarghooee, P. Dehghanian, and V. Terzija, "A practical multi-area bi-objective environmental economic dispatch equipped with a hybrid gradient search method and improved jaya algorithm," *IET Generation, Transmission & Distribution*, vol. 10, no. 14, pp. 3580–3596, 2016.

[111] M. A. Saffari, M. S. Misaghian, M. Kia, Heidari, and P. Dehghanian, "Robust/stochastic optimization of energy arbitrage in smart microgrids using electric vehicles," *Electric Power Systems Research*, 2019.

[112] M. Moeini-Aghtaie, A. Abbaspour, M. Fotuhi-Firuzabad, and P. Dehghanian, "Optimized probabilistic phev demand management in the context of energy hubs," *IEEE Transactions on Power Delivery*, vol. 30, no. 2, pp. 996–1006, 2015.

[113] M. Moeini-Aghtaie, P. Dehghanian, M. Fotuhi-Firuzabad, and A. Abbaspour, "Multi-agent genetic algorithm: An online probabilistic view on economic dispatch of energy hubs constrained by wind availability," *IEEE Transactions on Sustainable Energy*, vol. 5, no. 2, pp. 699–708, 2014.

[114] P. Dehghanian, S. H. Hosseini, M. Moeini-Aghtaie, and S. Arabali, "Optimal siting of dg units in power systems from a probabilistic multi-objective optimization perspective," *International Journal of Electrical Power and Energy Systems*, vol. 51, pp. 14–26, 2013.

[115] M. Moeini-Aghtaie, A. Abbaspour, M. Fotuhi-Firuzabad, and P. Dehghanian, "Phev's centralized/decentralized charging control mechanisms: Requirements and impacts," in *The 45th North American Power Symposium (NAPS)*, pp. 1–6, 2013.

[116] S. Lei, C. Chen, Y. Li, and Y. Hou, "Resilient disaster recovery logistics of distribution systems: Co-optimize service restoration with repair crew and mobile power source dispatch," *IEEE Transactions on Smart Grid*, 2019.

[117] B. Wang, J. A. Camacho, G. M. Pulliam, A. H. Etemadi, and P. Dehghanian, "New reward and penalty scheme for electric distribution utilities employing load-based reliability indices," *IET Generation, Transmission & Distribution*, vol. 12, no. 15, pp. 3647–3654, 2018.

[118] S. Lei, C. Chen, H. Zhou, and Y. Hou, "Routing and scheduling of mobile power sources for distribution system resilience enhancement," *IEEE Transactions on Smart Grid*, 2018.

[119] J. Kim and Y. Dvorkin, "Enhancing distribution system resilience with mobile energy storage and microgrids," *IEEE Transactions on Smart Grid*, 2018.

[120] S. Yao, P. Wang, and T. Zhao, "Transportable energy storage for more resilient distribution systems with multiple microgrids," *IEEE Transactions on Smart Grid*, 2018.

[121] M. S. Misaghian, M. Saffari, M. Kia, A. Heidari, P. Dehghanian, and B. Wang, "Electric vehicles contributions to voltage improvement and loss reduction in microgrids," in *2018 North American Power Symposium (NAPS)*, pp. 1–6, IEEE, 2018.

[122] H. Gao, Y. Chen, S. Mei, S. Huang, and Y. Xu, "Resilience-oriented pre-hurricane resource allocation in distribution systems considering electric buses," *Proceedings of the IEEE*, vol. 105, no. 7, pp. 1214–1233, 2017.

[123] Y. Ma, T. Houghton, A. Cruden, and D. Infield, "Modeling the benefits of vehicle-to-grid technology to a power system," *IEEE Transactions on power systems*, vol. 27, no. 2, pp. 1012–1020, 2012.

[124] H. Shin and R. Baldick, "Plug-in electric vehicle to home (v2h) operation under a grid outage," *IEEE Transactions on Smart Grid*, vol. 8, no. 4, pp. 2032–2041, 2017.

[125] S. Lei, J. Wang, C. Chen, and Y. Hou, "Mobile emergency generator pre-positioning and real-time allocation for resilient response to natural disasters," *IEEE Transactions on Smart Grid*, vol. 9, no. 3, pp. 2030–2041, 2018.

[126] J. A. Taylor and F. S. Hover, "Convex models of distribution system reconfiguration," *IEEE Transactions on Power Systems*, vol. 27, no. 3, pp. 1407–1413, 2012.

[127] T. E. McDermott, I. Drezga, and R. P. Broadwater, "A heuristic nonlinear constructive method for distribution system reconfiguration," *IEEE Transactions on Power Systems*, vol. 14, no. 2, pp. 478–483, 1999.

[128] Y.-K. Wu, C.-Y. Lee, L.-C. Liu, and S.-H. Tsai, "Study of reconfiguration for the distribution system with distributed generators," *IEEE transactions on Power Delivery*, vol. 25, no. 3, pp. 1678–1685, 2010.

[129] R. S. Rao, K. Ravindra, K. Satish, and S. Narasimham, "Power loss minimization in distribution system using network reconfiguration in the presence of distributed generation," *IEEE transactions on power systems*, vol. 28, no. 1, pp. 317–325, 2013.

[130] S. Iwai, T. Kono, M. Hashiwaki, and Y. Kawagoe, "Use of mobile engine generators as source of back-up power," in *INTELEC 2009-31st International Telecommunications Energy Conference*, pp. 1–6, IEEE, 2009.

[131] M. Lavorato, J. F. Franco, M. J. Rider, and R. Romero, "Imposing radiality constraints in distribution system optimization problems," *IEEE Transactions on Power Systems*, vol. 27, no. 1, pp. 172–180, 2012.

[132] M. E. Baran and F. F. Wu, "Network reconfiguration in distribution systems for loss reduction and load balancing," *IEEE Transactions on Power delivery*, vol. 4, no. 2, pp. 1401–1407, 1989.

[133] W. Wei, F. Liu, S. Mei, and Y. Hou, "Robust energy and reserve dispatch under variable renewable generation," *IEEE Transactions on Smart Grid*, vol. 6, no. 1, pp. 369–380, 2015.

[134] X. Yan, C. Duan, X. Chen, and Z. Duan, "Planning of electric vehicle charging station based on hierarchic genetic algorithm," in *2014 IEEE Conference and Expo Transportation Electrification Asia-Pacific (ITEC Asia-Pacific)*, pp. 1–5, IEEE, 2014.

[135] A. Briones, J. Francfort, P. Heitmann, M. Schey, S. Schey, and J. Smart, "Vehicle-to-grid (v2g) power flow regulations and building codes review by the avta," *Idaho National Lab., Idaho Falls, ID, USA*, 2012.

[136] H. H. Abdeltawab and Y. A.-R. I. Mohamed, "Mobile energy storage scheduling and operation in active distribution systems," *IEEE Transactions on Industrial Electronics*, vol. 64, no. 9, pp. 6828–6840, 2017.

[137] S. Lei, J. Wang, and Y. Hou, "Remote-controlled switch allocation enabling prompt restoration of distribution systems," *IEEE Transactions on Power Systems*, vol. 33, pp. 3129–3142, May 2018.

[138] H. H. Abdeltawab and Y. A. I. Mohamed, "Mobile energy storage scheduling and operation in active distribution systems," *IEEE Transactions on Industrial Electronics*, vol. 64, pp. 6828–6840, Sep. 2017.

[139] S. Lei, J. Wang, C. Chen, and Y. Hou, "Mobile emergency generator pre-positioning and real-time allocation for resilient response to natural disasters," *IEEE Transactions on Smart Grid*, vol. 9, pp. 2030–2041, May 2018.

[140] G. Wang, X. Zhang, H. Wang, J. Peng, H. Jiang, Y. Liu, C. Wu, Z. Xu, and W. Liu, "Robust planning of electric vehicle charging facilities with an advanced evaluation method," *IEEE Transactions on Industrial Informatics*, vol. 14, pp. 866–876, March 2018.

[141] O. K. Siirto, A. Safdarian, M. Lehtonen, and M. Fotuhi-Firuzabad, "Optimal distribution network automation considering earth fault events," *IEEE Transactions on Smart Grid*, vol. 6, pp. 1010–1018, March 2015.

Appendix A: Case Study Data for Modified IEEE 33-Node Test System, Mobile Power Sources and Photovoltaic Generation

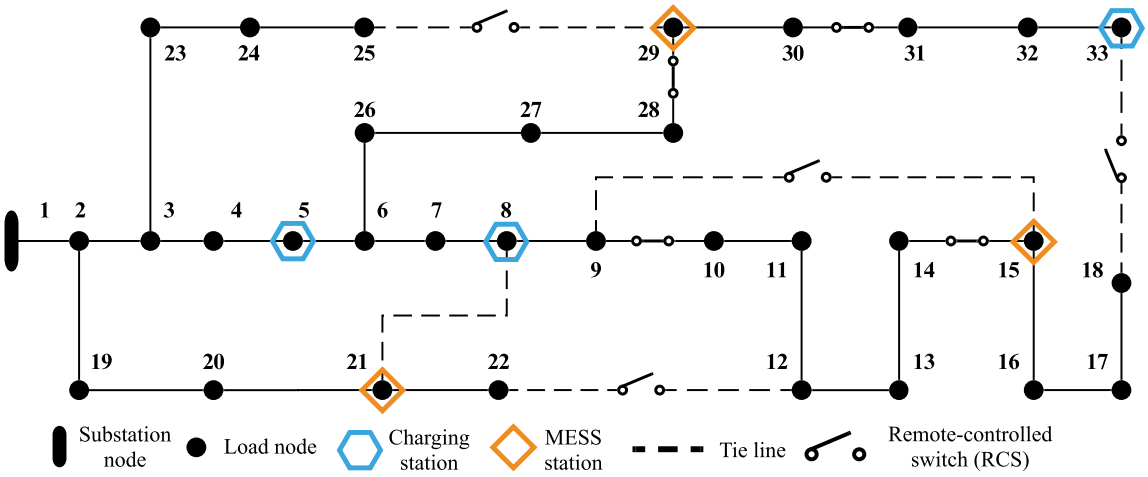

Figure A.1: The modified IEEE 33-node test system

Table A.1: IEEE 33-Node Test System Node Data

Node No.	Base Voltage (kV)	Voltage Max (kV)	Voltage Min (kV)	Nominal Load P (kV)	Nominal Load Q (kVar)	Priority*
1	12.66	13.293	12.027	0	0	4
2	12.66	13.293	12.027	100	60	2
3	12.66	13.293	12.027	90	40	4
4	12.66	13.293	12.027	120	80	7
5	12.66	13.293	12.027	60	30	4
6	12.66	13.293	12.027	60	20	9
7	12.66	13.293	12.027	200	100	9
8	12.66	13.293	12.027	200	100	5
9	12.66	13.293	12.027	60	20	10
10	12.66	13.293	12.027	60	20	3
11	12.66	13.293	12.027	45	30	5
12	12.66	13.293	12.027	60	35	4
13	12.66	13.293	12.027	60	35	6
14	12.66	13.293	12.027	120	80	8
15	12.66	13.293	12.027	60	10	5
16	12.66	13.293	12.027	60	20	5
17	12.66	13.293	12.027	60	20	1
18	12.66	13.293	12.027	90	40	7
19	12.66	13.293	12.027	90	40	4
20	12.66	13.293	12.027	90	40	7
21	12.66	13.293	12.027	90	40	10
22	12.66	13.293	12.027	90	40	6
23	12.66	13.293	12.027	90	50	9
24	12.66	13.293	12.027	420	200	6
25	12.66	13.293	12.027	420	200	8
26	12.66	13.293	12.027	60	25	1
27	12.66	13.293	12.027	60	25	7
28	12.66	13.293	12.027	60	20	1
29	12.66	13.293	12.027	120	70	5
30	12.66	13.293	12.027	200	600	7
31	12.66	13.293	12.027	150	70	5
32	12.66	13.293	12.027	210	100	4
33	12.66	13.293	12.027	60	40	6

$*$ The priority weights of loads are randomly generated ranging from $1 \sim 10$.

Table A.2: IEEE 33-Node Test System Distribution Line Data

Line No.	From Node	To Node	R (ohms)	X (ohms)	Maximum Capacity P (kW)	Maximum Capacity Q (kVAR)
1	1	2	0.0922	0.0470	4600	4600
2	2	3	0.4930	0.2511	4100	4100
3	3	4	0.3660	0.1864	2900	2900
4	4	5	0.3811	0.1941	2900	2900
5	5	6	0.8190	0.7070	2900	2900
6	6	7	0.1872	0.6188	1500	1500
7	7	8	0.7114	0.2351	1050	1050
8	8	9	1.0300	0.7400	1050	1050
9	9	10	1.0440	0.7400	1050	1050
10	10	11	0.1966	0.0650	1050	1050
11	11	12	0.3744	0.1298	1050	1050
12	12	13	1.4680	1.1550	500	500
13	13	14	0.5416	0.7129	450	450
14	14	15	0.5910	0.5260	300	300
15	15	16	0.7463	0.5450	250	250
16	16	17	1.2890	1.7210	250	250
17	17	18	0.7320	0.5740	100	100
18	2	19	0.1640	0.1565	500	500
19	19	20	1.5042	1.3554	500	500
20	20	21	0.4095	0.4784	210	210
21	21	22	0.7089	0.9373	110	110
22	3	23	0.4512	0.3083	1050	1050
23	23	24	0.8980	0.7091	1050	1050
24	24	25	0.8960	0.7011	500	500
25	6	26	0.2030	0.1034	1500	1500
26	26	27	0.2842	0.1447	1500	1500
27	27	28	1.0590	0.9337	1500	1500
28	28	29	0.8042	0.7006	1500	1500
29	29	30	0.5075	0.2585	1500	1500
30	30	31	0.9744	0.9630	500	500
31	31	32	0.3105	0.3619	500	500
32	32	33	0.3410	0.5302	100	100
33	8**	21**	2.0000	2.0000	1050*	1050*
34	9**	15**	2.0000	2.0000	1050*	1050*
35	12**	22**	2.0000	2.0000	500*	500*
36	18**	33**	0.5000	0.5000	500*	500*
37	25**	29**	0.5000	0.5000	1050*	1050*

$*$ The source data does not include the maximum capacities of Line 33 $\sim$ 37. The data listed here is assumed by the author.
$**$ denotes a tie-line

Table A.3: Mobile Power Sources Data

(a) Required Travel Time of MPSs Between Nodes

From Node	To Node	MPS		
		EV fleet 1	MESS 1	MEG 1
1	5	1	0	0
1	8	1	0	0
1	15	0	2	2
1	21	0	1	1
1	29	0	2	2
1	33	2	0	0
5	8	1	0	0
5	33	2	0	0
8	33	2	0	0
15	21	0	2	2
15	29	0	1	1
21	29	0	1	1

(b) Configuration of Electric Vehicle and Mobile Energy Storage System

Mobile Power Sources	State of Charge (SOC) Max (kWh)	State of Charge (SOC) Min (kWh)	Maximum Charging Power (kW)	Maximum Discharging Power (kW)	Maximum Reactive Power Output (kVar)
EV fleet 1	300	45	300	300	300
MESS 1	776	116.4	500	500	500

(c) Configuration of Mobile Emergency Generator

Mobile Power Source	Maximum Real Power Output (kW)	Maximum Reactive Power Output (kVar)
MEG 1	800	600

(d) Related Cost of Mobile Power Sources

Mobile Power Sources	Transportation Cost Coefficient	Power Rating Price ($/kWh)
EV fleet 1	1	0.1
MESS 1	1	0.1
MEG 1	1	0.1

Table A.4: IEEE 33-Node Test System Hourly Load Data (Part 1)

Real Power Demand (kW)	**Time Period (*t*)**							
Node No.	**1**	**2**	**3**	**4**	**5**	**6**	**7**	**8**
1	0	0	0	0	0	0	0	0
2	35.2422	35.2422	71.4027	71.4027	72.7467	72.7467	77.3493	77.3493
3	23.4948	23.4948	47.6018	47.6018	48.4978	48.4978	51.5662	51.5662
4	35.2422	35.2422	71.4027	71.4027	72.7467	72.7467	77.3493	77.3493
5	23.4948	23.4948	47.6018	47.6018	48.4978	48.4978	51.5662	51.5662
6	23.4948	23.4948	47.6018	47.6018	48.4978	48.4978	51.5662	51.5662
7	58.737	58.737	119.0045	119.0045	121.2445	121.2445	128.9155	128.9155
8	58.737	58.737	119.0045	119.0045	121.2445	121.2445	128.9155	128.9155
9	23.4948	23.4948	47.6018	47.6018	48.4978	48.4978	51.5662	51.5662
10	23.4948	23.4948	47.6018	47.6018	48.4978	48.4978	51.5662	51.5662
11	11.7474	11.7474	23.8009	23.8009	24.2489	24.2489	25.7831	25.7831
12	23.4948	23.4948	47.6018	47.6018	48.4978	48.4978	51.5662	51.5662
13	23.4948	23.4948	47.6018	47.6018	48.4978	48.4978	51.5662	51.5662
14	35.2422	35.2422	71.4027	71.4027	72.7467	72.7467	77.3493	77.3493
15	23.4948	23.4948	47.6018	47.6018	48.4978	48.4978	51.5662	51.5662
16	23.4948	23.4948	47.6018	47.6018	48.4978	48.4978	51.5662	51.5662
17	23.4948	23.4948	47.6018	47.6018	48.4978	48.4978	51.5662	51.5662
18	23.4948	23.4948	47.6018	47.6018	48.4978	48.4978	51.5662	51.5662
19	23.4948	23.4948	47.6018	47.6018	48.4978	48.4978	51.5662	51.5662
20	23.4948	23.4948	47.6018	47.6018	48.4978	48.4978	51.5662	51.5662
21	23.4948	23.4948	47.6018	47.6018	48.4978	48.4978	51.5662	51.5662
22	23.4948	23.4948	47.6018	47.6018	48.4978	48.4978	51.5662	51.5662
23	23.4948	23.4948	47.6018	47.6018	48.4978	48.4978	51.5662	51.5662
24	129.2214	129.2214	261.8099	261.8099	266.7379	266.7379	283.6141	283.6141
25	129.2214	129.2214	261.8099	261.8099	266.7379	266.7379	283.6141	283.6141
26	23.4948	23.4948	47.6018	47.6018	48.4978	48.4978	51.5662	51.5662
27	23.4948	23.4948	47.6018	47.6018	48.4978	48.4978	51.5662	51.5662
28	23.4948	23.4948	47.6018	47.6018	48.4978	48.4978	51.5662	51.5662
29	35.2422	35.2422	71.4027	71.4027	72.7467	72.7467	77.3493	77.3493
30	58.737	58.737	119.0045	119.0045	121.2445	121.2445	128.9155	128.9155
31	46.9896	46.9896	95.2036	95.2036	96.9956	96.9956	103.1324	103.1324
32	70.4844	70.4844	142.8054	142.8054	145.4934	145.4934	154.6986	154.6986
33	23.4948	23.4948	47.6018	47.6018	48.4978	48.4978	51.5662	51.5662

Table A.5: IEEE 33-Node Test System Hourly Load Data (Part 2)

Real Power Demand (kW)	**Time Period (t)**							
Node No.	**9**	**10**	**11**	**12**	**13**	**14**	**15**	**16**
1	0	0	0	0	0	0	0	0
2	83.715	83.715	86.9754	86.9754	94.5234	94.5234	97.9689	97.9689
3	55.81	55.81	57.9836	57.9836	63.0156	63.0156	65.3126	65.3126
4	83.715	83.715	86.9754	86.9754	94.5234	94.5234	97.9689	97.9689
5	55.81	55.81	57.9836	57.9836	63.0156	63.0156	65.3126	65.3126
6	55.81	55.81	57.9836	57.9836	63.0156	63.0156	65.3126	65.3126
7	139.525	139.525	144.959	144.959	157.539	157.539	163.2815	163.2815
8	139.525	139.525	144.959	144.959	157.539	157.539	163.2815	163.2815
9	55.81	55.81	57.9836	57.9836	63.0156	63.0156	65.3126	65.3126
10	55.81	55.81	57.9836	57.9836	63.0156	63.0156	65.3126	65.3126
11	27.905	27.905	28.9918	28.9918	31.5078	31.5078	32.6563	32.6563
12	55.81	55.81	57.9836	57.9836	63.0156	63.0156	65.3126	65.3126
13	55.81	55.81	57.9836	57.9836	63.0156	63.0156	65.3126	65.3126
14	83.715	83.715	86.9754	86.9754	94.5234	94.5234	97.9689	97.9689
15	55.81	55.81	57.9836	57.9836	63.0156	63.0156	65.3126	65.3126
16	55.81	55.81	57.9836	57.9836	63.0156	63.0156	65.3126	65.3126
17	55.81	55.81	57.9836	57.9836	63.0156	63.0156	65.3126	65.3126
18	55.81	55.81	57.9836	57.9836	63.0156	63.0156	65.3126	65.3126
19	55.81	55.81	57.9836	57.9836	63.0156	63.0156	65.3126	65.3126
20	55.81	55.81	57.9836	57.9836	63.0156	63.0156	65.3126	65.3126
21	55.81	55.81	57.9836	57.9836	63.0156	63.0156	65.3126	65.3126
22	55.81	55.81	57.9836	57.9836	63.0156	63.0156	65.3126	65.3126
23	55.81	55.81	57.9836	57.9836	63.0156	63.0156	65.3126	65.3126
24	306.955	306.955	318.9098	318.9098	346.5858	346.5858	359.2193	359.2193
25	306.955	306.955	318.9098	318.9098	346.5858	346.5858	359.2193	359.2193
26	55.81	55.81	57.9836	57.9836	63.0156	63.0156	65.3126	65.3126
27	55.81	55.81	57.9836	57.9836	63.0156	63.0156	65.3126	65.3126
28	55.81	55.81	57.9836	57.9836	63.0156	63.0156	65.3126	65.3126
29	83.715	83.715	86.9754	86.9754	94.5234	94.5234	97.9689	97.9689
30	139.525	139.525	144.959	144.959	157.539	157.539	163.2815	163.2815
31	111.62	111.62	115.9672	115.9672	126.0312	126.0312	130.6252	130.6252
32	167.43	167.43	173.9508	173.9508	189.0468	189.0468	195.9378	195.9378
33	55.81	55.81	57.9836	57.9836	63.0156	63.0156	65.3126	65.3126

Table A.6: IEEE 33-Node Test System Hourly Load Data (Part 3)

Real Power Demand (kW)	**Time Period (t)**							
Node No.	**17**	**18**	**19**	**20**	**21**	**22**	**23**	**24**
1	0	0	0	0	0	0	0	0
2	105.966	105.966	111.4509	111.4509	100.4544	100.4544	76.3959	76.3959
3	70.644	70.644	74.3006	74.3006	66.9696	66.9696	50.9306	50.9306
4	105.966	105.966	111.4509	111.4509	100.4544	100.4544	76.3959	76.3959
5	70.644	70.644	74.3006	74.3006	66.9696	66.9696	50.9306	50.9306
6	70.644	70.644	74.3006	74.3006	66.9696	66.9696	50.9306	50.9306
7	176.61	176.61	185.7515	185.7515	167.424	167.424	127.3265	127.3265
8	176.61	176.61	185.7515	185.7515	167.424	167.424	127.3265	127.3265
9	70.644	70.644	74.3006	74.3006	66.9696	66.9696	50.9306	50.9306
10	70.644	70.644	74.3006	74.3006	66.9696	66.9696	50.9306	50.9306
11	35.322	35.322	37.1503	37.1503	33.4848	33.4848	25.4653	25.4653
12	70.644	70.644	74.3006	74.3006	66.9696	66.9696	50.9306	50.9306
13	70.644	70.644	74.3006	74.3006	66.9696	66.9696	50.9306	50.9306
14	105.966	105.966	111.4509	111.4509	100.4544	100.4544	76.3959	76.3959
15	70.644	70.644	74.3006	74.3006	66.9696	66.9696	50.9306	50.9306
16	70.644	70.644	74.3006	74.3006	66.9696	66.9696	50.9306	50.9306
17	70.644	70.644	74.3006	74.3006	66.9696	66.9696	50.9306	50.9306
18	70.644	70.644	74.3006	74.3006	66.9696	66.9696	50.9306	50.9306
19	70.644	70.644	74.3006	74.3006	66.9696	66.9696	50.9306	50.9306
20	70.644	70.644	74.3006	74.3006	66.9696	66.9696	50.9306	50.9306
21	70.644	70.644	74.3006	74.3006	66.9696	66.9696	50.9306	50.9306
22	70.644	70.644	74.3006	74.3006	66.9696	66.9696	50.9306	50.9306
23	70.644	70.644	74.3006	74.3006	66.9696	66.9696	50.9306	50.9306
24	388.542	388.542	408.6533	408.6533	368.3328	368.3328	280.1183	280.1183
25	388.542	388.542	408.6533	408.6533	368.3328	368.3328	280.1183	280.1183
26	70.644	70.644	74.3006	74.3006	66.9696	66.9696	50.9306	50.9306
27	70.644	70.644	74.3006	74.3006	66.9696	66.9696	50.9306	50.9306
28	70.644	70.644	74.3006	74.3006	66.9696	66.9696	50.9306	50.9306
29	105.966	105.966	111.4509	111.4509	100.4544	100.4544	76.3959	76.3959
30	176.61	176.61	185.7515	185.7515	167.424	167.424	127.3265	127.3265
31	141.288	141.288	148.6012	148.6012	133.9392	133.9392	101.8612	101.8612
32	211.932	211.932	222.9018	222.9018	200.9088	200.9088	152.7918	152.7918
33	70.644	70.644	74.3006	74.3006	66.9696	66.9696	50.9306	50.9306

Table A.7: IEEE 33-Node Test System Hourly Load Data (Part 4)

Reactive Power Demand (kVar)	**Time Period (*t*)**							
Node No.	**1**	**2**	**3**	**4**	**5**	**6**	**7**	**8**
1	0	0	0	0	0	0	0	0
2	21.14532	21.14532	42.84162	42.84162	43.64802	43.64802	46.40958	46.40958
3	10.33771	10.33771	20.94479	20.94479	21.33903	21.33903	22.68913	22.68913
4	23.61227	23.61227	47.83981	47.83981	48.74029	48.74029	51.82403	51.82403
5	11.7474	11.7474	23.8009	23.8009	24.2489	24.2489	25.7831	25.7831
6	7.753284	7.753284	15.70859	15.70859	16.00427	16.00427	17.01685	17.01685
7	29.3685	29.3685	59.50225	59.50225	60.62225	60.62225	64.45775	64.45775
8	29.3685	29.3685	59.50225	59.50225	60.62225	60.62225	64.45775	64.45775
9	7.753284	7.753284	15.70859	15.70859	16.00427	16.00427	17.01685	17.01685
10	7.753284	7.753284	15.70859	15.70859	16.00427	16.00427	17.01685	17.01685
11	7.870758	7.870758	15.9466	15.9466	16.24676	16.24676	17.27468	17.27468
12	13.62698	13.62698	27.60904	27.60904	28.12872	28.12872	29.9084	29.9084
13	13.62698	13.62698	27.60904	27.60904	28.12872	28.12872	29.9084	29.9084
14	23.61227	23.61227	47.83981	47.83981	48.74029	48.74029	51.82403	51.82403
15	3.994116	3.994116	8.092306	8.092306	8.244626	8.244626	8.766254	8.766254
16	7.753284	7.753284	15.70859	15.70859	16.00427	16.00427	17.01685	17.01685
17	7.753284	7.753284	15.70859	15.70859	16.00427	16.00427	17.01685	17.01685
18	10.33771	10.33771	20.94479	20.94479	21.33903	21.33903	22.68913	22.68913
19	10.33771	10.33771	20.94479	20.94479	21.33903	21.33903	22.68913	22.68913
20	10.33771	10.33771	20.94479	20.94479	21.33903	21.33903	22.68913	22.68913
21	10.33771	10.33771	20.94479	20.94479	21.33903	21.33903	22.68913	22.68913
22	10.33771	10.33771	20.94479	20.94479	21.33903	21.33903	22.68913	22.68913
23	13.15709	13.15709	26.65701	26.65701	27.15877	27.15877	28.87707	28.87707
24	62.02627	62.02627	125.6688	125.6688	128.0342	128.0342	136.1348	136.1348
25	62.02627	62.02627	125.6688	125.6688	128.0342	128.0342	136.1348	136.1348
26	9.867816	9.867816	19.99276	19.99276	20.36908	20.36908	21.6578	21.6578
27	9.867816	9.867816	19.99276	19.99276	20.36908	20.36908	21.6578	21.6578
28	7.753284	7.753284	15.70859	15.70859	16.00427	16.00427	17.01685	17.01685
29	20.44048	20.44048	41.41357	41.41357	42.19309	42.19309	44.86259	44.86259
30	176.211	176.211	357.0135	357.0135	363.7335	363.7335	386.7465	386.7465
31	22.08511	22.08511	44.74569	44.74569	45.58793	45.58793	48.47223	48.47223
32	33.83251	33.83251	68.54659	68.54659	69.83683	69.83683	74.25533	74.25533
33	15.74152	15.74152	31.89321	31.89321	32.49353	32.49353	34.54935	34.54935

Table A.8: IEEE 33-Node Test System Hourly Load Data (Part 5)

Reactive Power Demand (kVar)	**Time Period (t)**							
Node No.	**9**	**10**	**11**	**12**	**13**	**14**	**15**	**16**
1	0	0	0	0	0	0	0	0
2	50.229	50.229	52.18524	52.18524	56.71404	56.71404	58.78134	58.78134
3	24.5564	24.5564	25.51278	25.51278	27.72686	27.72686	28.73754	28.73754
4	56.08905	56.08905	58.27352	58.27352	63.33068	63.33068	65.63916	65.63916
5	27.905	27.905	28.9918	28.9918	31.5078	31.5078	32.6563	32.6563
6	18.4173	18.4173	19.13459	19.13459	20.79515	20.79515	21.55316	21.55316
7	69.7625	69.7625	72.4795	72.4795	78.7695	78.7695	81.64075	81.64075
8	69.7625	69.7625	72.4795	72.4795	78.7695	78.7695	81.64075	81.64075
9	18.4173	18.4173	19.13459	19.13459	20.79515	20.79515	21.55316	21.55316
10	18.4173	18.4173	19.13459	19.13459	20.79515	20.79515	21.55316	21.55316
11	18.69635	18.69635	19.42451	19.42451	21.11023	21.11023	21.87972	21.87972
12	32.3698	32.3698	33.63049	33.63049	36.54905	36.54905	37.88131	37.88131
13	32.3698	32.3698	33.63049	33.63049	36.54905	36.54905	37.88131	37.88131
14	56.08905	56.08905	58.27352	58.27352	63.33068	63.33068	65.63916	65.63916
15	9.4877	9.4877	9.857212	9.857212	10.71265	10.71265	11.10314	11.10314
16	18.4173	18.4173	19.13459	19.13459	20.79515	20.79515	21.55316	21.55316
17	18.4173	18.4173	19.13459	19.13459	20.79515	20.79515	21.55316	21.55316
18	24.5564	24.5564	25.51278	25.51278	27.72686	27.72686	28.73754	28.73754
19	24.5564	24.5564	25.51278	25.51278	27.72686	27.72686	28.73754	28.73754
20	24.5564	24.5564	25.51278	25.51278	27.72686	27.72686	28.73754	28.73754
21	24.5564	24.5564	25.51278	25.51278	27.72686	27.72686	28.73754	28.73754
22	24.5564	24.5564	25.51278	25.51278	27.72686	27.72686	28.73754	28.73754
23	31.2536	31.2536	32.47082	32.47082	35.28874	35.28874	36.57506	36.57506
24	147.3384	147.3384	153.0767	153.0767	166.3612	166.3612	172.4253	172.4253
25	147.3384	147.3384	153.0767	153.0767	166.3612	166.3612	172.4253	172.4253
26	23.4402	23.4402	24.35311	24.35311	26.46655	26.46655	27.43129	27.43129
27	23.4402	23.4402	24.35311	24.35311	26.46655	26.46655	27.43129	27.43129
28	18.4173	18.4173	19.13459	19.13459	20.79515	20.79515	21.55316	21.55316
29	48.5547	48.5547	50.44573	50.44573	54.82357	54.82357	56.82196	56.82196
30	418.575	418.575	434.877	434.877	472.617	472.617	489.8445	489.8445
31	52.4614	52.4614	54.50458	54.50458	59.23466	59.23466	61.39384	61.39384
32	80.3664	80.3664	83.49638	83.49638	90.74246	90.74246	94.05014	94.05014
33	37.3927	37.3927	38.84901	38.84901	42.22045	42.22045	43.75944	43.75944

Table A.9: IEEE 33-Node Test System Hourly Load Data (Part 6)

Reactive Power Demand (kVar)	**Time Period (*t*)**							
Node No.	**17**	**18**	**19**	**20**	**21**	**22**	**23**	**24**
1	0	0	0	0	0	0	0	0
2	63.5796	63.5796	66.87054	66.87054	60.27264	60.27264	45.83754	45.83754
3	31.08336	31.08336	32.69226	32.69226	29.46662	29.46662	22.40946	22.40946
4	70.99722	70.99722	74.6721	74.6721	67.30445	67.30445	51.18525	51.18525
5	35.322	35.322	37.1503	37.1503	33.4848	33.4848	25.4653	25.4653
6	23.31252	23.31252	24.5192	24.5192	22.09997	22.09997	16.8071	16.8071
7	88.305	88.305	92.87575	92.87575	83.712	83.712	63.66325	63.66325
8	88.305	88.305	92.87575	92.87575	83.712	83.712	63.66325	63.66325
9	23.31252	23.31252	24.5192	24.5192	22.09997	22.09997	16.8071	16.8071
10	23.31252	23.31252	24.5192	24.5192	22.09997	22.09997	16.8071	16.8071
11	23.66574	23.66574	24.8907	24.8907	22.43482	22.43482	17.06175	17.06175
12	40.97352	40.97352	43.09435	43.09435	38.84237	38.84237	29.53975	29.53975
13	40.97352	40.97352	43.09435	43.09435	38.84237	38.84237	29.53975	29.53975
14	70.99722	70.99722	74.6721	74.6721	67.30445	67.30445	51.18525	51.18525
15	12.00948	12.00948	12.6311	12.6311	11.38483	11.38483	8.658202	8.658202
16	23.31252	23.31252	24.5192	24.5192	22.09997	22.09997	16.8071	16.8071
17	23.31252	23.31252	24.5192	24.5192	22.09997	22.09997	16.8071	16.8071
18	31.08336	31.08336	32.69226	32.69226	29.46662	29.46662	22.40946	22.40946
19	31.08336	31.08336	32.69226	32.69226	29.46662	29.46662	22.40946	22.40946
20	31.08336	31.08336	32.69226	32.69226	29.46662	29.46662	22.40946	22.40946
21	31.08336	31.08336	32.69226	32.69226	29.46662	29.46662	22.40946	22.40946
22	31.08336	31.08336	32.69226	32.69226	29.46662	29.46662	22.40946	22.40946
23	39.56064	39.56064	41.60834	41.60834	37.50298	37.50298	28.52114	28.52114
24	186.5002	186.5002	196.1536	196.1536	176.7997	176.7997	134.4568	134.4568
25	186.5002	186.5002	196.1536	196.1536	176.7997	176.7997	134.4568	134.4568
26	29.67048	29.67048	31.20625	31.20625	28.12723	28.12723	21.39085	21.39085
27	29.67048	29.67048	31.20625	31.20625	28.12723	28.12723	21.39085	21.39085
28	23.31252	23.31252	24.5192	24.5192	22.09997	22.09997	16.8071	16.8071
29	61.46028	61.46028	64.64152	64.64152	58.26355	58.26355	44.30962	44.30962
30	529.83	529.83	557.2545	557.2545	502.272	502.272	381.9795	381.9795
31	66.40536	66.40536	69.84256	69.84256	62.95142	62.95142	47.87476	47.87476
32	101.7274	101.7274	106.9929	106.9929	96.43622	96.43622	73.34006	73.34006
33	47.33148	47.33148	49.7814	49.7814	44.86963	44.86963	34.1235	34.1235

Table A.10: Photovoltaic Generation Data

(a) Maximum Available Real Power Output Hourly Data (500 kV Solar Farm)

Time Period (t)	1	2	3	4	5	6	7	8
Maximum Available Solar Real Power (kW)	6.31372	6.31372	20.0827	20.0827	73.7709	73.7709	30.3034	30.3034
Time Period (t)	9	10	11	12	13	14	15	16
Maximum Available Solar Real Power (kW)	91.6635	91.6635	156.757	156.757	371.807	371.807	363.241	363.241
Time Period (t)	17	18	19	20	21	22	23	24
Maximum Available Solar Real Power (kW)	328.24	328.24	275.461	275.461	200.954	200.954	41.2834	41.2834

(b) Related Cost of Solar Energy Curtailment

Value of Loss of Solar Energy PVC ($/kWh)	0.05